Fundamentals of Mass Transfer in Gas Carburizing

by

Olga Karabelchtchikova

A Dissertation

Submitted to the Faculty

of the

WORCESTER POLYTECHNIC INSTITUTE

In partial fulfillment of the requirements for the

Degree of Doctor of Philosophy

in

Materials Science and Engineering

_____

November 2007

APPROVED:

_____

Richard D. Sisson, Jr., George F. Fuller Professor, Advisor

Director of Manufacturing and Materials Engineering

ABSTRACT

Gas carburizing is an important heat treatment process used for steel surface hardening of automotive and aerospace components. The quality of the carburized parts is determined by the hardness and the case depth required for a particular application. Despite its worldwide application, the current carburizing process performance faces some challenges in process control and variability. Case depth variability if often encountered in the carburized parts and may present problems with i) manufacturing quality rejections when tight tolerances are imposed or ii) insufficient mechanical properties and increased failure rate in service. The industrial approach to these problems often involves trial and error methods and empirical analysis, both of which are expensive, time consuming and, most importantly, rarely yield optimal solutions.

The objective for this work was to develop a fundamental understanding of the mass transfer during gas carburizing process and to develop a strategy for the process control and optimization. The research methodology was based on both experimental work and theoretical developments, and included modeling the thermodynamics of the carburizing atmosphere with various enriching gasses, kinetics of mass transfer at the gas-steel interface and carbon diffusion in steel. The models accurately predict: 1) the atmosphere gas composition during the enriching stage of carburizing, 2) the kinetics of carbon transfer at the gas-steel surfaces, and 3) the carbon diffusion coefficient in steel for various process conditions and steel alloying. The above models and investigations were further combined to accurately predict the surface carbon concentration and the carbon concentration profile in the steel during the heat treatment process. Finally, these models were used to develop a methodology for the process optimization to minimize case depth variation, carburizing cycle time and total cycle cost. Application of this optimization technique provides a tradeoff between minimizing the case depth variation and total cycle cost and results in significant energy reduction by shortening cycle time and thereby enhancing carburizing furnace capacity.

ACKNOWLEDGEMENTS

The completion of this work is due to the support and guidance of many people. First, I would like to express my sincere appreciation and gratitude to my Ph.D. advisor, Professor Richard Sisson, Jr. for his support, guidance, enthusiasm and encouragements throughout my graduate studies and research progress.

I would like to thank Professor Diran Apelian, Professor Satya Shivkumar, Professor Makhlouf M. Makhlouf, Professor Mohammed Maniruzzaman, Professor Kevin Rong, and Professor Christopher Brown for sharing their vision of research, their continuous encouragements and invaluable feedback throughout my academic years at WPI.

I deeply appreciate opportunities that I have received through my internship with the Advanced Materials Technology group in Caterpillar, Inc. A lot of my work would have not been possible without their generous support. I give my sincere thanks to Scott Johnston, Michael Johnson and Gary Keil for their valuable discussions, for challenging my growth as a student, team player and an independent researcher.

I would like to thank the Center for Heat Treating Excellence at the Metal Processing Institute and the consortium member companies for their financial support and oversight of the project. I am so grateful for every little help that I was provided on my way up.

My friends and colleagues in the Materials Science and Engineering program and the Metal Processing Institute made my years at WPI an enjoyable experience. Being surrounded by such a positive group of people bestowed the feelings of family and forged lifelong relationships. Thank you for providing the support while pursuing my academic and personal goals.

I would like to thank my husband Matthew Ivan Rowan for his infinite love, support and encouragement. Thank you for being my everyday inspiration.

And finally, but most importantly, I would like to pay my deepest gratitude and love to my parents. Their love and belief in me lit my path in life and helped me strive to reach towards horizon and beyond.

TABLE OF CONTENT

CHAPTER I
INTRODUCTION

Gas carburizing in batch furnaces is a widely adapted procedure used for surface hardening, yet it faces some challenges in performance reliability and process control. The quality of the carburized parts is determined based on the hardness and case depth required for a particular application and on compliance with the specifications and tolerances. Therefore, to ensure a satisfactory and reliable service life of the carburized parts – it is imperative to understand the mechanism of carbon transfer and to accurately predict carbon concentration profile and case depth during the heat treatment process. Despite the importance of the carburizing applications and current challenges with the process control, the industrial approach to solving such problems often involves trial and error methods and empirical analysis, both of which are expensive and time consuming.

Successful carburizing performance depends on the effective control of the three principal variables: temperature, time and the carburizing atmosphere. Some research has been performed to investigate the effect of these process parameters on the carburizing kinetic coefficients, i.e. the mass transfer coefficient and carbon diffusivity in steel [1-10]. The mass transfer coefficient has been reported to be a complex function of the atmosphere gas composition, carburizing potential, temperature and surface carbon content [1-6]. The coefficient of carbon diffusion in austenite is another parameter determining the rate of carbon transport, which is strongly influenced by the carburizing temperature and carbon concentration in steel [7-10]. Although the mechanism of mass transport in carburizing appears to be known and understood, the results of the current industrial carburizing practices show that the carbon concentration profiles and case depths often deviate from those of the predicted ones.

The carburizing potential in the furnace is determined by the atmosphere gas composition. Accurate carbon potential calculation requires not only adequate measurement of the gas constituents (*CO, CH_4, CO_2, H_2O*) in the furnace but also representative sampling locations where the constituents are analyzed. Since surface carbon concentration and flux of carbon atoms from the atmosphere to the steel surface change with time, maintaining a constant atmosphere carbon potential during single stage carburization requires continuous adjustment of the set point until the parts meet the required specification. Dawes and Tranter [11] reported that variation of

0.05 wt% in the carburizing potential from the set point can be caused by an average temperature variation (10 °C) in the carburizing furnace.

An increase in the carburizing temperature increases the rate of mass transfer both in the furnace atmosphere and steel. It also promotes excessive austenite grain growth and deteriorates the furnace condition. The effect of time on case depth is interdependent with the carburizing temperature and is often estimated by using the Harris equation [12]. The equation, however assumes saturated austenite at the steel surface, and when the surface carbon content is less than the saturation limit, the resulting case depth prediction would be less than expected. Therefore, for the purpose of the carburizing process optimization and its further control, a more complex model should be used which would account for the variations of temperature and atmosphere carbon potential with time.

Overall, carburizing performance strongly depends on the choice of process parameters, operating furnace and atmosphere control, and materials characteristics. Each of these factors contribute to either the mass transfer coefficient or carbon diffusivity in austenite. Therefore, the goal of this project is to develop a fundamental understanding of the mechanism of mass transfer during gas carburizing and to investigate the effect of the process parameters' variations on the carburizing kinetics. Effective control of the mass transfer characteristics will help achieve the desired final properties of the carburized parts and improve process performance.

RESEARCH OBJECTIVES

The objective for this work was to develop a fundamental understanding of the mass transfer during gas carburizing process and to develop a strategy for the process control and optimization. The research methodology was based on both experimental work and theoretical developments, and included modeling the thermodynamics of the carburizing atmosphere with various enriching gasses, kinetics of mass transfer at the gas-steel interface and carbon diffusion in steel. The models accurately predict: 1) the atmosphere gas composition during the enriching stage of carburizing, 2) the kinetics of carbon transfer at the gas-steel surfaces, and 3) the carbon diffusion coefficient in steel for various process conditions and steel alloying. The above models and investigations were further combined to accurately predict the surface carbon concentration and the carbon concentration profile in the steel during the heat treatment process. Finally, this

model was used to develop a methodology for the process optimization to minimize case depth variation, carburizing cycle time and total cycle cost. Application of this optimization technique provides a tradeoff between minimizing the case depth variation and total cycle cost and results in significant energy reduction by shortening cycle time and thereby enhancing carburizing furnace capacity.

RESEARCH PLAN

This section describes the research plan for this project, which consists of both theoretical developments and experimental investigations. Theoretical developments focus on modeling the kinetics and thermodynamics of the gas carburizing atmosphere, developing a method of direct flux integration to calculate the mass transfer coefficient and carbon diffusion in steel, and finally, on modeling the overall heat treatment process.

Experimental work focuses on understanding the effect of the process parameters and materials characteristics on the kinetics of mass transfer during carburizing. The results of these investigations will then be used in conjugation with the developed models and help determine the critical kinetic parameters for the boundary conditions and process modeling.

Overall, the proposed research plan allows studying each of the stages of carbon transfer path from the gas atmosphere to the steel surface individually, yet links them together to allow overall process modeling, control and optimization.

Theoretical developments:

1. Gas carburizing atmosphere development (submitted to *Metallurgical Transactions*)
    1.1. Carburizing atmosphere reactions and carbon potential calculations
    1.2. Thermodynamic model for endothermic carrier gas and carburizing atmosphere
2. Carbon diffusion in steels – a numerical analysis based on direct flux integration (published in *Journal of Phase Equilibria and Diffusion,* 26 (6), 598-604)
    2.1. Kinetics of carbon transfer in carburizing
    2.2. Numerical approach to calculate the mass transfer coefficient and carbon diffusivity
    2.3. Direct flux method validation

3. Calculation of gas carburizing kinetic parameters from carbon concentration profiles based on direct flux integration

   (published in *Defect and Diffusion Forum,* vol. 266, 171-180)

   3.1. Mass transfer coefficient and carbon diffusivity (AISI 8620)

   3.2. Model and method validation

4. Carburizing process modeling

   (published in *Proc.* MS&T 2006, Cincinnati, OH, 375-386)

   4.1. Governing PDE and Boundary conditions

   4.2. Numerical simulation

   4.3. Model validation and sensitivity analysis

Experimental investigations:

5. Gas consumption and cost model optimization of the carburizing boost stage

   (submitted to *Metallurgical Transactions*)

   5.1. Stabilized atmosphere composition

   5.2. Carburized case characteristics

   5.3. Cost model – heat treating operating cost

6. Effect of surface roughness on the kinetics of mass transfer during gas carburizing

   (submitted to *International Journal of Heat Treatment and Surface Engineering*)

   6.1. Surface area characterization

   6.2. Average carbon flux and mass transfer coefficient

   6.3. Modeling carbon concentration profile

7. Effect of alloy composition on carburizing performance of steel

   (submitted to *Metallurgical Transactions*)

   7.1. Calculation of carbon diffusivity in unalloyed plain carbon steel (AISI 1018) and medium-alloyed steels (AISI 4820, 5120, 8620)

   7.2. Validation of the method of direct flux integration with DICTRA simulation results

8. Carburizing process optimization

   (submitted to *Metallurgical Transactions*)

   8.1. Minimizing total cycle cost and processing time to achieve a desired case depth

   8.2. Optimizing the carburizing process parameters to minimize case depth variation

CHAPTER II

LITERATURE REVIEW

Gas Carburizing Atmosphere Reactions

Endothermic carburizing atmospheres consist of a mixture of carburizing agents (*CO, CH_4*) and decarburizing (*CO_2, H_2O*) agents, the ratio of which determines the carburizing potential in the furnace. As the driving force for carburizing is determined by the gradient between the carbon potential in the atmosphere and carbon at the steel surface, it is imperative to maintain a high carburizing potential throughout the whole process.

From a thermodynamic standpoint, the generation of the carburizing atmosphere is a rather complex process involving the interaction of numerous gases. Endothermic gas is most commonly produced by mixing air and natural gas in a fixed proportion, where the ratio may range from 2.5 to 5. To accelerate the chemical reactions, the gas mixture is passed through a chamber with a NiAl catalyst. Endothermic gas is then cooled to stabilize its chemical composition and is delivered into the furnace. The carrier gas entering the furnace is composed of *CO, CO_2, CH_4, H_2, H_2O* and N_2. It has been estimated that nearly 180 chemical reactions occur simultaneously in the carburizing atmosphere, among which, only the following three reactions are important and determine the rate of carbon transfer from the carburizing atmosphere to the steel surface [13]:

$$2CO \rightarrow C_{(\gamma-Fe)} + CO_2, \tag{1}$$

$$CH_4 \rightarrow C_{(\gamma-Fe)} + 2H_2, \tag{2}$$

$$CO + H_2 \leftrightarrow C_{(\gamma-Fe)} + H_2O. \tag{3}$$

While carburizing most rapidly proceeds by *CO* molecule decomposition, the by-products of the carburizing reactions (*CO_2* and *H_2O*) act as decarburizing agents. The presence of *CO_2* even in small quantities requires a high *CO* concentration to balance this decarburizing action. Therefore, for the process to proceed further, these decarburizing species must be reduced. Generally, the maximum amount of *CO_2* that is tolerated at a particular carburizing temperature without causing decarburization can be determined based on thermodynamic calculations [14].

Since carburizing with endogas only is practically inefficient and requires large flow rates, the endothermic carrier gas is enriched by blending with an additional hydrocarbon gas [15]. The purpose of the enriching gas is to react with CO_2 and H_2O, thus reducing their concentration and producing more CO and H_2 as reaction products:

$$CH_4 + CO_2 \leftrightarrow 2CO + 2H_2, \tag{4}$$

$$CH_4 + H_2O \leftrightarrow CO + 3H_2. \tag{5}$$

Although enriching reactions (4) and (5) are slow and do not approach equilibrium, the effectiveness of the carburizing process is determined by the atmosphere carbon potential and controlled by the ratio of CO / CO_2 and H_2 / H_2O components in the heterogeneous water-gas reaction:

$$CO + H_2O \leftrightarrow CO_2 + H_2. \tag{6}$$

Carbon Potential Calculation

Carbon potential (C_P) in the furnace atmosphere is defined as the amount of carbon in the furnace atmosphere that is in thermodynamic equilibrium with the surface carbon content in unalloyed steel. The atmosphere carbon potential is calculated from the chemical reactions (1-3) for the given carburizing temperature and gas chemical composition. In the non-equilibrium conditions of an industrial carburizing practice [16], carbon activity (a_C) and the reaction rate coefficient (k) for these reactions differ according to equations (7-9). Therefore, to calculate the effective carbon activity and C_P in the furnace atmosphere, the reaction with the highest reaction rate should be considered [17].

$$a_{C_1} = \frac{P_{CO}^2}{P_{CO_2}} \cdot \exp\left(\frac{20530.65}{T} - 20.98\right), \qquad k_1 = 184 \cdot \left(\frac{P_{CO_2}}{P_{CO}}\right)^{-0.3} \cdot P_{CO_2} \cdot \exp\left(\frac{-22,400}{T}\right). \tag{7}$$

$$a_{C_2} = \frac{P_{CH_4}}{P_{H_2}^2} \cdot \exp\left(\frac{10949.68}{T} - 13.31\right), \qquad k_2 = 1.96 \cdot 10^{-2} \cdot P_{H_2}^{1.5} \cdot \exp\left(\frac{-17,600}{T}\right). \tag{8}$$

$$a_{C_3} = \frac{P_{CO} \cdot P_{H_2}}{P_{H_2O}} \cdot \exp\left(\frac{16333.11}{T} - 17.26\right), \qquad k_3 = \frac{4.75 \cdot 10^5 \cdot \exp\left(\frac{-27{,}150}{T}\right) \cdot \frac{P_{H_2O}}{\sqrt{P_{H_2}}}}{1 + 5.6 \cdot 10^6 \cdot \exp\left(\frac{-12{,}900}{T}\right) \cdot \frac{P_{H_2O}}{\sqrt{P_{H_2}}}} \,. \tag{9}$$

Table 1 shows the reaction rate coefficients (k_1, k_2, and k_3) for the carburizing reactions (1-3), calculated for the typical endothermic atmosphere composition (19.8% CO, 0.1% CO_2, 40 % H_2, 0.3 % H_2O and balance N_2) at 925 °C.

Table 1. Reaction rate coefficients for the carburizing chemical reactions (1-3).

	Reaction 1	Reaction 2	Reaction 3
Reaction rate (k, cm/s)	$6.83 \cdot 10^{-9}$	$2.07 \cdot 10^{-9}$	$2.08 \cdot 10^{-7}$
Normalized rate coefficient	0.03	0.01	1

The data in Table 1 suggest that carburizing reaction (3) is several orders of magnitude faster than the reactions (1) and (2), and therefore, it determines the rate of carbon adsorption during the process. The effective carbon activity calculated from Equation (9) is then related to the atmosphere carbon potential using the following model [18,19]:

$$\log_{10} a_C = \frac{3770}{T} + 2.72 \cdot \log_{10} T - 10.525 + \frac{3860 \cdot y}{T} + \log_{10}\left(\frac{y}{1-y}\right), \tag{10}$$

$$C_P = \frac{1201 \cdot y}{55.85 + 12.01 \cdot y} \,. \tag{11}$$

where a_C is carbon activity in austenite, T is temperature in K, and y is the wt.% of carbon in austenite at the steel surface.

Carbon Transfer Mechanisms During Gas Carburizing

The mass transfer mechanism during gas carburizing is a complex phenomenon which involves three distinct stages: 1) carbon transport from the atmosphere to the steel surface, 2) surface chemical reactions, and 3) diffusion of the absorbed carbon atoms towards the bulk of the steel down the chemical potential gradient. Total carbon transfer from the atmosphere to the steel is thus determined by the limiting process, which kinetically becomes the rate controlling stage of

carburizing [1-6,20-24]. Figure 1 schematically shows the mechanisms of carbon transfer during carburizing and the primary control parameters: the mass transfer coefficient (β) defining carbon atoms flux (J) from the atmosphere to the steel surface and the coefficient of carbon diffusion in steel (D) at austenizing temperatures.

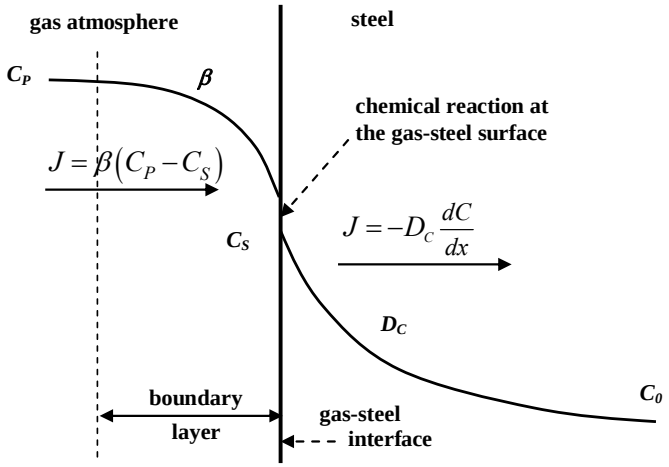

Figure 1. Schematic representation of carbon transport in carburizing.

Considering kinetics of the process, the maximum carburization rate is obtained when the carbon transfer from the atmosphere is equal to or greater than the carbon diffusion rate in the solid state. Such a diffusion controlled process has no deficiency of carbon supplied to the interface for its further transport into the solid; an assumption of constant surface carbon content may then be justified. In practice, however, the non-equilibrium carbon transfer from the atmosphere to the solid boundary including surface reaction is often reported to be the rate limiting factor [1,6] especially at the start of the carburizing process. After this initial stage, the process becomes mixed controlled [20-22] and should be modeled correspondingly.

Mass transfer coefficient

The mass transfer coefficient in the gas phase controls the rate of carbon uptake during the initial stage of carburizing [1-6]. As shown in Figure 2, the mass transfer coefficient determines the thickness of the boundary gas layer (D/β) at the gas-solid interface and defines the maximum flux of carbon atoms reaching the steel surface and available for further carbon diffusion towards the bulk of the steel [1].

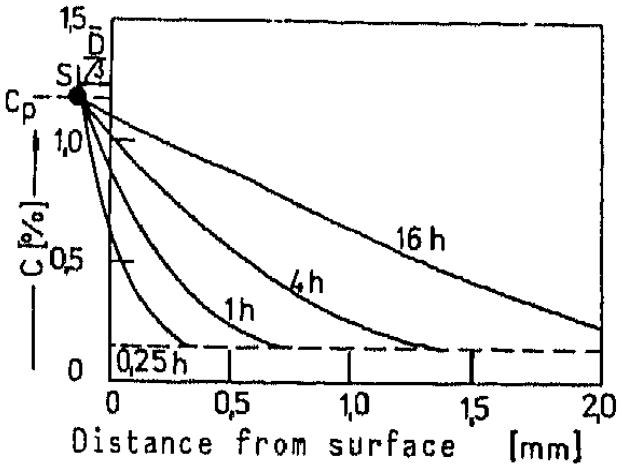

Figure 2. Graphical representation of the significance of the mass transfer coefficient β [1].

Several models have been proposed [20,23] to model the evolution of surface carbon content with carburizing time; most of them have some limitations and do not always yield accurate results. One of such models was suggested by Yan [20] as follows

$$C_S = C_P - \frac{C_P - C_0}{1 + \beta\sqrt{\frac{3t}{D}} \cdot \exp\left(-\frac{D}{3\beta^2 t}\right)}, \tag{12}$$

where C_S is surface carbon concentration in wt.%, C_0 is the bulk carbon concentration in the steel, and t – carburizing time. While the model was derived analytically, some correction factors were applied to compensate for the assumed constant carbon diffusivity.

The mass transfer coefficient is very sensitive to the changes in the atmosphere composition and carburizing potential [1-6,24-27]. Several independent authors [1,2] measured β using thin foils in the carburizing atmospheres of various CO-CO_2 ratios. Even though the magnitude of β varies, their findings indicate a similar trend: β changes drastically in the range of 0-30 % of each of these gas constituents. Also, in such atmospheres β is only slightly dependent on the atmosphere carbon potential. When the ratio of these gases is in the range of 30-70 % β becomes independent of the atmosphere composition and is influenced by the carbon potential only.

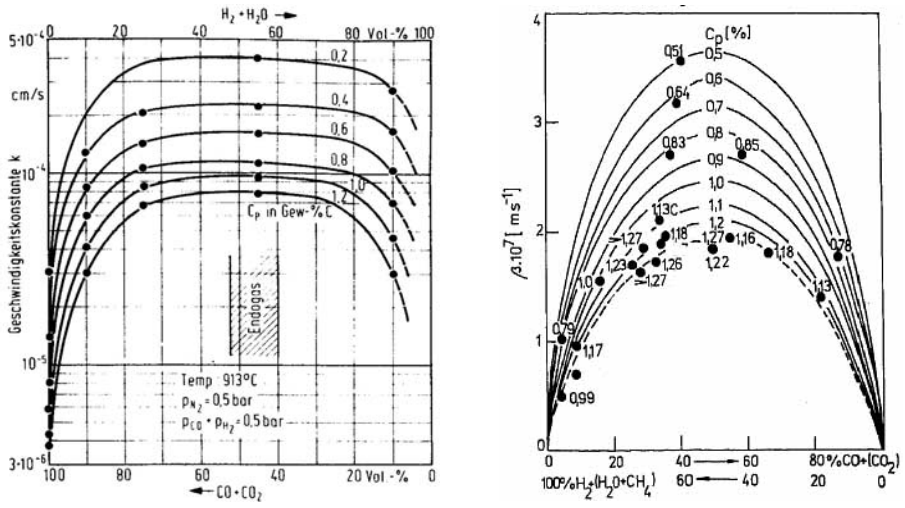

a) b)

Figure 3. Variation in β with gas atmosphere composition and C_P: (a) according to Rimmer et.al. at 913 °C [2], and (b) according to Stolar at 920 °C [1].

Munts and Baskakov [3] suggested that the mass transfer coefficient should increase linearly with the concentration of water vapor in the carburizing atmosphere. And since carbon activity in the gas phase is inversely proportional to the concentration of water vapor, the β coefficient should decrease with increasing carbon potential. Assuming that partial pressures of the atmosphere gas components are known and carbon activity in the gas is controlled, the following mass transfer coefficient model was suggested [24,25]:

$$\beta = \frac{6.31 \cdot 10^5 \cdot \exp\left(\frac{-22350}{T}\right) \cdot \frac{P_{H_2O}}{\sqrt{P_{H_2}}}}{1 + 5.6 \cdot 10^6 \cdot \exp\left(\frac{-12900}{T}\right) \cdot \frac{P_{H_2O}}{\sqrt{P_{H_2}}}} \tag{13}$$

While information on β as a function of the gas atmospheres is agreeable among most researchers [2,4,24,25], there is a large discrepancy in the reported effect of carburizing temperature on this coefficient [3,5,6,26,27]. Wünning [5] studied carburizing of iron foils in an endothermic atmosphere at 850-980 °C and found $\beta = 10^{-5}$ cm/s to be consistent with the carburizing temperature. Rimmer and co-authors also reported β to be independent of carburizing temperature [2]. Using mixtures of pure gases similar to endogas composition, the authors observed β values on the order of 10^{-4} cm/s. As opposed to the first group of work, a number of studies [3,6,26] observed a significant change in β given changes in carburizing temperature.

Munts and Baskakov [3] measured β ranging from $2 \cdot 10^{-5}$ to $2 \cdot 10^{-4}$ cm/s at 800-1000 °C. β values also varied with carburizing temperature and carbon potential in the atmosphere. Once carbon potential approached near-solubility limit in γ-Fe for steels with carbon content greater than 0.5 wt.%, the value of β was $2 \cdot 10^{-5}$ cm/s and became consistent with temperature.

Carbon diffusivity in austenite

Once *CO* molecules reach the surface and dissociate into adsorbed carbon atoms and carbon dioxide ($2CO \rightarrow C_{ad} + CO_2$), the mechanism of further carbon transport becomes limited by the rate of carbon diffusion in steel. Carbon diffusivity (*D*) in austenite varies both with carbon concentration and carburizing temperature [7-10] as shown in Table 2 and Figure 4. Considering that carbon concentration depends on its activity in austenite and that the finite repulsive interactions exist between neighboring carbon atoms in octahedral sites, Babu and Bhadeshia [28] modeled carbon diffusivity in accordance with kinetic and thermodynamic behavior of carbon in austenite. Siller and McLellan [29] suggested that the repulsive forces between the neighboring carbon atoms influence carbon diffusivity by reducing probability of interstitial sites occupancy in the vicinity of the site already occupied by carbon atom. Therefore, in a concentration gradient, carbon atom attempting random motion faces exaggerated difference in the number of available sites, which enhances carbon diffusion down the concentration gradient.

Interstitial carbon diffusivity is strongly affected by the atomic interactions with substitutional solute, i.e., alloying elements present in the steel [30]. If these interactions are positive, substitutional solute atoms tend to attract interstitial carbon atoms. Such deviation from randomness in the interstitial atoms distribution impedes long range diffusion of carbon in the austenite lattice, and therefore decreases the effective coefficient of carbon diffusion. Similar effect but of the opposite nature will be expected with solute components of negative interactions: as their binding energy decreases there will be localized volumes with increased carbon diffusivity. The described effect has appreciable contribution to the total diffusivity, and therefore should be considered in medium- and high-alloyed steels to achieve an adequate prediction of the carburizing performance. Despite its significant contribution, little theoretical and experimental knowledge is available to quantitatively describe the effect of alloying on carbon diffusivity. As a result, most applications assume carbon diffusivity to be either constant at fixed temperature or vary with carbon concentration only.

Table 2. Carbon diffusivity models

Coefficient of carbon diffusion (D_C)	Equation number	Reference
$D_{C(\gamma-Fe)} = 0.738 \cdot \exp\left(\frac{-159,000}{RT}\right)$, $\mathrm{cm^2/s}$, $R = 1.99$ cal/mol·K	Equation A1	[48]
$D_{C(\gamma-Fe)} = 0.03919 \cdot \exp\left(\frac{-129,340}{RT}\right)$, $\mathrm{cm^2/s}$, $R = 1.99$ cal/mol·K	Equation A2	[49]
$D_{C(\gamma-Fe)} = 0.668 \cdot \exp\left(\frac{-157,000}{RT}\right)$, $\mathrm{cm^2/s}$, $R = 8.31$ J/mol·K	Equation A3	[50]
$D_{C(\gamma-Fe)} = 0.162 \cdot \exp\left(\frac{-137,800}{RT}\right)$, $\mathrm{cm^2/s}$, $R = 8.31$ J/mol·K	Equation A4	[23]
$D_{C(\gamma-Fe)} = 0.47 \cdot \exp\left(\frac{-155,310}{RT}\right)$, $\mathrm{cm^2/s}$, $R = 8.31$ J/mol·K	Equation A5	[51]
$D_{C(\gamma-Fe)} = 0.47 \cdot \exp\left(-1.6 \cdot C - \frac{37,000 - 6,600 \cdot C}{RT}\right)$, $\mathrm{cm^2/s}$ $R = 1.99$ cal/mol·K, C, wt.%	Equation A6	[52]
$D_{C(\gamma-Fe)} = (0.07 + 0.06 \cdot C) \cdot \exp\left(-\frac{32,000}{RT}\right)$, $\mathrm{cm^2/s}$ $R = 1.99$ cal/mol·K, C, wt.%	Equation A7	[7]
$D_{C(\gamma-Fe)} = (1 - 0.23 \cdot C) \cdot \exp\left(\frac{4300 \cdot C^{1.5} - 18900}{T} - 2.63 \cdot C^{1.5} - 0.38\right)$, $\mathrm{cm^2/s}$, $R = 8.31$ J/mol·K, C, wt.%	Equation A8	[22]
$D_{C(\gamma-Fe)} = 0.78 \cdot \exp\left[-\frac{18,900}{T} + \left(\frac{4,300}{T} - 2.63\right) C^{1.5}\right]$, $\mathrm{cm^2/s}$ $R = 8.31$ J/mol·K, C, wt.%	Equation A9	[8]
$D_{C(\gamma-Fe)} = 4.53 \cdot 10^{-3} \cdot \left(1 + Y_C (1 - Y_C) \frac{8,339.9}{T}\right) \times$ $\times \exp\left(-\left(\frac{1}{\mathrm{T}} - 2.221 \cdot 10^{-4}\right) \cdot (17,767 - Y_C \cdot 26,436)\right)$, $\mathrm{cm^2/s}$ $Y_C = \frac{X_C}{1 - X_C}$, X_C – mole fraction	Equation A10	[9,53]
$D_{C(\gamma-Fe)} = 1.43 \cdot \exp\left(-\frac{19,900}{T}\right) \cdot (1 - 23.2 \cdot C) \cdot \exp\left(0.242 \cdot C \cdot \exp\left(\frac{6790}{T}\right)\right)$ $\mathrm{cm^2/s}$, $R = 8.31$ J/mol·K, C, wt.%	Equation A11	[10]

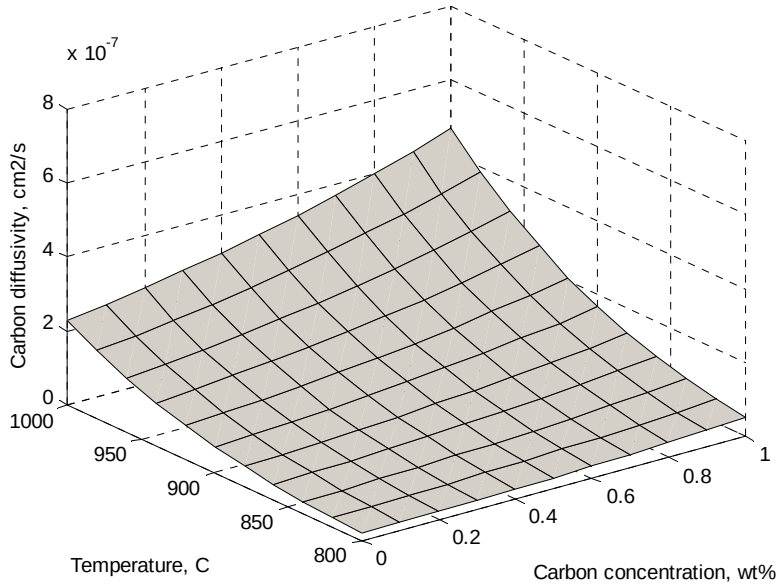

a)

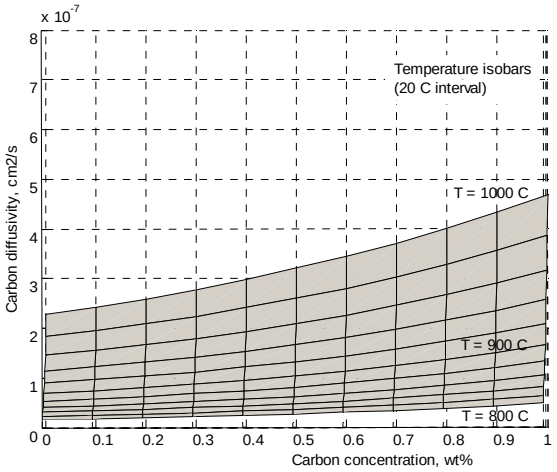

b)

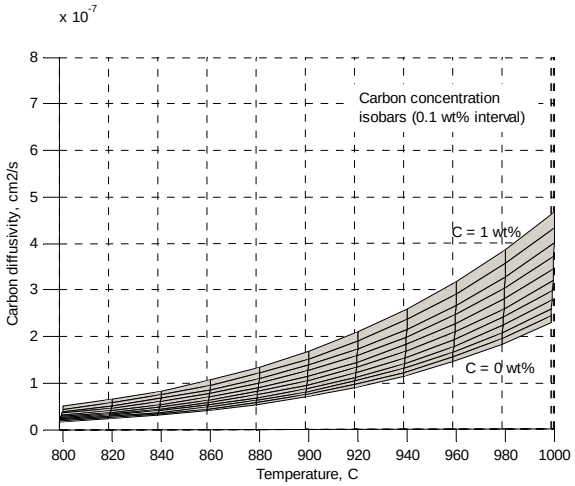

c)

Figure 4. Mean values of the coefficient of carbon diffusion in austenite (Equations A6-A11): a) surface representation, b) as a function of carbon content, c) as a function of temperature.

REFERENCES

1. P. Stolar and B. Prenosil, "Kinetics of Transfer of Carbon from Carburizing and Carbonitriding Atmospheres," *Metallic Materials (English translation of Kovove Materialy)*, 22 (5) (1984), 348-353.

2. K. Rimmer, E. Schwarz-Bergkampf, and J. Wunning, "Surface Reaction Rate in Gas Carburizing," *Haerterei-Technische Mitteilungen*, 30 (3) (1975), 152-160.

3. V.A. Munts, and A.P. Baskatov, "Rate of Carburizing of Steel," *Metal Science and Heat Treatment (English Translation of Metallovedenie i Termicheskaya Obrabotka Metallov),* 22 (5-6) (1980), 358-360.

4. V.A. Munts, and A.P. Baskakov, "Mass Exchange in Carburization and Decarburization of Steel," *Metal Science and Heat Treatment (English Translation of Metallovedenie i Termicheskaya Obrabotka Metallov),* 25 (1-2) (1983), 98-102.

5. J. Wunning, "Advances in Gas Carburizing Technique," *Haerterei-Technische Mitteilungen*, 23 (3) (1968), 101-109.

6. B.A. Moiseev, Y.M. Brunzel', and L.A. Shvartsman, "Kinetics of Carburizing in an Endothermal Atmosphere," *Metal Science and Heat Treatment (English translation of Metallovedenie i Termicheskaya Obrabotka Metallov)*, 21 (5-6) (1979), 437-442.

7. J.I. Goldstein and A.E. Moren, "Diffusion Modeling of the Carburization Process," *Metallurgical and Materials Transactions A,* 9 (11) (1978), 1515-1525.

8. George E. Totten and Maurice A.H. Howes, *Steel Heat Treatment Handbook* (New York, NY: Marcell Dekker, Inc., 1997).

9. J. Agren, "Revised Expression for the Diffusivity of Carbon in Binary Fe-C Austenite," *Scripta Metallurgica*, 20 (11) (1986), 1507-1510.

10. R.M. Asimow, "Analysis of the Variation of the Diffusion Constant of Carbon in Austenite with Concentration," *Transactions of AIME,* 230 (3) (1964), 611-613.

11. C. Dawes, and D.F. Tranter, "Production Gas Carburizing Control," *Heat Treatment of Metals,* 31 (4) (2004), 99-108.

12. F.E. Harris, "Case Depth - an Attempt at a Practical Definition," *Metal Progress*, 44 (1943), 265-272.

13. R. Collin, S. Gunnarson and D. Thulin, "Mathematical Model for Predicting Carbon Concentration Profiles of Gas-Carburized Steel," *Journal of the Iron and Steel Institute*, 210(10) (1972), 785-789.

14. American Society for Metals, (1977). Carburizing and Carbonitriding. Metals Park, OH: ASM International.

15. B. Edenhofer, "Case-hardening - a Process with New Evolutions and Perspectives," Proceedings of the 5th ASM Heat Treatment and Surface Engineering Conference, Jun 7-9 2000, Gothenburg, Sweden, ASM International.

16. C.A. Stickels, "Gas Carburizing of Steel," in Metals Handbook (1981), vol.4, American Society for Metals.

17. M.L. Schmidt, "Pre-oxidation Prior to Gas Carburizing: Theory and its Effect on Pyrowear 53 Alloy. Carburizing Processing and Performance," Metals Park, OH, ASM International, (1989), 83-100.

18. M.J. Bannister, "Control of Carbon Potential Using an Oxygen Sensor," *Industrial Heating*, 51(3) (1984), 24-26.

19. S. Ban-Ya, J.F. Elliott, J. Chipman, "Thermodynamics of Austenitic Fe-C Alloys," *Metallurgical and Materials Transactions A*, 1(5) (1970),1313-2130.

20. Yan, M., Z. Liu, and G.Zu, "The Mathematical Model of Surface Carbon Concentration Growth during Gas Carburization," *Materials Science Progress* (in Chinese) 6(3) (1992), 223-225.

21. Turpin, T., J. Dulcy, and M. Gantois, "Carbon Diffusion and Phase Transformations during Gas Carburizing of High-Alloyed Stainless Steels: Experimental Study and Theoretical Modeling," *Metallurgical and Materials Transactions A*, 36(10) (2005): 2751-2760.

22. Ruck, A., D. Monceau, and H.J.Grabke, "Effects of Tramp Elements Cu, P, Pb, Sb and Sn on the Kinetics of Carburization of Case Hardening Steels," *Steel Research*, 67(6) (1996), 240-246.

23. Yan, M.F., Z.R. Liu, and T. Bell, "Effect of Rare Earths on Diffusion Coefficient and Transfer Coefficient of Carbon During Carburizing," *Journal of Rare Earths*, 19(2) (2001), 122-124.

24. K.T. Raic, "Control of Gas Carburizing by Diagram Method," *Scandianvian Journal of Metallurgy*, 22 (1993), 50-54.

25. V.A. Munts and A. P. Baskakov, "Mass Exchange in Carburization and Decarburization of Steel," *Metal Science and Heat Treatment (English Translation of Metallovedenie i Termicheskaya Obrabotka Metallov),* 25(1-2) (1983), 98-102.

26. Sobusiak, T. Method of Measuring Carbon Potential and Carbon Transfer Coefficient, Heat Treatment Shanghai '83, Proceedings of the 3rd International Congress on Heat Treatment of Materials (1984) Shanghai, China: Metals Society (Book 310), London, England.

27. Zamyatin, M.M., Kinetics of Chemicothermal Treatment of Steel (1951), Moscow: Metallurgizdat.

28. Babu, S.S. and H.K.D.H. Bhadeshia, "Diffusion of Carbon in Substitutionally Alloyed Austenite," *Journal of Materials Science Letters*, 14(5) (1995), 314-316.

29. Siller, R. and R. McLellan, "Variation with Composition of Diffusivity of Carbon in Austenite," *Transactions of AIME*, 245(4) (1969), 697-700.

30. K.E. Blazek and P. R. Cost, "Carbon Diffusivity in Iron-Chromium Alloys," *Transactions of the Japan Institute of Metals*, 17(10) (1976), 630-636.

CHAPTER III

PUBLICATIONS

This section summarizes the results for the outlined theoretical work and experimental investigations. The section is structured as a collection of papers – each presented as a subsection outlined in the research plan.

PAPER # 1: THERMODYNAMICS OF THE CARBURIZING ATMOSPHERES WITH VARIOUS ENRICHING HYDROCARBON GASES

(submitted to *Metallurgical Transactions*)

Abstract

The effect of various hydrocarbon enrichment processes on carbon potential and carburizing atmosphere evolution has been investigated both theoretically and experimentally. A thermodynamic model has been developed to predict the equilibrium gas composition. A series of industrial experiments were performed to validate the model predictions and to experimentally investigate the enriching potential of selected hydrocarbon gases. It was observed that enriching the endothermic carrier gas with propane significantly enhanced the rate of carbon potential evolution and produced richer carbon atmospheres. These benefits were attributed not only to the advantage in higher carbon availability per unit volume of propane molecule, but also to the thermodynamics and kinetics of its decomposition. The atmosphere tendency to soot was evaluated in terms of deviation of the atmosphere composition from equilibrium and the amount of residual methane. An equivalent atmosphere carbon potential was achieved by using four times lower flow of enriching propane over conventional natural gas enrichment. Such carburizing atmospheres also exhibited lower residual methane and lower tendency to soot. Overall, using propane enrichment proved to be an attractive alternative to conventional natural gas enrichment by shortening total cycle time and lowering enriching gas consumption; both resulting in better energy utilization.

Introduction

Endothermic atmospheres produced by mixing endogas and enriching hydrocarbon gas have been successfully used in industrial gas carburizing for over 50 years. Compared to the previous carburizing methods, such as salt- or pack carburizing, it offers an advantage of carbon potential control and therefore produces more uniform and repeatable results. Geographically, where natural gas supply is scarce or not available, gas carburizing atmospheres with composition similar to endothermic gas can be produced either by using methanol-nitrogen in a 60%-40% ratio [1-4] or by in-situ mixing of air and propane or butane [5-8]. Despite a number of recent advances in in-situ gas atmospheres [9-12], carburizing with endogas-generated atmospheres enriched with natural gas dominates the heat-treating market in North America.

In industrial settings, carburizing cycles are generally designed through plant trials and empirical methods, and are rarely optimized [13]. In addition, anticipated shortages in natural gas supply and energy resources demand industry to search for alternative lower-cost solutions and efficient energy utilization [14,15]. In the view of a competitive market this would require shortening cycle time and reducing gas consumption, which would decrease cycle cost and increase furnace productivity. The most common approach to reduce the cycle time is to carburize at higher temperatures. This would increase the rate of carbon transfer from the gas atmosphere to the steel surface and increase carbon diffusion in steel [16,17]. Such a solution, however, has limitations due to its deteriorating effect on the furnace life and excessive growth of austenite grain size [18]. Therefore, optimizing the enriching stage of the atmosphere development would help reduce the time necessary for the furnace to raise the carburizing potential to a desired set point, and potentially, reduce the overall gas consumption. From this standpoint, an optimal carburizing atmosphere can be defined as the atmosphere that promotes faster carburizing rates and achieves high carbon potential without sooting.

The objectives of this work were three-fold: i) to investigate the enriching potential of various hydrocarbon gases and to analyze their propensity to soot, ii) to model the equilibrium gas composition of various carburizing atmospheres, and iii) to optimize endothermic carburizing atmosphere by maximizing the rate of carbon potential evolution and minimizing the enriching gas consumption without impairing the carburizing properties of the gases. Specifically, the goal of this work was to develop a better understanding of the effect of

enriching gas composition and flow rate on the evolution of carbon potential and the carburizing atmosphere composition during the process. The endothermic carburizing atmospheres were generated by varying the volumetric flow rate of the enriching hydrocarbon gas and maintaining a steady flow of the endothermic carrier gas. A thermodynamic model was developed to predict the equilibrium gas composition upon carbon potential stabilizing. The experimental work was performed at an industrial research facility and the data were used to validate the model predictions.

Environmental impact is another driver for reducing gas consumption, which was also addressed in this paper. The major barrier for the industrial sector is the difficulty to cost-effectively reduce emmision and at the same time increase efficiency of the process [15]. Deducing an optimal combination of the type of hydrocarbon enriching gas and its flow rate will help lower the environmental impact by reducing gas consumption and emission of the by-product gases without impairing the carburizing properties. Accelerating the rates of the carburizing reactions would permit carburizing larger workloads with greater efficiency, reducing total cycle time required to achieve a desired case depth and increasing furnace capacity.

Gas Carburizing Atmosphere Reactions

Endothermic carburizing atmospheres consist of a mixture of carburizing agents (*CO, CH_4*) and decarburizing (*CO_2, H_2O*) agents, the ratio of which determines the carburizing potential in the furnace. As the driving force for carburizing is determined by the gradient between the carbon potential in the atmosphere and carbon at the steel surface, it is imperative to maintain a high carburizing potential throughout the whole process. From a thermodynamic standpoint, the generation of the carburizing atmosphere is a complex process involving the interaction of numerous gases. Endothermic gas is most commonly produced by mixing air and natural gas and consists of *CO*, *CO_2*, *CH_4*, *H_2*, *H_2O* and *N_2*. Among various chemical reactions occurring simultaneously in the carburizing atmosphere, only the following three reactions are important and determine the rate of carbon transfer [19]:

$$2CO \rightarrow C_{(Fe)} + CO_2, \quad (1)$$

$$CH_4 \rightarrow C_{(Fe)} + 2H_2, \quad (2)$$

$$CO + H_2 \leftrightarrow C_{(Fe)} + H_2O. \quad (3)$$

While carburizing most rapidly proceeds by CO molecule decomposition, the by-products of the carburizing reactions (CO_2 and H_2O) act as decarburizing agents. The presence of CO_2 even in small quantities requires high CO concentration to balance this decarburizing action, therefore, these decarburizing species must be reduced. Generally, the maximum amount of CO_2 that is tolerated at a particular carburizing temperature without causing decarburization can be determined based on thermodynamic calculations [20]. Since carburizing strictly with endogas is practically inefficient and requires large flow rates, endothermic gases are enriched by blending with an additional hydrocarbon gas. As such, the purpose of the enriching gas is to react with CO_2 and H_2O, thus reducing their concentration and producing more CO and H_2 as reaction products:

$$CH_4 + CO_2 \leftrightarrow 2CO + 2H_2, \tag{4}$$

$$CH_4 + H_2O \leftrightarrow CO + 3H_2. \tag{5}$$

When the enriching hydrocarbon gas reacts fully and approaches equilibrium, the amount of residual methane in the furnace atmosphere is low. However, in industrial carburizing processes the enriching reactions (4-5) deviate from equilibrium and result in a large amount of residual methane in the carburizing chamber. An increased concentration of methane is observed in all types of carburizing atmospheres, and therefore a limited amount of it is considered normal [1]. The degree of methane decomposition depends on the quantity and type of the hydrocarbon gas entering the furnace, furnace operating temperature, and workload characteristics [21]. Large concentration of residual methane gives a strong driving force for graphite precipitation through the chemical reaction (2) and may result in formation of soot [12]. To prevent soot formation, it is important that the amount of enriching hydrocarbon gas does not exceed carbon demand in the furnace. Several researchers suggested that buildup of residual methane is an indication on the atmosphere tendency to soot, and therefore, monitoring residual methane should be used as a part of the atmosphere control [1,10,22]. Based on the experimental and empirical observations [5], a threshold soot criterion used in this work was residual methane above 1 vol.% in the gas atmosphere composition.

The potential candidates for the enriching carburizing gases include unsaturated hydrocarbons (C_2H_4, C_3H_6) and saturated hydrocarbons (CH_4, C_3H_8). Unsaturated hydrocarbons are not typically used in the enriching process since they are less stable and tend to form free carbon in the

atmosphere before coming into contact with the steel surface. Ultimately, this leads to sooting and impedes the carburizing process control. Conversely, saturated hydrocarbon gases are more stable at the carburizing temperatures and thermally decompose at the steel surface rather than in the atmosphere. Although the enriching reactions (4) and (5) are slow and do not approach equilibrium [18], the effectiveness of the carburizing process is determined by the carbon potential in the atmosphere and is controlled by the water-gas reaction and the ratio of CO to CO_2 and H_2 to H_2O components:

$$CO + H_2O \leftrightarrow CO_2 + H_2 . \quad (6)$$

To investigate the effect of enriching gas composition and its flow rate on the evolution of the carbon potential and the carburizing atmosphere composition, the following criteria were met:

- Endothermic carrier gas flow was set to the lowest required flow rate that would enable an effective purging time for the given carburizing furnace, i.e., volume of the carburizing chamber
- The flow of the enriching hydrocarbon gas should be high enough to raise the atmosphere carbon potential to a desired level, but without causing sooting (i.e. CH_4 below 1 vol.% in the furnace gas atmosphere)
- The criteria for achieving high carbon potential in the furnace atmosphere must comply with established safety regulations.

Experimental Procedure

The experiments were carried out at 925 °C in a box furnace in the heat treatment laboratory at Caterpillar Inc., USA. Figure 1 shows the schematic of the carburizing furnace setup. The furnace was electrically heated and had a carburizing chamber of 3.058 m^3. To promote an effective gas circulation, the furnace was equiped with a fan mounted in the ceiling of the carburizing chamber. Hydrocarbon enriching gases were supplied to the furnace directly into the fan, which ensured effective atmosphere mixing in the carburizing chamber. Gas atmosphere composition was continuously monitored throughout the cycle using IR CO, CO_2, CH_4 and H_2 analyzers, and an oxygen probe. Carbon potential was calculated from the atmosphere gas composition and the carburizing temperature [23].

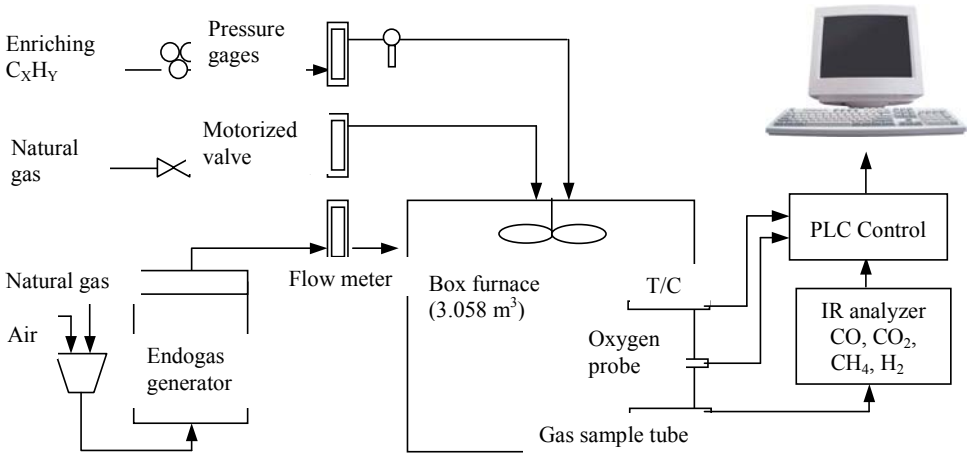

Figure 1. The schematic of the carburizing furnace setup.

For a representative surface area, the load of gears (36.3 kg total) shown in Figure 2, was repeatedly recarburized and shot blasted between each cycle. It was assumed that carburizing the same load does not influence the ability of enriching gases to raise the atmosphere carbon potential from its endogas level. To validate this assumption the initial green load was carburized and the gas analysis was recorded. Then using the same cycle the gears were recarburized several times. No differences in the carburizing atmosphere composition were observed, confirming the initial assumption.

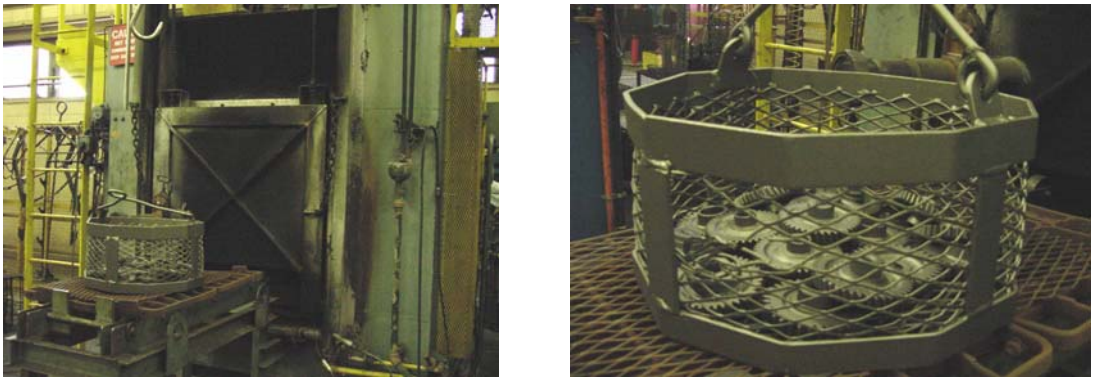

Figure 2. Workload and batch furnace used for the initial carburizing experiments.

For uniform atmosphere composition, the gas flow rate must be low to increase residence time of the gases in the furnace. Lowering flow rate, however, may cause long purging times, and result in slow response in the carbon potential evolution and an increase the total cycle time. To accurately investigate the effect of the enriching gas flow rate and the type of enriching

hydrocarbon gas, the experimental procedure consisted of two stages. Initially, the endothermic carrier gas was allowed to stabilize in the furnace for 1 hour. After this, the enriching hydrocarbon gas was introduced into the furnace at various fixed rates, shown in Table 1. While the atmosphere response to different gas flow rates will differ depending on the volume and capacity of the carburizing chamber, relative volume fraction (or vol.%) of the enriching gas flow to the total gas flow was used throughout this paper.

Table 1. Relative rates of endogas and enriching gas flow during carburizing

Endogas flow rate	*CxHy* flow rate	Enriching *CxHy* vol.% total gas flow	Mean residence time t_m=Volume(furnace)/flow
9.91 m^3/h (350 ft^3/h)	0.14 m^3/h (5 ft^3/h)	1.43%	0.304 h
9.91 m^3/h (350 ft^3/h)	0.28 m^3/h (10 ft^3/h)	2.86%	0.3 h
9.91 m^3/h (350 ft^3/h)	0.42 m^3/h (15 ft^3/h)	4.29%	0.296 h
9.91 m^3/h (350 ft^3/h)	0.57 m^3/h (20 ft^3/h).	5.71%	0.291 h

It was assumed that the furnace atmosphere was homogeneous, i.e. in-flowing gas mixed completely and instantly with the gas in the carburizing chamber [12]. The flow of enriching gas is inversely proportional to the mean residence time of the gases in the atmosphere. As such, it will affect the kinetics of the carburizing enriching reactions and the time for the carburizing atmosphere to stabilize. To ensure reproducible results, two experiments were performed for each set of the experimental conditions. After every experiment the workload was examined for soot formation.

Thermodynamic Calculations

Endothermic Carrier Gas

Although gas carburizing is a non-equilibrium process, reactions (3) and (6) approach equilibrium fast enough to allow thermodynamic calculations of the stabilized atmosphere composition. Mixing air and natural gas (assumed 100% CH_4 for computational convenience) in a fixed ratio (K*) at a constant temperature produces an atmosphere consisting of 7 gaseous species: CO, CO_2, H_2, H_2O, CH_4, O_2 and base N_2. Since gas carburizing is performed at atmospheric pressure, summation of the partial pressures of all gas species in the atmosphere is 1.

Consequently, if the partial pressures of 6 gas components are known, the partial pressure of the 7th component can be determined. The following expressions were used to relate the unknown partial pressures of the atmosphere gas constituents:

- ratio of *C/H* atoms fixed by the stoichiometry of the natural gas:

$$\frac{n_C}{n_H}=\frac{1}{4},\qquad \frac{n_{CH_4}+n_{CO}+n_{CO_2}}{2n_{H_2}+2n_{H_2O}+4n_{CH_4}}=\frac{1}{4}.$$

Assuming $\frac{n_i}{\sum n_i}=\frac{P_i}{\sum P_i}=\frac{i}{100}\%$, the following can be derived:

$$2P_{CO}+2P_{CO_2}=P_{H_2}+P_{H_2O}, \tag{7}$$

where n_i is the number of moles and P_i is the partial pressure of *i*-th gas constituent in the furnace gas atmosphere.

- ratio of *O/N* atoms in air:

$$\frac{n_O}{n_N}=\frac{21}{79},\qquad \frac{n_{H_2O}+2n_{O_2}+n_{CO}+2n_{CO_2}}{2n_{N_2}}=\frac{21}{79},$$

$$P_{N_2}=1.88\cdot P_{CO}+3.76\cdot P_{CO_2}+1.88\cdot P_{H_2O}+3.76\cdot P_{O_2} \tag{8}$$

- ratio of *C/O* atoms from the air-to-fuel gas ratio:

$$\frac{n_O(air)}{n_C(CH_4)}=0.42\cdot K^*,\qquad \frac{n_{CO}+2n_{CO_2}+n_{H_2O}+2n_{O_2}}{n_{CH_4}+n_{CO}+n_{CO_2}}=0.42\cdot K^*,$$

$$P_{CH_4}=\frac{1-0.42\cdot K^*}{0.42\cdot K^*}P_{CO}+\frac{2-0.42\cdot K^*}{0.42\cdot K^*}P_{CO_2}+\frac{P_{H_2O}}{0.42\cdot K^*}+\frac{P_{O_2}}{0.21\cdot K^*} \tag{9}$$

- total pressure in the furnace:

$$P_{CO}+P_{CO_2}+P_{H_2}+P_{H_2O}+P_{CH_4}+P_{O_2}+P_{N_2}=1 \tag{10}$$

- $H_2O \rightarrow H_2+\frac{1}{2}O_2,\quad \Delta G=247{,}500-55.85\cdot T$ [24]

$$P_{H_2O}=P_{H_2}\cdot\sqrt{P_{O_2}}\cdot\exp\left(-\frac{29{,}767.63}{T}+6.717\right) \tag{11}$$

Here and throughout the whole paper the expressions of the Gibbs free energy for all chemical reactions are given in [Joule].

- $CO + \frac{1}{2}O_2 \rightarrow CO_2, \quad \Delta G = -282,400 + 86.81 \cdot T$ [24]

$$P_{CO_2} \cdot P_{H_2} = P_{CO} \cdot P_{H_2O} \cdot \exp\left(\frac{33,965.17}{T} - 10.44\right) \tag{12}$$

- $CH_4 + CO_2 \leftrightarrow 2CO + 2H_2, \quad \Delta G = 261,740 - 285.16 \cdot T$ [24]

$$P_{CH_4} = \frac{P_{CO}^2 \cdot P_{H_2}^2}{P_{CO_2}} \cdot \exp\left(\frac{31,480.3}{T} - 34.297\right) \tag{13}$$

Further mathematical simplifications reduce the above 7 equations to a system of 4 equations with 4 unknowns, which were solved simultaneously using a non-linear least square optimization routine in Matlab [25]. Table 2 shows the results of the thermodynamic calculations and the experimental data for the endothermic carrier gas produced from air and natural gas mixed in a 2.5 ratio. The calculated data for the major carburizing components (*CO, H_2*) appear to be in very good agreement with the experimental data.

Table 2. Endothermic gas composition at 925 °C (vol.%).

	CO	*CO_2*	*H_2*	*H_2O*	*CH_4*	*N_2*	*a (C)*
Thermodynamic calculations	19.76	0.31	39.37	0.77	0.064	39.76	0.27
Experimental data	19.89	0.38	40.78	0.98*	0.083	37.89**	0.30

* *H_2O* concentration was not measured but calculated from the equilibrium gas reactions

** *N_2* was calculated as the balance between the total pressure in the furnace and the sum of all gas constituents

Carburizing Atmosphere after Enriching

Similar thermodynamic calculations were performed to predict the atmosphere composition after the enriching stage. Since thermodynamic calculations do not depend on the sequence of the chemical reactions, the total amount of *CH_4* [in the case of natural gas enrichment] reacting with air will change with the flow of the enriching hydrocarbon gas. As such, the ratios of *C/H* and *C/O* atoms in the atmosphere should be recalculated correspondingly. If *C_3H_8* is used as the enriching gas, the ratios of *C/H* and *C/O* atoms in the carburizing atmosphere can be recalculated

based on the mixing ratio of natural gas (used for the endothermic carrier gas generation) and the flow of enriching C_3H_8 gas:

$$\frac{n_C}{n_H} = \frac{n_{CH_4} + n_{CO} + n_{CO_2} + 3n_{C_3H_8}}{2n_{H_2} + 2n_{H_2O} + 4n_{CH_4} + 8n_{C_3H_8}} = \frac{X_{CH_4} + 3X_{C_3H_8}}{4X_{CH_4} + 8X_{C_3H_8}} \tag{14}$$

and

$$\frac{n_C}{n_O} = \frac{n_{CH_4} + n_{CO} + n_{CO_2} + 3n_{C_3H_8}}{n_{CO} + 2n_{CO_2} + n_{H_2O} + 2n_{O_2}} = \frac{X_{CH_4} + 3X_{C_3H_8}}{0.42 \cdot X_{air}}, \tag{15}$$

where n_i is the number of moles of i-th gas constituent in the atmosphere, and X_i is the mole fraction of the corresponding gases. To express the partial pressure of C_3H_8 in terms of the other gas components, two additional chemical reactions were introduced:

$$C_3H_8 \leftrightarrow C + 2CH_4, \quad \Delta G = -49,544 - 103.087 \cdot T \quad [26]$$

and

$$2CO \leftrightarrow C + CO_2, \quad \Delta G = -170,700 + 174.46 \cdot T \quad [26]$$

yielding

$$P_{C_3H_8} = \frac{P_{CO}^2 \cdot P_{CH_4}^2}{P_{CO_2}} \cdot \exp\left(\frac{14,571.82}{T} - 33.379\right). \tag{16}$$

As in the calculations with natural gas enriching, a system of 8 equations with 8 unknowns (partial pressure of the atmosphere gas constituents) was reduced to a system of 4 equations, and was solved simultaneously using a non-linear least square optimization routine in Matlab [25].

Table 3 compares the thermodynamic calculations with the experimental data for the carburizing atmospheres with various flow rates of enriching natural gas and propane at 925 °C.

Table 3. Carburizing atmosphere composition at 925 °C: comparison of the predicted and experimental (in brackets) data.

Gas species	Enriching gas (CH_4), vol.% total gas flow			Enriching gas (C_3H_8), vol.% total gas flow			
	2.78%	4.11%	5.41%	1.41%	2.78%	4.11%	5.41%
CO	20.23 (20.33)	20.06 (20.12)	19.89 (19.84)	20.24 (20.35)	19.44 (20)	18.74 (18.9)	18.03 (18.7)
CO_2	0.0212 (0.095)	0.0109 (0.087)	0.01 (0.072)	0.013 (0.078)	0.007 (0.058)	0.004 (0.05)	0.003 (0.049)
H_2	40.4 (43.06)	40.1 (43.4)	39.8 (44.79)	40.3 (43.32)	41.8 (44.7)	42.9 (47.1)	44.1 (48)
CH_4	1.033 (0.53)	1.209 (0.59)	1.942 (0.87)	0.6 (0.57)	1.21 (0.78)	1.78 (1.05)	2.27 (1.3)

The prediction for the main carburizing component, *CO*, is very accurate for all carburizing atmospheres. The difference between the experimental and predicted H_2 concentration is within 3-5 vol.%, which may originate from the non-equilibrium nature of the industrial carburizing process and, possibly, from the assumption of pure CH_4 as the enriching natural gas. Experimental CO_2 values are consistently higher than the predicted theoretical values, which indicate that the atmosphere chemical reactions did not reach equilibrium [1,5,27].

Results and Discussion

Effect of Flow Rate of the Enriching Gases

Natural gas enrichment

Figure 3 shows the effect of flow rate of the enriching natural gas on the carburizing atmosphere composition and the corresponding carbon potential (C_P). As seen from the concentration profiles, greater flow rate of the enriching natural gas increases carbon availability in the atmosphere and results in a higher C_P. This occurs due to a higher *C/H* ratio and greater kinetics of CO_2 and H_2O reduction from their endogas concentrations. A shorter mean residence time, however, shifted the atmosphere composition further from equilibrium and resulted in a greater amount of residual methane in the furnace. A slight decrease in *CO* concentration has also

been observed, which shifted equilibrium of the heterogeneous water gas reaction (Equation 6) to the right and resulted in H_2 buildup.

Analysis of the atmosphere gas composition suggests that the kinetics of methane decomposition is slower than the rate of carbon supply from the enriching hydrocarbon gas to the furnace. If the threshold soot criterion is taken as 1 vol.% of residual CH_4 in the furnace atmosphere, the flow of natural gas in excess of 4.2 vol.% of the total gas flow should be avoided.

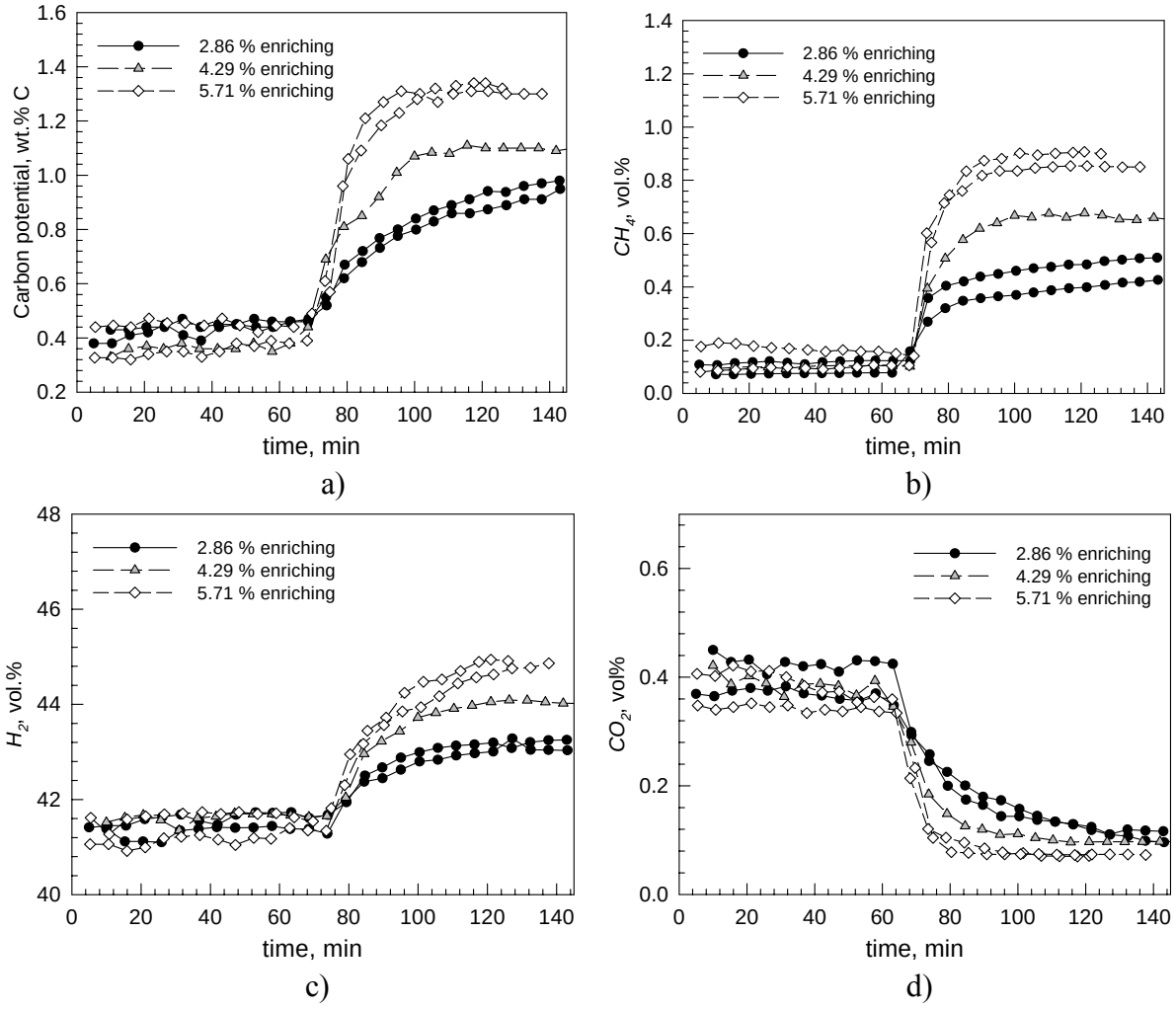

Figure 3. Carbon potential and gas composition in the atmosphere with endogas (first 1 hour) and natural gas enrichment (after 1 hour).

The data in Table 4 show the changes in the atmosphere composition before and after the enriching stage. Positive values indicate an increase in the composition of the respective gas, while negative values indicate a reduction of these species after enriching.

Table 4. Changes in the atmosphere composition due to natural gas enriching.

CH_4 flow rate	CH_4 vol.%	Endogas, vol.%	Δ (time), min	Δ (C_P) wt.%	Δ (CO), vol.%	Δ (CO_2), vol.%	Δ (CH_4), vol%	Δ (H_2), vol.%
10 ft^3/h	2.86	97.22	110	0.73	0.141	-0.328	0.464	1.591
15 ft^3/h	4.29	95.89	67	0.76	-0.228	-0.188	0.53	1.916
20 ft^3/h	5.71	94.59	37	0.87	-0.483	-0.242	0.755	3.325

As follows from Table 4, increasing the flow rate enhanced the kinetics of the atmosphere enrichment and the rate of C_P evolution. Specifically, increasing the enriching gas flow from 2.86 to 5.71 vol.% of the total gas flow reduced the time to achieve a stabilized atmosphere composition from 110 to 37 min. This observation can be explained by a faster rate of CO_2 and H_2O conversion with a greater enriching gas flow. A shorter residence time of the gases in such atmospheres causes further deviation from thermodynamic equilibrium, and results in residual CH_4 and H_2 build-up. Therefore, carburizing atmosphere should be produced such that it would offer a compromise between the rate of C_P evolution and the amount of residual CH_4.

Propane enrichment

Evolution of the atmosphere gas composition with propane enrichment is shown in Figure 4. Higher flow rates of the enriching gas enhance the rate of C_P evolution and stabilize it at higher C_P level. Rich carbon atmospheres (high C/H ratio), however, inherently contain a greater amount of residual CH_4 in the furnace atmosphere. Therefore, using atmospheres with a high flow of enriching propane would increase the atmosphere tendency to form soot during longer carburizing cycles [10].

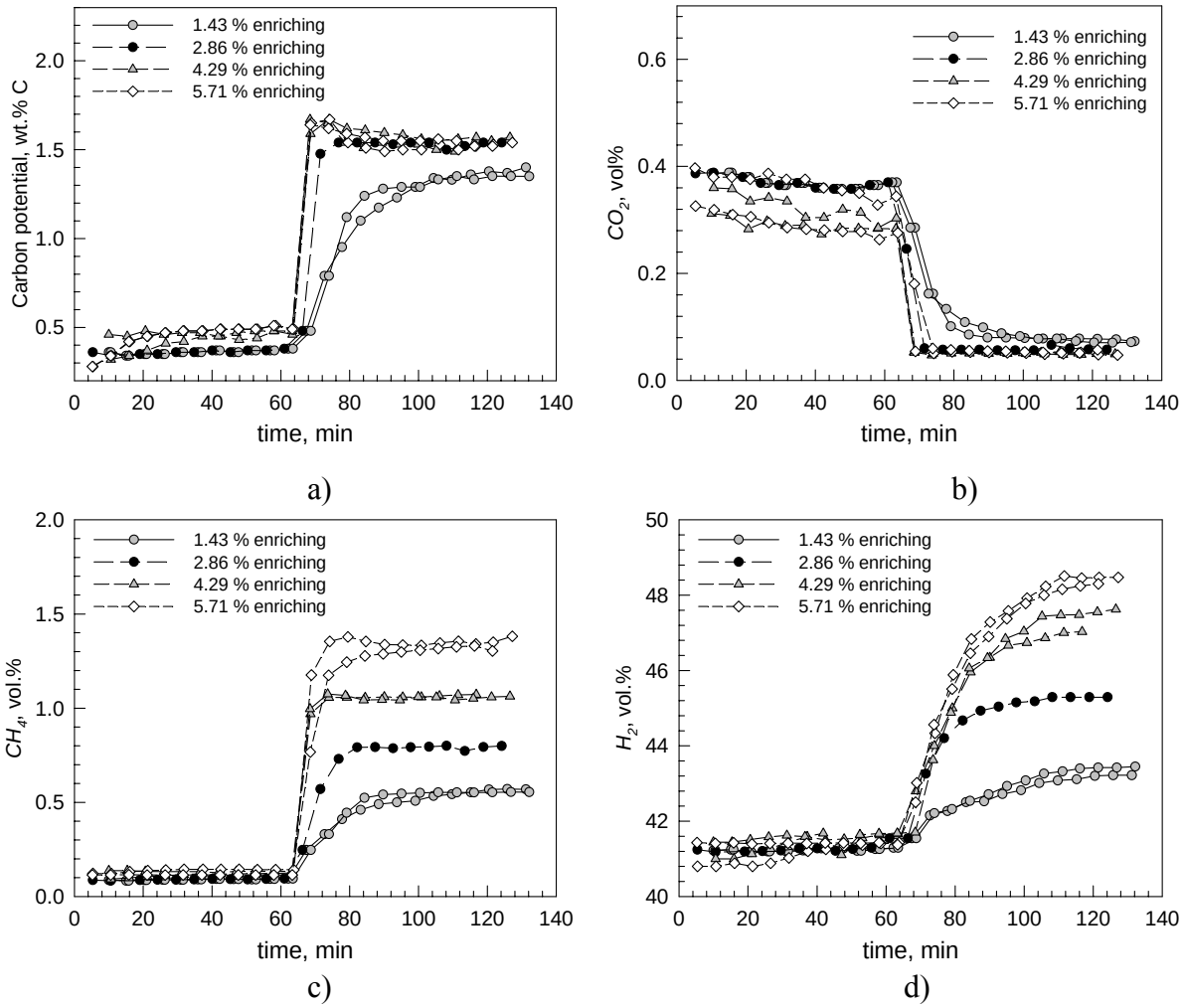

Figure 4. Carbon potential and gas atmosphere composition in the atmosphere with endogas (first 1 hour) and propane enrichment (after 1 hour).

Compared to the atmospheres produced with natural gas enrichment, a distinct inflection point in C_P evolution was observed during the initial time of C_3H_8 enriching. This phenomenon occurred due to fast CO_2 conversion and H_2 dilution. In the beginning of the enriching stage, C_3H_8 rapidly reduces CO_2 and H_2O to regenerate CO and H_2. As time proceeds, the atmosphere soon becomes depleted of CO_2 and decreases the driving force for the enriching reactions. The resulting changes in the atmosphere composition (relative ratio of CO/CO_2) and H_2 dilution cause a slight drop in the calculated C_P before it stabilizes at the achieved level.

Table 5 shows the changes in the atmosphere gas composition during propane enrichment. Positive values indicate an increase in the composition of the respective gas, while negative values indicate reduction in the gas component after enriching. Increasing the enriching gas flow from 1.43 to 5.71 vol.% of the total gas flow shortened the time to stabilize the atmosphere from

37 to 12 min. Although no soot was observed in any of the experimental runs, carburizing with enriching propane greater than ~4 vol.% of total gas flow produce large amount of residual CH_4, and may result in sooting during longer carburizing time [10]

Table 5. Changes in the atmosphere composition due to propane enriching.

C_XH_Y flow rate	C_XH_Y vol.%	Endogas, vol.%	Δ (time), Min	Δ (C_P) wt.%	Δ (CO), vol.%	Δ (CO_2), vol.%	Δ (CH_4), vol%	Δ (H_2), vol.%
5 ft^3/h	1.43	98.59	37	1.05	0.170	-0.302	0.480	2.120
10 ft^3/h	2.86	97.22	26	1.16	-0.280	-0.376	0.658	3.450
15 ft^3/h	4.29	95.89	21	1.05	-1.263	-0.225	0.937	5.464
20 ft^3/h	5.71	94.59	12	1.03	-1.259	-0.234	1.186	6.719

Effect of C_XH_Y Enriching Gas

Figure 5 compares carbon potential evolution and the atmosphere gas composition during natural gas and propane enrichment. The data clearly indicate that enriching the endothermic carrier gas with propane significantly enhances the rate of carbon potential evolution and produces a higher C_P atmosphere compared to conventional natural gas enrichment. The molecules of C_3H_8 inherently contain a higher C/H atoms ratio, which enables a greater number of carbon atoms to be supplied to the furnace even with lower [than natural gas] enriching gas flow. The corresponding increase in the atmosphere carburizing potential, however, results not only from sheer advantage in higher carbon availability per unit volume of C_3H_8 molecule, but also from the thermodynamics of its decomposition.

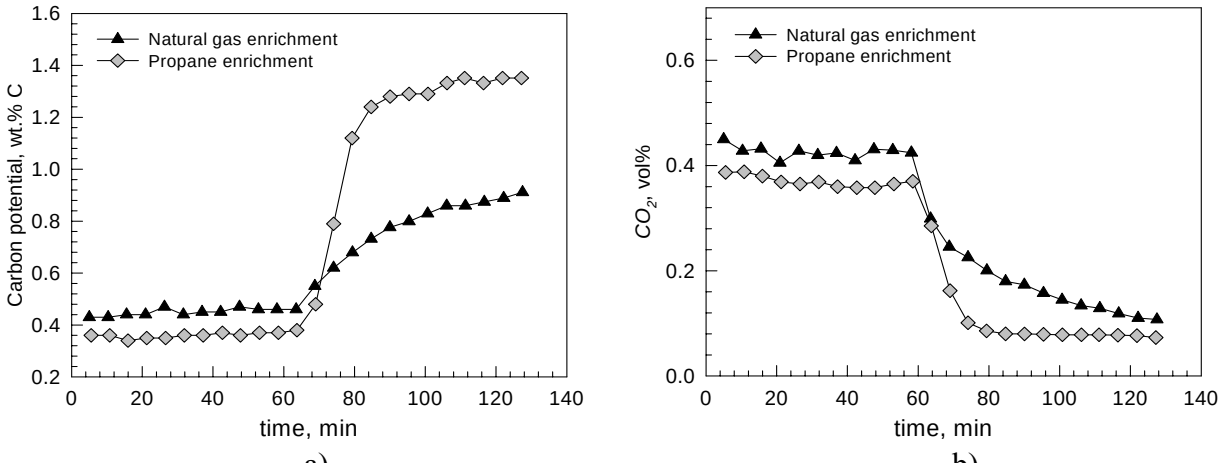

Figure 5. Carbon potential and gas atmosphere composition during natural gas and propane enrichment (both at 2.86 vol.% of total gas flow).

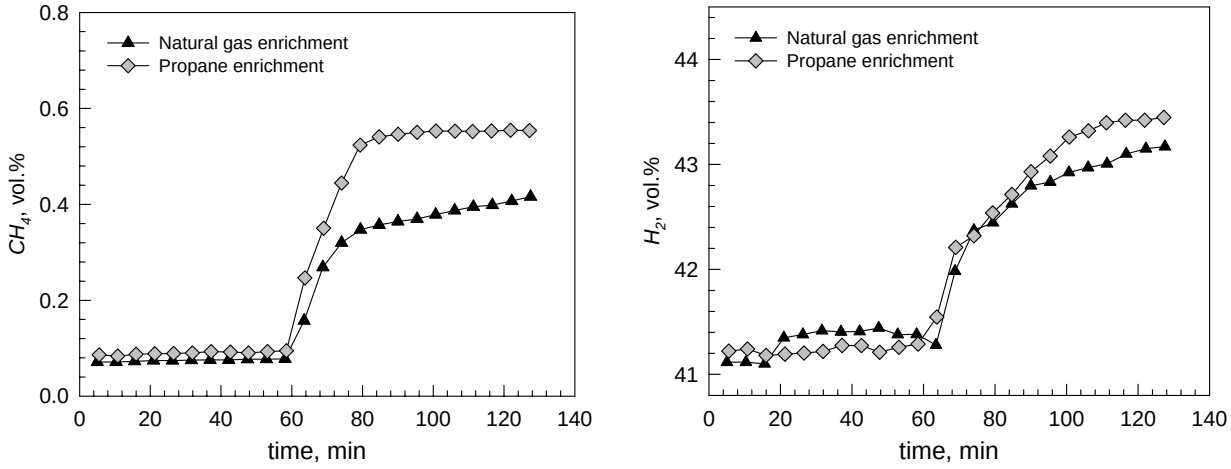

Figure 5 (Cont.). Carbon potential and gas atmosphere composition during natural gas and propane enrichment (both at 2.86 vol.% of total gas flow).

As opposed to the natural gas enrichment, where CH_4 is directly reacting with endothermic carrier gas and reduces H_2O and CO_2 concentrations, carburizing atmospheres enriched with propane decompose through the intermediate step-reaction of dehydrogenation of a C_3H_8 molecule into an elementary C atom and two CH_4 molecules

$$C_3H_8 \rightarrow C + 2CH_4 . \qquad (17)$$

As seen from the chemical reaction (17), one mole of C_3H_8 produces two moles of CH_4. The first product of the decomposition reaction, elementary C, gives a rapid raise to carbon concentration in the atmosphere and thus enhances the rate of C_P evolution. The second product component, CH_4, further participates in the enriching chemical reactions (4-5) and reduces H_2O and CO_2 concentrations in the atmosphere with rate twice as fast than with the equivalent flow of natural gas enrichment.

Caution must be taken when controlling the flow of enriching C_3H_8. While a greater flow of the enriching gas increases carbon availability in the gas atmosphere, the carbon formed by the initial breakdown (reaction 17) has an unfortunate propensity to cause sooting [28]. An increase in the enriching gas flow rate above ~4 vol.% is likely to cause saturation of the carburizing atmosphere with free C contributing to soot formation.

Carburized Atmosphere Optimization

When evaluating the efficiency of the gas carburizing atmospheres, the primary characteristics that should be considered are C_P (relative ratio of CO/CO_2) and the residual methane in the furnace. High carburizing potential in the atmosphere ensures a sufficient driving force for carbon transfer from the atmosphere to the steel surface, while residual methane indicates the tendency of such atmospheres to soot.

Figure 6 compares the carbon potential and the corresponding residual methane level observed in the endothermic carburizing atmospheres with natural gas and propane enrichment. As discussed in the previous sections, for any given flow rate of the enriching hydrocarbon gas – atmospheres enriched with propane provide higher carbon availability and greater kinetics of CO_2 and H_2O conversion, thus promoting a richer carburizing atmosphere. Specifically, atmospheres enriched with 1.43 vol.% propane produced a higher carbon potential than in the atmosphere with 5.71 vol.% natural gas enrichment. Such a carburizing atmosphere also produces a lower level of residual methane, and therefore, it exhibits a lower tendency to soot.

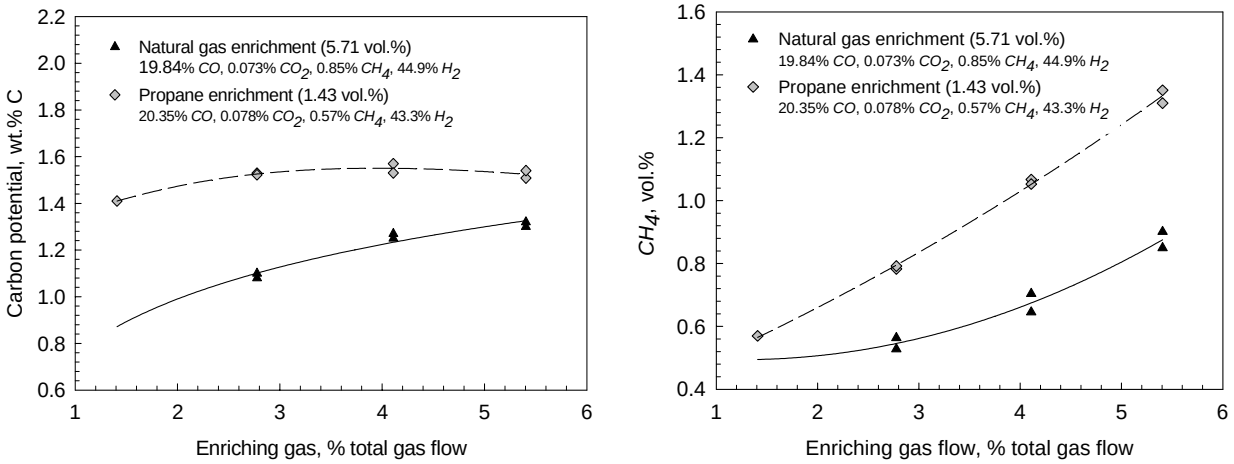

a) b)

Figure 6. The carburizing potential (a) and the residual methane (b) in the atmospheres with natural gas and C_3H_8 enriching of various flow rates.

Overall, given the same transient time to stabilize the atmosphere composition (37 min), enriching the endothermic atmosphere with propane offers an advantage of higher CO and C_P level (refer to Figure 6). In addition to the lower gas consumption, the smaller amount of H_2 in the atmosphere composition indicates better enriching gas utilization. All of the above observations suggest that using a four times smaller amount of propane as enriching gas over the

conventional carburizing practice with natural gas enrichment would produce a comparable effect on the steel carburizing efficiency, as will be discussed in Part II of this series of papers.

Conclusions

This paper presented the results and analysis of both theoretical and experimental investigation of the effect of carburizing atmosphere enriching using two hydrocarbon gases. Thermodynamic models were developed and validated to predict carburizing atmosphere composition. Based on the observed phenomena and the experimental data, the following conclusions have been made:

1. Greater flow rates of enriching gas provide a richer carbon atmosphere. Such atmospheres, however, deviate further from the equilibrium atmosphere composition due to a lower mean residence time. This deviation was primarily observed in CO_2 conversion and residual CH_4. Higher flow rates of enriching gas enhance the rate of carbon potential development and shorten time for a carburizing atmosphere to stabilize.

2. Atmospheres with propane enrichment provide greater carbon availability and enhance the kinetics of the gas enriching reactions. Increasing the enriching gas flow rate above 2.86 % of the total gas flow, however, does not contribute to further carbon potential evolution but results in higher residual methane.

3. Equivalent atmosphere carbon potential can be achieved by using four times lower flow of enriching propane over natural gas enrichment. Such atmospheres also exhibit a lower level of residual methane, and therefore lower the tendency to soot.

4. Findings of this paper (Part I) enhance our understanding of the carburizing atmosphere enriching reactions, compare the performance of the alternative enriching hydrocarbon gas with the baseline carburizing (natural gas enrichment) and serve as a basis for Part II (Gas consumption and cost model optimization for gas carburizing).

Acknowledgements

The support of the Center for Heat Treating Excellence (CHTE) at Worcester Polytechnic Institute and the member companies is gratefully acknowledged. This work was performed at Caterpillar Inc. and its support through facilities and experimental work is greatly appreciated. The authors would also like to thank Advanced Materials Technology (AMT) group for their assistance and valuable discussions.

References

1. J. Slycke and L. Sproge: *J. Heat Treat.*, 1988, vol. 5, n. 2, pp. 97-114.
2. B. Edenhofer: *Heat Treat. Met.*, 1955, vol. 22, n. 3, pp. 55-60.
3. J.H. Kaspersma and R.J. Peartree: US Patent No. 4306918, Air Products and Chemicals, Inc., Allentown, PA, December 1981.
4. L. Lefevre, and D. Domergue: *Heat Treat. Met.,* 2001, vol. 28, n. 3, pp. 59-62.
5. C.A. Stickels, C. M. Mack and M. Brachaczek: *Metall. Trans. B*, 1980, vol. 11B, n.3, pp. 471-79.
6. C.A. Stickels and C. M. Mack: *Metall. Trans. B*, 1980, vol. 11B, n. 3, pp. 481-84.
7. C.A. Stickels, C. M. Mack and J.A. Pieprzak: *Metall. Trans. B*, 1980, vol. 11B, n. 3, pp. 485-91.
8. C.A. Stickels, C. M. Mack and J.A. Pieprzak: *Metall. Trans. B*, 1982, vol. 13B, n. 4, pp. 613-23.
9. M.L. Fenstermaker and M.A. Pellman: US Patent No. 4597807, Air Products and Chemicals, Inc., Allentown, PA, July 1986.
10. T. Naito, K. Ogihara, A. Wakatsuki, T. Nakahiro, H. Inoue and Y. Nakashima: US Patent No. 6106636, Dowa Mining Co., Ltd, Tokyo, Japan, August 2000.
11. D. Garg, J.N. Armor, D.J. Martenak and P.T. Kilhefner: US Patent No. 6287393, Air Products and Chemicals, Inc., Allentown, PA, September 2001.
12. L. Sproge and J. Agren: *J. Heat Treat.*, 1988, vol. 6, n. 1, pp. 9-19.
13. S.S. Sahay, and K. Mitra: *Surf. Eng.*, 2004, vol. 20, n. 5, pp. 379-84.
14. F. Kuhn: *Industrial Heating*,1983, vol. 50, n. 11, pp. 25-30.

15. U.S. Department of Energy Report No. 2044323 Washington, DC, March 2001.
16. V.A. Munts and A.P. Baskatov: *Met. Sci. Heat Treat.*, 1980, vol. 22, n. 5-6, pp. 358-60.
17. J. Agren: *Scripta Metall.*, 1986, vol. 20, n. 11, pp. 1507-510.
18. C.A. Stickels: *Metals Handbook*, 9 th ed., vol. 4, Metals Park, OH, 1981, pp. 312-324.
19. R. Collin, S. Gunnarson and D. Thulin: *J. Iron Steel Inst.*, 1972, vol. 210, n. 10, pp. 785-89.
20. H. Boyer: *Case Hardening of Steel*, American Society for Metals, Metals Park, OH, 1987, pp. 1-12.
21. J. Slycke and L. Sproge, *J. Heat Treat.*, 1988, vol. 5, n. 2, pp. 97-114.
22. T. Naito, K. Ogihara, A. Wakatsuki, T. Nakahiro, H. Inoue, Y. Nakashima: US Patent No. 6051078, Dowa Mining Co., Ltd., Tokyo, Japan, April 2000.
23. M.J. Bannister: *Ind. Heating*, 1984, vol. 51, n. 3, pp. 24-26.
24. D.R. Gaskell: *Introduction to the Thermodynamics of Materials*, 4 th ed., Taylor & Francis, New York - London, 2003, pp. 582-83.
25. MATLAB® Manual, Version 6, The Math Works, Inc., Natick, MA, November 2000.
26. HSC Chemistry® Manual, Version 6.0, Outocumpu, Espoo, Finland, August 2006.
27. U. Wyss, R. Hoffmann and F. Neumann: *J. Heat Treat.*, 1980, vol. 1, n. 3, pp. 14-23.
28. A. Cook: *Heat Treat. Met.*, 1976, vol. 3, n. 1, pp. 15-18.

PAPER # 2: GAS CONSUMPTION AND COST MODEL OPTIMIZATION OF THE GAS CARBURIZING 'BOOST' STAGE IN BATCH FURNACE

(submitted to *Metallurgical Transactions*)

Abstract

This paper focuses on optimizing the enriching gas supply to ensure a fast rate of carbon potential evolution and consequently a fast rate of carbon transfer during the 'boost' stage of carburizing. The optimization is based on understanding the kinetics and thermodynamics of the enriching gas reactions. Three combinations of pure hydrocarbon gases and their mixtures were investigated to produce similar carbon potential atmospheres, while a cost model was developed to quantify the benefits of reducing enriching gas consumption and the total carburizing time. It was observed that using propane, instead of natural gas enrichment increased the kinetics of the enriching gas reactions which shortened the time for the carbon potential to stabilize from 63 min [natural gas] to 25 min [propane]. This atmosphere also revealed lower level of residual methane indicating more efficient enriching gas utilization and slightly lower tendency to soot. While carburizing with propane enrichment reduced the enriching gas consumption by 65 % and shortened the total cycle time by 38 min, the metallurgical and metallographic analysis revealed no significant differences in the carburized case characteristics. Overall, carburizing with propane enriching gas provides a lower-cost alternative to an endothermic atmosphere carburizing with more efficient energy utilization.

Introduction

Paper 1 of this thesis reported the results of theoretical and experimental investigations on the carburizing potential of endothermic atmospheres enriched with propane and natural gas [1]. The goal of the current analysis is to understand the effect of the type of enriching hydrocarbon gases and their flow rates on the carbon potential evolution and the stabilized atmosphere composition. While the initial investigations used the same fixed volumetric flow rates for both hydrocarbon enriching gases, this paper optimizes various combinations of pure hydrocarbon enriching gases and their mixtures to produce similar carbon potential atmospheres for 'boost' stage carburizing. The optimization approach is based on minimizing the total operating cost including cycle time

and gas consumption, and producing a desired carbon potential in the atmosphere with a low tendency to soot.

The carburizing atmosphere determines the rate of carbon transfer from the atmosphere to the steel surface, hence, it has the major effect on the 'boost' stage carburizing. During the 'diffuse' stage, the rate of carbon transfer becomes limited by the carbon diffusion in austenite [2], which is primarily determined by the carburizing temperature and alloy composition of the steel [3]. Therefore, optimization of the carburizing atmosphere in this work focuses on the enriching gas supply to ensure faster rate of carbon transfer and faster carbon potential evolution during the 'boost' stage carburizing. The stabilized atmosphere composition after propane and natural gas enrichment and their flow rates have been analyzed based on the experimental data from Paper 1 of this series of papers [1]. A cost model was developed to identify combinations of the experimental settings yielding an atmosphere with maximum efficiency and minimum overall heat treating cost. Three selected experiments were performed to validate the findings. Metallurgical analysis of the carburized parts was combined with the cost analysis of enriching gas consumption and furnace operating time to ensure efficiency of the process.

The driving force for carbon transfer in gas carburizing is proportional to the difference between the carbon potential in the atmosphere (C_P) and the steel surface concentration (C_S). Hence, an optimal carburizing atmosphere was defined as the atmosphere that promotes faster carburizing rate while maintaining a high carburizing potential in the furnace. The target enriching gas should rapidly raise the carburizing potential without sooting. Ultimately, accelerating the rate of the carburizing atmosphere evolution to achieve a high stabilized carbon potential during the 'boost' stage carburizing would result in a shorter total cycle time to produce the desired case depth, and therefore, in greater furnace capacity.

Stabilized Atmosphere Composition

Analysis of the stabilized atmosphere composition is based on the experimental data from Paper 1 [1]. The box furnace [with carburizing chamber of 1.37 m width × 1.47 m height × 1.52 m length] was operated at 925 °C and the atmosphere composition was monitored by an IR analyzer and oxygen-probe. For a representative surface area, the same load of gears (36.3 kg) was carburized and shot blasted between each cycle. It was assumed and validated that for the given set of experimental conditions, carburizing the same load did not have a significant affect

on the ability of enriching gases to raise the carbon potential from its endogas level. The enriching hydrocarbon gases included natural gas (assumed 100% CH_4 for computational convenience) and propane (C_3H_8). Endothermic carrier gas was supplied to the furnace at a fixed flow rate of 9.91 m^3/hr, while the flow of the enriching gases varied from 0.14 to 0.57 m^3/hr, i.e., 1.43 % to 5.71 % of the total gas flow.

For carburizing at a fixed temperature, the primary atmosphere control parameters include the carbon potential (C_P) and the residual methane (CH_4). The carbon potential in the furnace determines the driving force for carbon transfer from the gas atmosphere to the steel surface, while the residual methane may serve as indication of the atmosphere tendency to soot [4,5]. Figure 1 shows stabilized C_P and residual CH_4 for the carburizing atmospheres with various combinations of the enriching gas flow and the type of C_XH_Y gas. If the threshold soot criteria is considered as 1 vol.% of residual CH_4 in the furnace atmosphere [6], the 'boost' stage atmosphere optimization should be based on achieving maximized C_P with minimum or just below 1 vol.% CH_4.

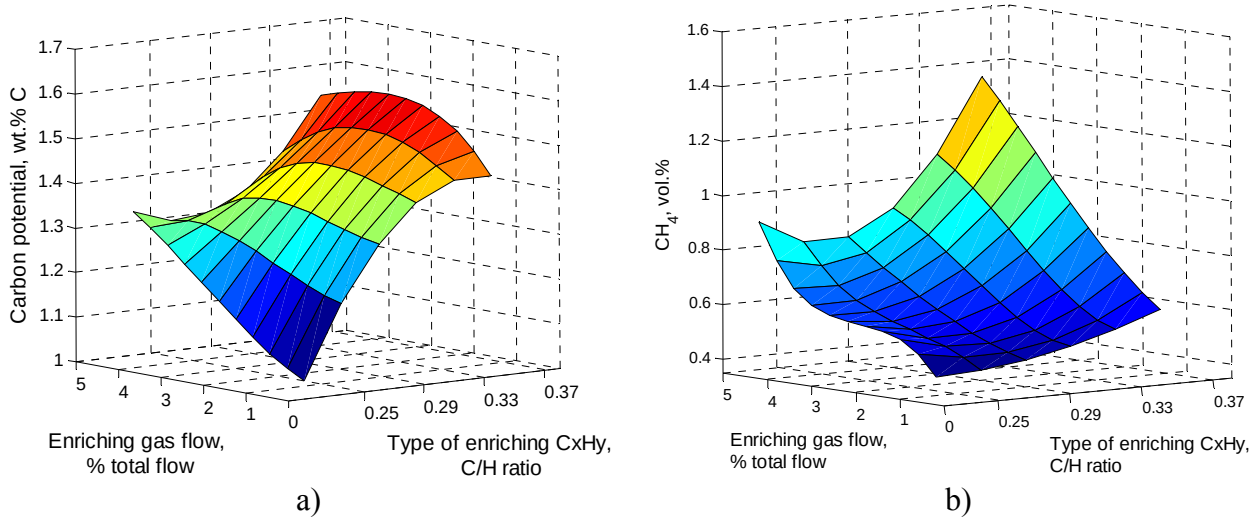

Figure 1. Stabilized carbon potential and residual CH_4 in the carburizing atmospheres produced by blending endothermic carrier gas with a various enriching C_XH_Y gases and flow rates at 925 ºC.

As follows from Figure 1, similar carbon potential atmospheres can be produced by several combinations of the enriching C_XH_Y gases and the corresponding flow rates. Therefore, such carburizing atmospheres can be optimized based on the flow rate (gas consumption) of various C_XH_Y gases (gas cost) and the carburizing time (furnace operating cost).

Heat Treating Operating Cost

A simple cost model has been developed to analyze the efficiency of various carburizing atmospheres shown in Figure 1. The model is based on the following mathematical expressions which consider both the enriching gas consumption and the furnace operating cost:

$$Cost_{cycle} = Cost_{\substack{gas \\ consumption}} + Cost_{\substack{furnace \\ operation}}, \tag{1}$$

$$Cost_{\substack{gas \\ consumption}} = \sum_{i}^{n} \left(\frac{ft^3}{hr} \cdot \frac{\$}{ft^3} \right)_i \cdot \left(\Delta t + t_{Carb} \right), \tag{2}$$

$$Cost_{\substack{furnace \\ operation}} = \left(\frac{\$\ furnace}{hr} + \frac{\$\ operator}{hr} \right), \tag{3}$$

where n is the number of gases used to produce carburizing atmosphere, Δt is the time to stabilize the carbon potential upon parts loading (enriching transient time), and t_{Carb} is the carburizing cycle time at constant carbon potential and temperature.

The estimated prices for the hydrocarbon gases and furnace operating time were obtained from the public resources of the Department of Energy [7] and from the industrial heat treating partners of the Center for Heat Treating Excellence (CHTE). Although the actual cost numbers are furnace-specific and will differ from one manufacturer to another, the total cycle cost can easily be adjusted to a particular manufacturer and recalculated according to Equations (1-3). The calculated cost for a 2 hrs 'boost' carburizing cycle was normalized to the maximum cost value and presented in Figure 2.

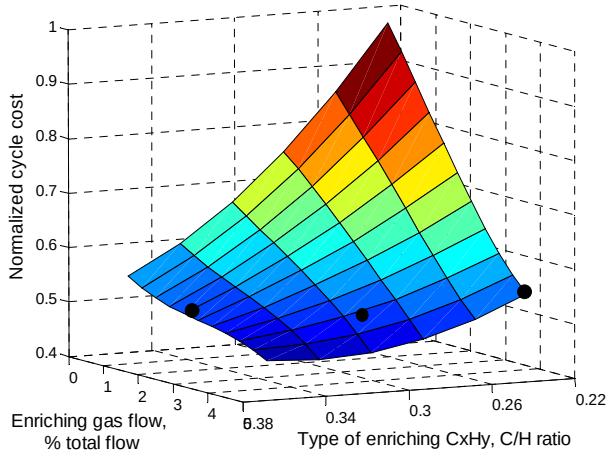

Figure 2. Normalized carburizing process cost: endogas with C_XH_Y enriching, 2 hrs at 925 °C (the dark dots indicate three sets of the experimental factors for further investigations)

As follows from Figure 2, the highest heat treating operating cost corresponds to the cycles with carburizing atmospheres produced by natural gas enrichment. Although the cost of natural gas is significantly lower than the cost of propane [7], such atmospheres require a greater flow of the enriching gas to reach a high carbon potential in the furnace. More importantly, they require longer time for the carbon potential to stabilize. On the other hand, despite the higher cost of propane, carburizing with this enriching gas can be justified economically by taking into account the faster rate of CO_2 and H_2O conversion [1] and, therefore shorter time for such carburizing atmosphere to reach a stabilized high carbon potential.

Based on the observed data, further optimization of the 'boost' stage carburizing was performed by considering the kinetics (time to stabilize the atmosphere) and thermodynamics (stabilized C_P and CH_4) of the enriching chemical reactions with various C_XH_Y enrichment. Three sets of the experiments were performed (marked on Figure 2), which included carburizing in endothermic atmospheres enriched with natural gas (baseline process), propane, and a mixture (1:1) of these two gases. It was hypothesized that equivalent carbon potentials could be achieved with various C_XH_Y gases by compensating for their carburizing power with the flow of the enriching gas. If so, comparable case depth characteristics should be expected while consuming a lower amount of higher-order hydrocarbon enriching gases and shortening the carburizing cycle time.

Experimental Procedure

The experimental setup is shown in Figure 3. Three cylindrical test coupons (2.48 cm diameter and 5.1 cm height) were carburized for metallographic examination and a carbon step bar (5.08 cm diameters and 15.24 cm height) was carburized for carbon profile measurements. The test coupons and carbon step bars were made of 41xx series chromium-molybdenum steel with 0.2 wt.% base carbon concentration. Twelve sheets of AISI 1018 steel (1.62 mm thick) were also added to the carburized workload to provide a representative steel surface area (5.2 m^2). Providing additional mass and surface area was intended to mimic a representative workload of carburized steel components for a more accurate heat-up rate and gas consumption during the process.

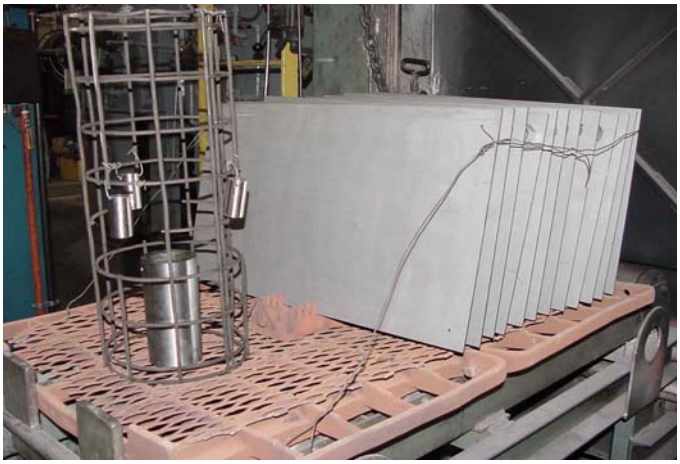

Figure 3. Experimental setup: test coupons, carbon step bar and additional surface area.

The carburizing atmospheres in the box furnace were produced by blending endothermic gas (9.91 m^3/hr) with: 1) natural gas (0.65 m^3/hr), 2) propane (0.23 m^3/hr), and 3) a mixture of natural gas (0.2 m^3/hr) and propane (0.2 m^3/hr). All parts were carburized in the box furnace at 925 °C. After 2 hrs carburizing, the basket with the test coupons and carbon step bar was taken out of the furnace and quenched in highly agitated oil at 39 °C in an open quench tank for 3 min. The carbon step bars were tempered at 600 °C and analyzed for carbon concentration profile using a standard step bar procedure [8]. The test coupons were subjected to a typical carburized steel tempering operation (1 hr at 177 °C) prior to microstructural evaluation.

The carburizing performance of various atmospheres was evaluated in terms of the gas atmosphere analysis (gas composition and carbon potential evolution) and test coupons characterization (weight gain, carbon concentration profiles and microstructural analysis). Laboratory scales sensitive to 1 μg were used for weight gain measurements. Microhardness measurements were collected with a Knoop indenter (500 gf) on an automated LECO Microhardness tester. Surface carbon concentration was measured by spectral analysis on an LECO-OES (Optical Emission Spectroscopy) with ± 0.01 measurement error. Carbon concentration profiles were obtained using a standard carbon step bar procedure [8].

Results and Analysis

Carbon Potential Evolution

The recorded temperature recovery after the parts loading and carbon potential evolution during the carburizing cycles are shown in Figure 4-a. Although the flow rate of enriching propane (C_3H_8) was only about one third of the flow of natural gas, the carburizing atmosphere reached the same carbon potential of 1.26 wt.% C. It was observed that using propane as the enriching gas provided a more rapid kinetics of the carburizing reactions, which shortened the time (Δt) for the carbon potential to stabilize from 63 min [natural gas] to 25 min [propane]. Mixing propane and natural gas in equal proportions ($CH_4 : C_3H_8 = 1:1$) revealed an intermediate rate of carbon potential evolution during the enriching stage (34 min) compared to using either one of the pure component gases.

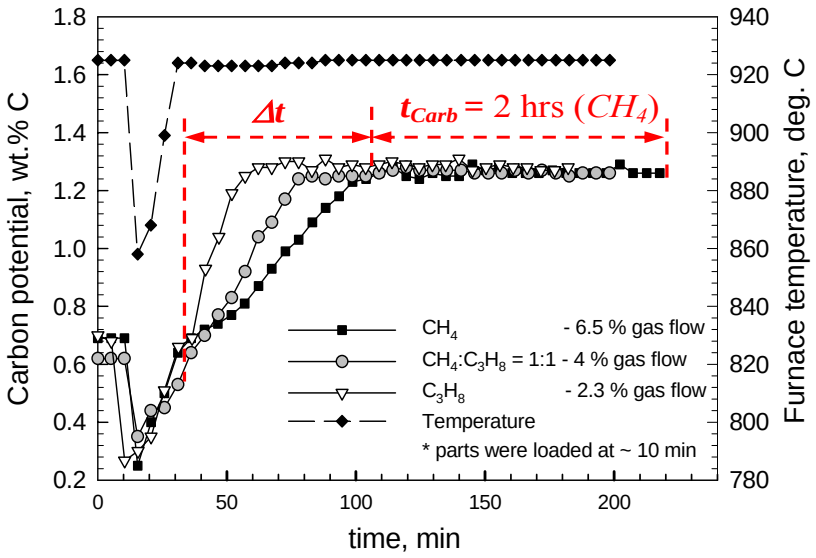

a)

Figure 4. Gas atmosphere characteristics: a) temperature recovery and carbon potential evolution, b) residual methane for the carburizing cycles with various levels of enrichment.

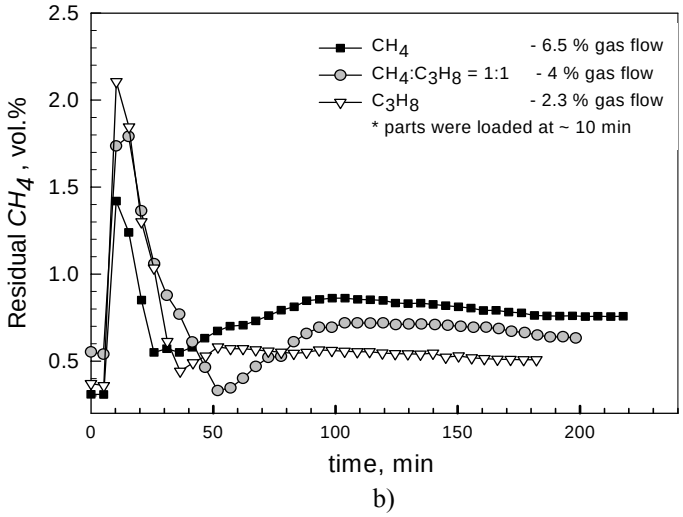

b)

Figure 4 (Cont.). Gas atmosphere characteristics: a) temperature recovery and carbon potential evolution, b) residual methane for the carburizing cycles with various levels of enrichment.

Figure 4-b shows the residual methane in the furnace atmosphere for all three cycles. The amount of residual methane indicates the completion of the gas carburizing chemical reactions and depends on the flow and the type of hydrocarbon enriching gases. If the level of residual methane in the furnace atmosphere continuously increases with carburizing time beyond the point of carbon potential stabilizing, the effluent hydrocarbon gas is being exhausted and has little contribution to further CO_2 and H_2O conversion. The amount of residual methane in all carburizing cycles was observed to be below 1 vol.% and no sooting was observed after 2 hrs carburizing. A sharp increase in the residual methane was observed for up to 40 min, which corresponded to the parts loading and temperature recovery, and therefore, should not be considered in the analysis. During the 2 hrs carburizing cycle at the constant temperature and carbon potential, the atmosphere with natural gas enrichment exhibited the highest level of residual methane. The lowest level of residual methane was observed in the atmosphere with propane enrichment, which suggests a more efficient enriching gas utilization and slightly lower tendency of the atmosphere to soot.

From the experimental data and the theoretical calculations in this series of papers, it was observed that the atmospheres enriched with propane provide a richer carbon atmosphere compared to the baseline carburizing atmospheres with natural gas enrichment. The molecules of C_3H_8 inherently contain a higher *C/H* atoms ratio, which enables a greater flux of carbon atoms supplied to the furnace even with a lower [than natural gas] enriching gas flow. The

corresponding increase in the carburizing potential, however, results not only from the advantage in higher carbon availability per unit volume of C_3H_8, but also from the thermodynamics of the gas molecule decomposition. As opposed to the natural gas enrichment, where CH_4 is directly reacting with the endothermic gas composition and reduces H_2O and CO_2 concentrations, carburizing atmospheres enriched with propane (C_3H_8) decompose through an intermediate step-reaction of elementary C atom and lower-order C_XH_Y gas (methane) before reacting in the enriching chemical reactions (5-6):

$$C_3H_8 \leftrightarrow C + 2CH_4 \tag{4}$$

$$CH_4 + CO_2 \leftrightarrow 2CO + 2H_2, \tag{5}$$

$$CH_4 + H_2O \leftrightarrow CO + 3H_2. \tag{6}$$

As follows from the chemical reaction (4) one mole of C_3H_8 produces 2 moles of CH_4. The first product of the decomposition reaction, elementary C atom, rapidly raises the carbon concentration in the atmosphere and thus enhances the rate of C_P evolution. The second product component, CH_4, further participates in the enriching chemical reactions (5-6) and reduces H_2O and CO_2 concentrations in the atmosphere with twice the rate as the equivalent flow of natural gas enrichment.

Carburized Case Characteristics

Microstructural analysis of the carburized test coupons revealed a mixture of martensite and retained austenite near the surface (Figure 5-a) and a mixture of martensite and bainite in the core (Figure 5-b). Intergranular oxidation was observed in all samples within 3 μm from the steel surface. While martensite is the desired phase in a carburized case, a large amount of retained austenite (>55 %) resulted from direct quenching of the parts from 925 °C. This was pursued to evaluate and compare metallographic characteristics between the parts at the end of 'boost' stage, rather than to evaluate the final carburized parts characteristics.

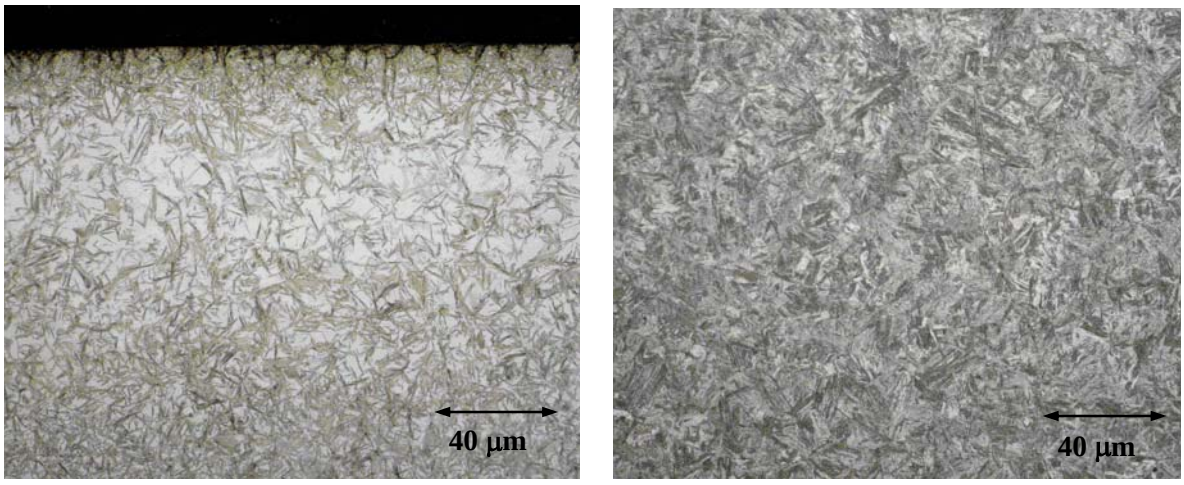

a) b)

Figure 5. Microstructure of carburized test coupons, 2% nital etch: a) surface, b) core.

Figure 6 shows the carbon concentration profile obtained from a standard carbon step bar (subsurface) and from the surface carbon measurements on the carburized test coupons. Upon quenching from 925 °C, the surface hardness on the step bars was greater than Rc 40. Turning the step bars in such as-quenched condition would have caused excessive overheating, which could have obscured the results of the carbon gradient analysis. The bars were subsequently tempered for 1 hr at 600 °C prior to machining the bars. The results of carbon concentration measurements after tempering the bars revealed a decarburized layer up to a depth of 0.12 mm. Therefore, to help reconstruct the carbon gradient, the surface carbon concentration was measured on the test coupons and reported together with the subsurface step bar measurement in Figure 6.

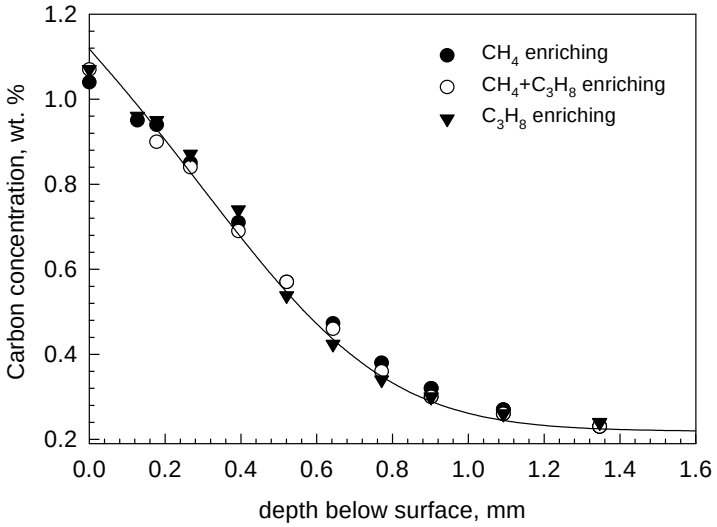

Figure 6. Carbon concentration profile obtained from surface carbon measurements (test coupons) and carbon step bar analysis (subsurface measurements).

Table 1 compares the data obtained from all three carburizing experiments. Despite the different levels of the hydrocarbon enrichment, all carburizing atmospheres produced a similar carbon potential in the furnace. Therefore, after 2 hrs carburizing at the same constant temperature and carbon potential, all parts revealed comparable carburizing performance, i.e., similar weight gain, surface carbon concentration and the carburized case depth.

Table 1. Carburizing atmosphere and the case depth characteristics.

Atmosphere	Enriching, % total gas flow	Δt (time to stabilize C_P)	t_{Carb}, hrs	C_P, wt.%C	Weight gain, mg	Surface carbon, wt.%	Case depth to 0.4 wt.%C
Endo + CH_4	6.5	1 hr 3 min	2	1.26 ± 0.01	181.2	1.05+/-0.02	0.71 mm
Endo + mixture (CH_4+C_3H_8)	4	34 min	2	1.26 ± 0.01	181.8	1.07+/-0.02	0.71 mm
Endo + C_3H_8	2.3	25 min	2	1.28 ± 0.02	182	1.05+/-0.02	0.69 mm

Beyond the inherent errors in the experimental data (such as, flow meter sensitivity and carbon concentration measurement error) as well as the natural variations during the carburizing process (carbon potential and temperature variations with time), no significant differences either in metallurgical or metallographic analyses were observed. Thus, carburizing parts with propane as the enriching gas proved to produce the same case characteristics with lower gas consumption and shorter furnace operating time.

Modeling Carbon Concentration Profiles

In order to explain the effect of carbon potential evolution and cycle time on the carburizing performance of parts in different gas atmospheres, the carbon concentration profiles were modeled using the recorded C_P-time and temperature data from Figure 4-a. The carburizing model is based on the finite difference approximation of the parabolic equation governing carbon diffusion in steel and a set of boundary conditions [9], which account for the mass transfer in the atmosphere and the kinetics of the interfacial reactions. Figure 7 shows the predicted carbon profile evolution for two time segments during the carburizing cycle and the final carbon concentration profile.

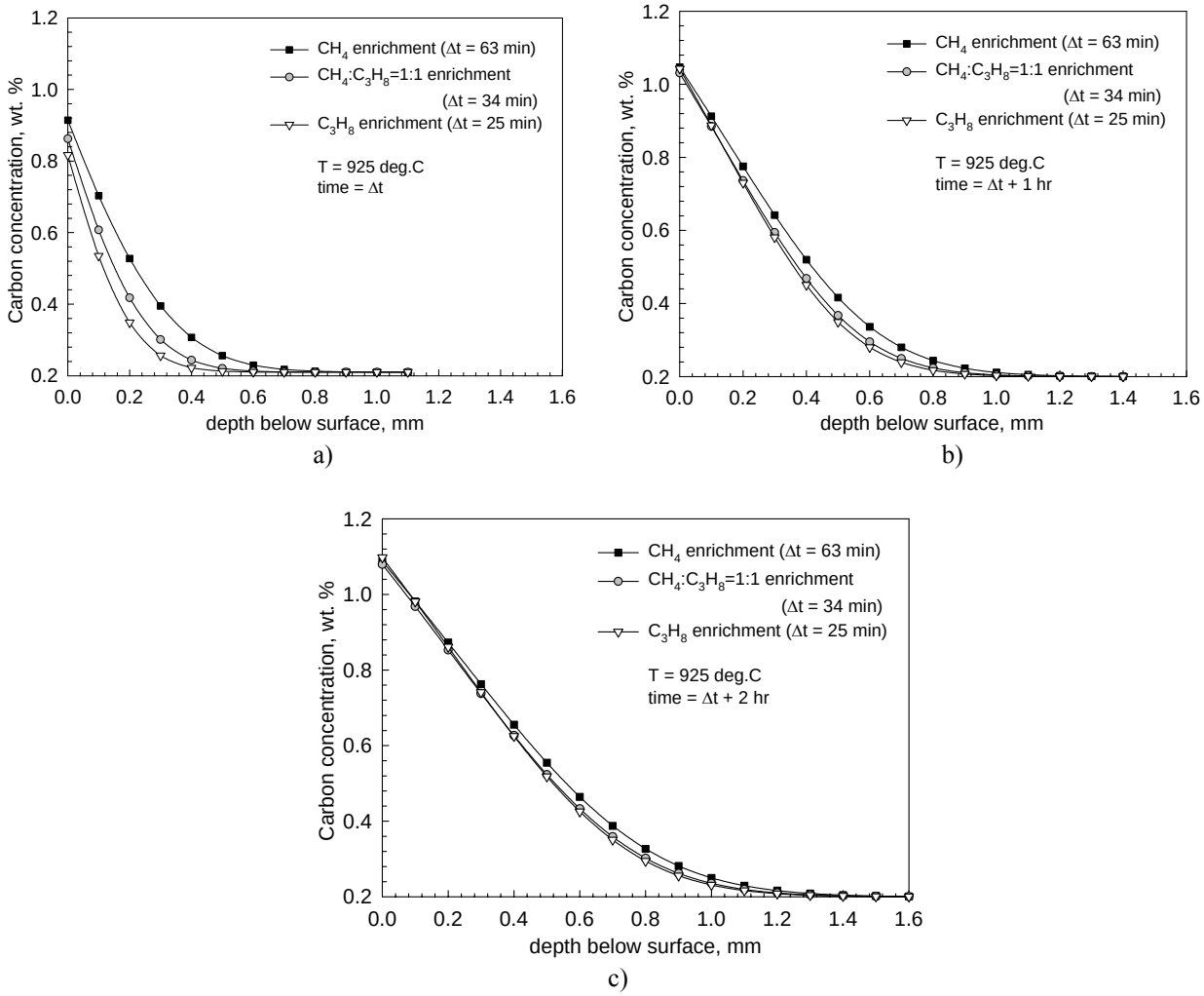

Figure 7 (Cont.). Predicted carbon profile evolution during the carburizing cycle: a) after carbon potential stabilizing (Δt); b) 1 hr carburizing (Δt + 1 hr); c) 2 hrs carburizing (Δt + 2 hrs).

Figure 7-a shows the predicted carbon concentration profiles for all three atmospheres upon carbon potential stabilizing. Despite the differences in the atmosphere stabilizing time (Δt) between the cycles, the atmospheres enriched with propane exhibit larger driving force for carbon transfer from the atmosphere to the steel surface, i.e., larger (C_P - C_S), and therefore, result in relatively small differences in the surface carbon concentration. At this stage, the differences in the subsurface carbon concentration are significant and originate from the different Δt times allowed for carbon diffusion. Hence, for shallow- and medium- case carburizing cycles [up to ~ 0.5 mm] different diffusion times should be determined for such atmospheres to produce a desired case depth. As the carburizing time proceeds, the differences in the carbon concentration profiles (Figure 7-b) decrease due to the parabolic nature of diffusion. The final carbon concentration profiles for all three cycles overlap, which explains the nearly equal weight gain measured experimentally in all parts after carburizing.

Cost Analysis

As discussed in the previous sections, all carburized parts exhibited similar carburized case characteristics, and therefore, the goal of cost analysis is to determine the efficiency of these carburizing cycles in terms of the enriching gas consumption and the furnace operating time. The atmospheres enriched with propane (C_3H_8) provided greater carbon availability in the furnace atmosphere and more rapid kinetics of the carburizing chemical reactions (4-6) even with lower [than natural gas] enriching gas flow. As a result, for the given experimental setup similar carbon potential atmosphere was produced with 65 % lower enriching gas consumption and 21% lower furnace operating cost.

Table 2. Cost analysis of the carburizing atmospheres.

Carburizing atmosphere	Enriching gas consumption		Furnace operating time			
	C_XH_Y gas consumption, m^3/hr	Normalized C_XH_Y gas consumption	Δt (time to stabilize C_P)	t_{Carb},	Total cycle time, hr	Normalized cycle cost
Endo + CH_4	0.65	1.00	63 min	2 hrs	3 hrs 3 min	1
Endo + mixture (CH_4+C_3H_8)	0.4	0.61	34 min	2 hrs	2 hrs 34 min	0.84
Endo + C_3H_8	0.23	0.35	25 min	2 hrs	2 hrs 25 min	0.79

* Total cycle cost was calculated based on the cost model given by Equation 1-3.

As hypothesized, carburizing with propane enriching gas provides a lower-cost alternative to endothermic atmosphere carburizing with more efficient energy utilization. Using such atmospheres would help lower the environmental impact by reducing gas consumption and emission of the by-product gases without impairing the carburizing properties. Accelerating the rates of the carburizing reactions would also permit carburizing larger workloads with greater efficiency, reducing total cycle time required to achieve a desired case depth and increasing furnace capacity.

The major advantage of using the carburizing atmospheres with enriching propane (C_3H_8) is the significant reduction in the total cycle time (38 min) achieved by shortening the atmosphere stabilizing time. This becomes especially significant for shorter carburizing cycles times intended for shallow and medium case depths. Reducing production time to perform an additional carburizing cycle would increase capacity of the furnace and lower cost per kg/part.

Conclusions

1. The 'boost' stage of gas carburizing was analyzed by evaluating the thermodynamics and kinetics of carburizing reactions with enriching natural gas, propane, and a mixture of these two gases. The cost model was developed to quantify the corresponding benefits in the enriching gas consumption and the total carburizing time.

2. The same atmosphere carbon potential was obtained by using 2.3 vol. % (total gas flow) of enriching C_3H_8 as opposed to 6.5 vol.% of natural gas, which lowered hourly enriching gas consumption by 65 %. Greater carbon availability of the C_3H_8 molecules and the thermodynamics of their step-reaction decomposition also reduced time to stabilize the carbon potential, which shortened total cycle time by 38 min.

3. Analyses of the carburized parts revealed similar case characteristics in all three carburizing cycles. The atmospheres enriched with C_3H_8 provided faster carbon potential evolution, which shortened the total carburizing cycle time while providing a similar microstructure, case depth and carbon gradient characteristics.

4. Although enriching with a mixture of natural gas and C_3H_8 (1:1) enhanced the rate of carbon potential evolutions, the effect was primarily dominated by C_3H_8. Simultaneous addition of CH_4 and C_3H_8 lowered the activity of C_3H_8 and increased the amount of residual CH_4 remaining in the furnace. Therefore, carburizing with pure C_XH_Y is preferred to using gas mixtures.

Acknowledgements

The support of the Center for Heat Treating Excellence (CHTE) at Worcester Polytechnic Institute and the member companies is gratefully acknowledged. This work was performed at Caterpillar Inc. and its support through facilities and experimental work is greatly appreciated. The authors would also like to thank Advanced Materials Technology (AMT) group for their assistance and valuable discussions.

References

1. O. Karabelchtchikova, S.A. Johnston and R.D. Sisson, Jr: submitted to *Metall. Trans.*
2. J.I. Goldstein and A.E. Moren: *Metall. Trans. A,*1978, vol. 9 A, n. 11, pp. 1515-25.
3. J. Agren: *Scripta Metallurgica*, 1986, vol. 20, n. 11, pp. 1507-10.
4. J. Slycke and L. Sproge: *J. Heat Treat.*, 1988, vol. 5, n. 2, pp. 97-114.
5. T. Naito, K. Ogihara, A. Wakatsuki, T. Nakahiro, H. Inoue and Y. Nakashima: US Patent No. 6106636, Dowa Mining Co., Ltd, Tokyo, Japan, August 2000.
6. C.A. Stickels, C. M. Mack and M. Brachaczek: *Metall. Trans. B*, 1980, vol. 11B, n.3, pp. 471-79.
7. Department of energy, Energy Information Administration: www.eia.doe.gov
8. American Society for Metals: *Carburizing and Carbonitriding*, ASM International, Metals Park, OH, 1977, pp. 18-25.
9. O. Karabelchtchikova and R.D. Sisson, Jr.: *J. Phase Equilib. Diffusion*, 2006, vol. 26, n. 6, pp. 598-604.

PAPER # 3: CARBURIZING PROCESS MODELING AND SENSITIVITY ANALYSIS USING NUMERICAL SIMULATION

(published in *Proc.* MS&T 2006, Cincinnati, OH, 375-386)

Abstract

Industry often faces problems in maintaining uniform case depth during the gas carburization heat treatment processes. Two important control parameters that control the carburization of steel: environmental reaction rate that causes carbon to be absorbed at the surface and the carbon diffusion rate from the steel surface to the interior of the part. In this study a computer model is developed to investigate the effect of temperature and gas composition on the mass transfer coefficients at the steel surface and the effect of carbon content and temperature on the carbon diffusion rate in low and medium carbon steels. A series of computer experiments are performed to investigate the sensitivity of the carburizing performance characteristics to the variation in these control parameters and to determine the potential route to reduce case depth variability and the cycle time.

Introduction

Gas carburizing in batch furnaces is a widely accepted procedure for surface hardening, yet it faces certain challenges in performance reliability and process control. The quality of the carburized parts is determined based on the hardness and case depth required for a particular application and on compliance with the specifications and tolerances. In particular, carburizing performance is often evaluated by the surface hardness, surface carbon concentration, and the case depth. Despite the importance of the carburizing applications and current challenges with the process control, the industrial approach to solving this problem often involves trial and error methods and empirical analysis, both of which are both expensive and time consuming.

Successful carburizing performance depends on the effective control of the three principal variables: temperature, time and the carburizing atmosphere. Much research has been performed to investigate the effect of these process parameters on the carburizing kinetic parameters, i.e. the mass transfer coefficient and carbon diffusivity in steel [1-10]. In particular, the mass transfer coefficient has been reported to be a complex function of the atmosphere gas composition, carburizing potential,

temperature and surface carbon content [1-6]. The coefficient of carbon diffusion in steel is another parameter defining the rate of carbon transport, which is strongly influenced by the carburizing temperature and steel carbon concentration [7-10]. Even though the mechanism of mass transport in carburizing appears to be well understood, experimental results have shown that for different carburizing atmospheres, the carbon concentration curves often deviate from those of the predicted ones. Therefore, the goal of this paper is to develop a better understanding of the effect of process parameters' variations on the carburizing kinetic coefficients, which effective control will help achieving the desirable final properties of the parts and in improved process performance.

The carburizing potential in the furnace atmosphere is a function of the gas composition. This requires not only accurate measurement of the gas constituents (CO, CH_4, CO_2, H_2O) in the furnace but also representative sampling locations where the constituents are analyzed. Since surface carbon concentration and flux of carbon atoms from the atmosphere to the steel surface change with time, maintaining a constant atmosphere carbon potential during single stage carburization requires continuous adjustment of the set point until the parts meet the required specification. Dawes and Tranter [11] reported that variation of 0.05 wt% in the carburizing potential from the set point can be caused by an average temperature variation (10 °C) in the carburizing furnace. As such, an accurate control of the carburizing atmosphere may be achieved only with accurate control of temperature in the furnace.

An increase in the carburizing temperature increases the rate of mass transfer both in the furnace atmosphere and steel. It also promotes excessive austenite grain growth and deteriorates the furnace condition. The effect of time on case depth is interdependent with the carburizing temperature and is often estimated by using the Harris equation [12]. The equation, however assumes saturated austenite at the steel surface, and when the surface carbon content is less that the saturation limit, the resulting case depth prediction would be less than expected. Therefore, for the purpose of the carburizing process optimization and its further control, more complex model should be used which would account for the variations of temperature and atmosphere carbon potential with time.

Overall, carburizing performance strongly depends on the choice of process parameters, type of furnace, atmosphere control, and materials characteristics. All of these factors contribute to either the mass transfer coefficient or carbon diffusivity in austenite. As a part of the carburizing process optimization and control, the objectives of the paper are to: 1) identify the effective

control parameters as a functions of the process parameters to manipulate the desired case depth and surface carbon content variability, 2) evaluate the effect of the process parameters' variations on the carburizing kinetics and 3) determine the potential route to the process optimization in order to achieve desired properties with minimal processing time.

Modeling of Carburizing Heat Treatment

Carbon Transfer Mechanisms During Carburizing

The mass transfer mechanism in carburizing, as shown in Figure 1, consists of three stages: 1) carbon transport from the atmosphere through the boundary layer, 2) chemical reaction at the steel surface and 3) carbon diffusion in steel. Total carbon transfer from the atmosphere to the steel is thus determined by the limiting process, which kinetically becomes the rate controlling stage of carburizing. In particular, the two control parameters determining final carbon distribution in steel after carburizing are: the mass transfer coefficient (β) defining carbon atoms flux from the atmosphere to the steel surface and the coefficient of carbon diffusion in steel (D_C) at austenizing temperature.

The mass transfer coefficient defines carbon flux from the atmosphere to the steel surface, and limits the rate of carburizing in the beginning of the process [1-6]. After this initial stage, the process becomes mixed controlled [13-15] and the thickness of the boundary gas in front of the gas-solid interface is estimated as the (D_C/β) ratio [1]. The mass transfer coefficient is very sensitive to the changes in the atmosphere composition and carburizing potential (C_P). Munts and Baskakov [3] suggested that β increases linearly with the concentration of water vapor in the carburizing atmosphere. Since carbon activity in the gas phase is inversely proportional to the concentration of water vapor, β should decrease with increasing C_P. Various researchers reported β ranging from $1 \cdot 10^{-5}$ to $3.5 \cdot 10^{-5}$ cm/s [1-4] and agreed that β is sensitive to the change in CO and H_2 in the atmosphere, and is maximized by increasing the product of partial pressures of these components [1,2]. While there is a general agreement in the mass transfer coefficient measurements as a function of the gas atmospheres [1-4], there is a large discrepancy in the reported effect of carburizing temperature on this coefficient [2,3,5,6]. Rimmer and Wünning [2,5] reported β to be independent of carburizing temperature. On the other hand, a number of studies [3,6] indicated

significant change in β from the change in carburizing temperature, which may range from $2 \cdot 10^{-5}$ to $2 \cdot 10^{-4}$ cm/s at 800-1000 °C carburizing temperatures.

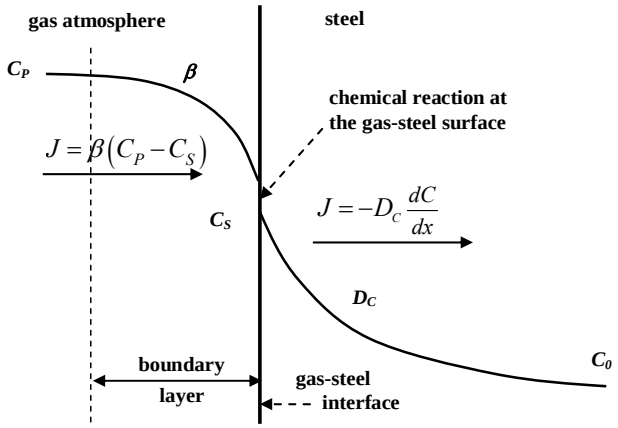

Figure 1. Schematic representation of carbon transport in carburizing [16].

Once the *CO* molecules reach the surface and dissociate into adsorbed carbon atoms and carbon dioxide ($2CO \rightarrow C_{ad} + CO_2$), the mechanism of further carbon transport in the steel becomes diffusion controlled. As such, the coefficient of carbon diffusion in austenite is another control parameter defining carburizing process performance. Generally accepted to be a function of alloying elements, the models available for carbon diffusivity calculation either consider only temperature effect or temperature and carbon content at most [7-10]. In this work, to model carbon diffusion in the steel at the austenizing temperatures the following diffusivity model was adopted [8]:

$$D_{C(\gamma-Fe)} = 0.78 \cdot \exp\left[-\frac{18,900}{T} + \left(\frac{4,300}{T} - 2.63 \right) C^{1.5} \right], \quad (1)$$

where D_C is carbon diffusivity in cm^2/s, T is absolute temperature in K, C is carbon concentration in wt%.

Governing PDE and Boundary Conditions

Carburizing process is modeled using a second-order parabolic partial differential equation for carbon diffusion in steel and a set of boundary conditions accounting for the mass transfer coefficient at the steel surface and kinetics of the interfacial reactions:

$$\frac{\partial C}{\partial t} = \frac{\partial}{\partial x}\left(D_C \frac{\partial C}{\partial x} \right) + u \cdot \frac{D_C}{r + ux} \cdot \frac{\partial C}{\partial x}, \tag{2}$$

where $u = -1$ for convex surface, $u = 0$ for plane surface and $u = 1$ for concave surface, D_C is the coefficient of carbon diffusion in steel, r is radius of the curvature, x is distance from the surface.

With the flux balance at the gas-steel interface, one may assume that the amount of carbon produced by the surface reaction is equal to the flux of carbon atoms in the steel described by Fick's law of diffusion:

$$\sum_i^n \frac{k_i}{a_C^{surf_i}} \left(C_P - C_S \right) = -D_C \frac{dC_S}{dx}. \tag{3}$$

where a_C^{surf} is carbon activity at the steel surface and k_i is the reaction rate coefficient of the carburizing chemical reactions, C_P is the atmosphere carburizing potential, and C_S is carbon concentration at the steel surface.

If the summation term $\sum k_i / a_C^{surf_i}$ is defined as β, the total mass transfer coefficient would include both carbon transfer through the gas layer near the steel surface and the kinetics of the surface reaction, i.e., the resistance barrier to carbon uptake at the steel/gas interface. The rate of exchange at the surface is directly proportional to the difference between its surface carbon concentration at any given time and the carburizing potential of the atmosphere. Therefore, the flux balance boundary condition at the surface can be re-written as

$$\beta \left(C_P - C_S \right) = -D_C \frac{\partial C}{\partial x}. \tag{4}$$

where $\frac{\partial C}{\partial x}$ is the carbon concentration gradient at the surface and β is the mass transfer coefficient.

Numerical Simulation

Since an analytical solution to carbon diffusion in steel (Equation 2) with the flux balance boundary conditions (Equation 4) is not available for concentration dependent diffusivity, the carburizing process was modeled numerically. The governing PDE with the corresponding boundary condition was transformed into a set of finite difference equations and solved sing

MATLAB. Concentration profiles were computed iteratively using the Dusinberre numerical method [17] and assuming semi-infinite geometry initially at uniform constant carbon concentration. This method is second order accurate and provides a stable and convergent solution. For a simple plane geometry and one-dimensional diffusion carbon profiles were calculated using the following numerical expression:

$$C_i^{t+\Delta t} = \frac{\Delta t}{(\Delta x)^2}\left[D_i^t \left(C_{i-1}^t - 2C_i^t \left(\frac{(\Delta x)^2}{D_i^t \Delta t} - 2 \right) + C_{i+1}^t \right) + \frac{\left(D_{i+1}^t - D_{i-1}^t\right)\left(C_{i+1}^t - C_{i-1}^t\right)}{4} \right], \tag{5}$$

where C is carbon concentration corresponding to a particular location (node i) and time t, Δx is space increment between the nodes, and Δt is time increment.

Given the mass transfer coefficient at the steel surface, carbon concentration at the boundary nodes was calculated as

$$C_{surf}^{t+1} = \frac{1}{M} \cdot \left[2N \cdot C_P + \left[M - (2N+2) \right] C_{surf}^t + 2C_{x_1}^t \right], \tag{6}$$

where

$$M = \frac{D_C \cdot \Delta t}{(\Delta x)^2} \quad \text{and} \quad N = \frac{\beta}{D_C} \cdot \Delta x\,. \tag{7}$$

The two stability criteria were assured to be fulfilled simultaneously: $M > 2$, and $M > 2N + 2$, which combination provides a criteria for calculating the maximum stable time increment from the previously determined grid space interval, D_C and β values:

$$\Delta t < \frac{(\Delta x)^2}{2\beta \cdot \Delta x + 2D_C}\,. \tag{8}$$

Results and Discussion

The results of the carburizing heat treatment modeling are given in Figure 2. Since surface flux and surface carbon content vary with time even with a fixed carburizing potential, the mass balance at the gas-steel interface served as the boundary condition. To validate adequacy of the

model, the numerically modeled results were compared with the available analytical solution for the same boundary conditions, but with a constant carbon diffusivity given by the following equation [18].

$$\frac{C(x,t)-C_0}{C_P-C_0} = erfc\left(\frac{x}{2\sqrt{Dt}}\right) - \exp\left(\frac{\beta x+\beta^2 t}{D}\right)\cdot erfc\left(\frac{x+2\beta t}{2\sqrt{Dt}}\right). \quad (9)$$

The numerical simulation accurately repeated the analytical solution for any carburizing time greater than 0.25 hour with no error associated with it. This comparison validated the developed model and was further used to calculate carbon distribution profiles using concentration dependent diffusivities (Figure 2).

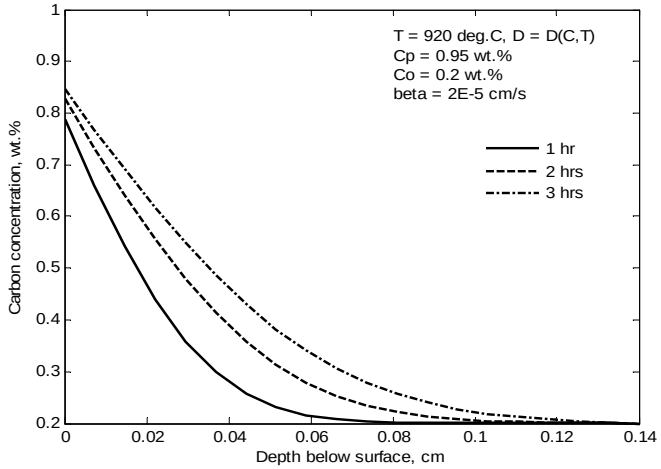

Figure 2. Numerically calculated carbon concentration profiles after 1, 2, and 3 hrs carburizing.

As identified in the previous section, the primary sources of variation in the carburizing performance are the temperature and carburizing gas atmosphere. While the surface carbon concentration and carbon gradient depend on accurate control of the atmosphere and its carburizing potential, the case depth is primarily influenced by the temperature in the furnace and the duration of the carburizing process. Therefore, a set of computer experiments was performed for sensitivity analysis to evaluate the effect of variation in these parameters during the industrial carburizing on the final carbon distribution profiles.

Effect of Temperature and the Mass Transfer Coefficient on Carburizing

Depending on the gas composition and the method of the carburizing atmosphere control, the mass transfer coefficient may vary from $1 \cdot 10^{-5}$ to $3.5 \cdot 10^{-5}$ cm/s [1-4]. Figure 3 shows the effect of such variation in β on the carbon concentration profile after 2 hours of carburizing. When β changes from $1 \cdot 10^{-5}$ to $4 \cdot 10^{-5}$ cm/s, the following changes in the concentration profile occur: surface carbon content increases from 0.74 wt% to 0.88 wt%, while effective case depth (defined to 0.4 wt% C) changes from 0.0332 to 0.0420 cm. Also, carbon profile sensitivity to β increases with increasing temperatures, causing an even larger variation in the surface carbon content and the case depth.

An interesting observation is that variations in the carbon concentration profile decrease with an increasing β. Therefore, if a higher mass transfer coefficient is established and maintained in the carburizing furnace, it may not only increase the rate of carbon flux from the atmosphere to the steel surface, but will also result in smaller variations in the concentration profiles.

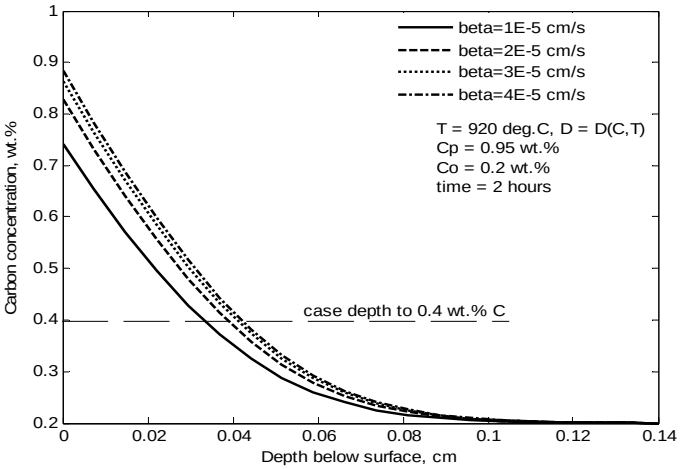

Figure 3. Effect of variation in the mass transfer on carbon concentration profile.

The temperature distribution in the batch furnace should be uniform to produce consistent case depth between the parts of the same load. Often, however, a temperature gradient exists in the industrial furnaces throughout the carburizing cycle. The two factors which may lead to a non-uniform case depth in the carburized parts are: 1) the temperature gradient during heating between the parts at various locations in the furnace and 2) the temperature gradient, which persists in the furnace throughout the whole carburizing cycle due to non-uniform heating in the furnace. While the temperature gradient due to the heating rates is reduced with time, the

temperature gradient in a poorly controlled furnace may persist throughout the entire carburizing cycle and will result in non-uniform case depths.

To simulate the effect of the internal furnace temperature gradients on the effective case depths (specified to 0.4 wt% C), a set of computer experiments was performed. Figure 4 shows the numerical model predicted concentration profiles corresponding to the specified range of temperatures. Assuming a constant mass transfer coefficient and concentration dependent model for carbon diffusivity, the calculated case depth variation was 0.0386 ± 0.0027 cm.

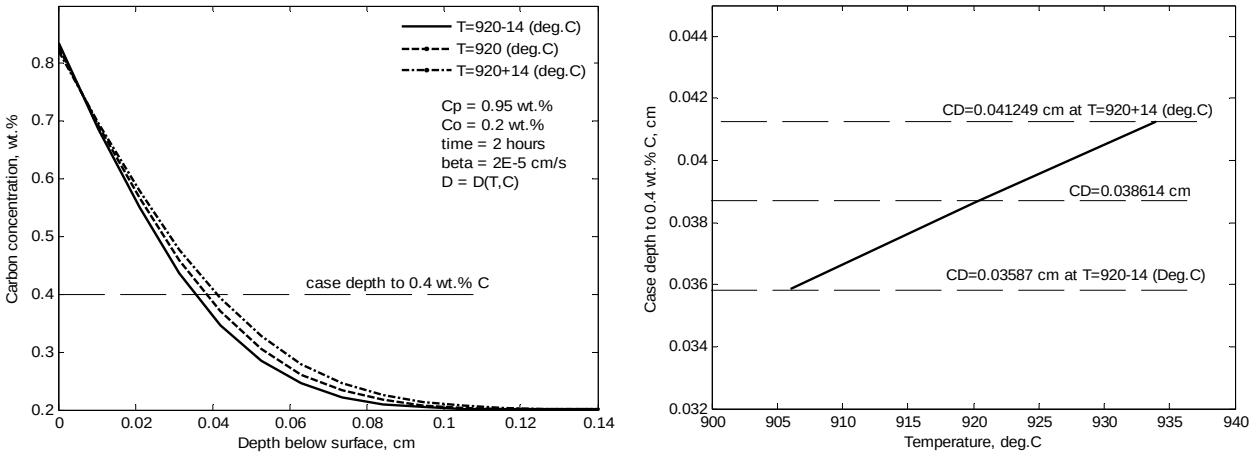

a) b)

Figure 4. Effect of temperature gradient in the furnace on case depth (CD) variation: a) carbon concentration profiles, b) case depth variation for the specified temperature tolerance.

Effect of Variation in the Atmosphere Potential on Carburizing

Another source of case depth variation is the variation in the atmosphere carbon potential, which is a complex function of the gas atmosphere composition. The average fluctuation of the carburizing potential may reach ±0.05 % depending on the control loop in the gas supply to the carburizing chamber [11]. The effect of such fluctuation in C_P on the concentration profiles at constant temperature is shown in Figure 5. While the case depth variation was ±0.0016 cm, the major difference in the predicted profiles was observed near the surface where surface carbon concentration ranged from 0.78 to 0.86 wt% C.

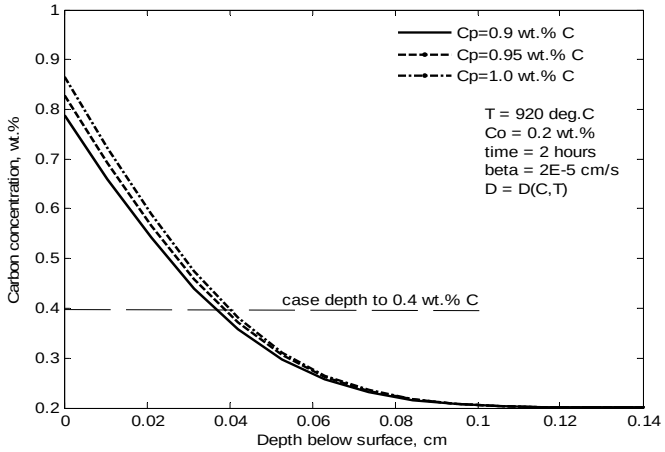

Figure 5. Effect of carburizing potential variation on the concentration profile.

Summary

The objectives of this paper were to identify effective control parameters in terms of the process parameters and to evaluate the effect of their variation on the carburizing performance. The carburizing heat treatment was modeled using finite difference method. The model prediction was validated by comparing the modeled concentration profiles with the analytical solution available for a constant diffusion coefficient. The average variation in the mass transfer coefficient revealed significant variation both in the surface carbon content and the case depth. These variations increased greatly at higher carburizing temperatures. It was also observed that beyond a certain value ($\sim 3.5 \cdot 10^{-5}$ cm/s), carbon concentration profiles become nearly insensitive to further changes in β. As such, increasing β will not only enhance carbon flux from the atmosphere to the steel surface, but will also help achieve uniform case depth.

As follows from the sensitivity analysis, an average temperature variation (14 °C) in the industrial carburizing furnace is capable of producing as much as 7% of the case depth variation. This temperature gradient will also inevitably lead to variation in the atmosphere carburizing potential [11]. In particular, C_P variations of only ±0.05 wt% from the preset value cause dramatic changes in the resulting surface carbon content and the corresponding case depth. Therefore, by controlling temperature fluctuations in the industrial furnace better control of the carburizing atmosphere may be achieved. Process control must be maintained by checking the control parameters with their preset values. In the event that the difference between the two

values becomes greater than a specified level, the heat input (for temperature control) and/or enriching gas flow (for atmosphere control) must be adjusted correspondingly.

The material presented in the paper is an integral part of carburizing process optimization. The work is currently in progress and some experimental carburizing work is planned to be performed in an industrial setting. The experimental data will be used to further validate the models and to gain better understanding on the effect of the process parameters on the coefficients of mass transfer and carbon diffusion in the steel. Together with the results of the carburizing process modeling, sensitivity analysis and the experimental data, the derived functional correlations will then be used to search for a set of the process parameters which would maximize the case characteristics with minimized variation in the observed data.

References

1. P. Stolar and B. Prenosil, “Kinetics of Transfer of Carbon from Carburizing and Carbonitriding Atmospheres,” *Metallic Materials (English translation of Kovove Materialy)*, 22 (5) (1984), 348-353.

2.K. Rimmer, E. Schwarz-Bergkampf, and J. Wunning, ”Surface Reaction Rate in Gas Carburizing,” *Haerterei-Technische Mitteilungen*, 30 (3) (1975), 152-160.

3.V.A. Munts, and A.P. Baskatov, "Rate of Carburizing of Steel," *Metal Science and Heat Treatment (English Translation of Metallovedenie i Termicheskaya Obrabotka Metallov),* 22 (5-6) (1980), 358-360.

4.V.A. Munts, and A.P. Baskakov, “Mass Exchange in Carburization and Decarburization of Steel,” *Metal Science and Heat Treatment (English Translation of Metallovedenie i Termicheskaya Obrabotka Metallov),* 25 (1-2) (1983), 98-102.

5.J. Wunning, “Advances in Gas Carburizing Technique,” *Haerterei-Technische Mitteilungen*, 23 (3) (1968), 101-109.

6.B.A. Moiseev, Y.M. Brunzel', and L.A. Shvartsman, “Kinetics of Carburizing in an Endothermal Atmosphere,” *Metal Science and Heat Treatment (English translation of Metallovedenie i Termicheskaya Obrabotka Metallov)*, 21 (5-6) (1979), 437-442.

7.J.I. Goldstein and A.E. Moren, “Diffusion Modeling of the Carburization Process,” *Metallurgical and Materials Transactions A,* 9 (11) (1978), 1515-1525.

8.George E. Totten and Maurice A.H. Howes, *Steel Heat Treatment Handbook* (New York, NY: Marcell Dekker, Inc., 1997).

9.J. Agren, “Revised Expression for the Diffusivity of Carbon in Binary Fe-C Austenite,” *Scripta Metallurgica*, 20 (11) (1986), 1507-1510.

10. R.M. Asimow, “Analysis of the Variation of the Diffusion Constant of Carbon in Austenite with Concentration,” *Transactions of AIME,* 230 (3) (1964), 611-613.

11. C. Dawes, and D.F. Tranter, “Production Gas Carburizing Control,” *Heat Treatment of Metals,* 31 (4) (2004), 99-108.

12. F.E. Harris, "Case Depth - an Attempt at a Practical Definition," *Metal Progress*, 44 (1943), 265-272.

13. T. Turpin, J. Dulcy, and M. Gantois, “Carbon Diffusion and Phase Transformations during Gas Carburizing of High-Alloyed Stainless Steels: Experimental Study and Theoretical Modeling,” *Metallurgical Transactions A*, 36 (10) (205), 2751-2760.

A. Ruck, D. Monceau, and H.J.Grabke, “Effects of Tramp Elements Cu, P, Pb, Sb and Sn on the Kinetics of Carburization of Case Hardening Steels,” *Steel Research,* 67 (6) (1996), 240-246.

14. R. Collin, S. Gunnarson, and D. Thulin, “Mathematical Model for Predicting Carbon Concentration Profiles of Gas-Carburized Steel,” *Journal of the Iron and Steel Institute*, 210 (1972), 785-789.

15. J. Dulcy, P. Bilger, D. Zimmermann, and M. Gantois, “Characterization and Optimization of a Carburizing Treatment in Gas Phase: Definition of a New Process,” *Metallurgia Italiana*, 91 (4) (1999), 39-44.

16. William H. McAdams, *Heat Transmission* (New York, NY: McGraw-Hill, 1954), 43-50.

17. John Crank, *The Mathematics of Diffusion*, 1st ed., (Oxford, UK: Clarendon Press, 1956), 42-62.

PAPER # 4: EFFECT OF SURFACE ROUGHNESS ON THE KINETICS OF MASS TRANSFER DURING GAS CARBURIZING

(submitted to *International Journal of Heat Treatment and Surface Engineering*)

Abstract

Gas carburizing is one of the oldest heat treatment processes used for steel surface hardening. Despite its worldwide application, the process faces certain challenges in control and variability. Beyond the established knowledge regarding the effect of process parameters and atmosphere control, no carburization model accounts for the effect of surface roughness and is able to predict the observed case depth variations. Therefore, the objectives of this work are to (i) investigate the effect of surface roughness on gas carburizing performance, (ii) develop a functional relationship between the surface roughness characteristics and the mass transfer coefficient, and (iii) model surface roughness effect on the carbon concentration profile and the corresponding case depth variations. AISI 8620 steel samples were finished by sandblasting, two abrasive wire brush operations and grinding to 120 and 800 grit. A scanning laser microscope was used to measure 3D roughness parameters and surface area via area-scale fractal analysis. Carburizing performance was analyzed in terms of weight gain, microhardness and carbon concentration profiles. The measured weight gain and surface carbon concentration were used to calculate the mass transfer coefficient. The carburizing kinetics was found to be directly proportional to the surface roughness and was a function of surface area available for carbon transfer. These calculated mass transfer coefficients were compared to those reported in literature and served as input to the carburization model. Experimentally determined concentration profiles validated the model prediction and can be used to estimate initial surface conditions for improved carburizing performance and effective process control.

Introduction

Gas carburizing is a heat treating process used for saturating the near-surface layers of steel with carbon. This hardens the surface and enables the part to withstand large work forces without causing premature wear or fatigue. The mass transfer during gas carburizing proceeds in three

stages: 1) carbon transfer from the atmosphere to the steel surface, 2) surface chemical reactions, and 3) diffusion of the absorbed carbon atoms into the bulk of the steel. The rate of carburizing depends on the process parameters as well as steel composition and surface characteristics of the part. Although the effect of the process parameters has been investigated in-depth [1-5], the effect of surface roughness on carburizing kinetics has not been reported. Therefore, the objectives of this work are to (i) experimentally investigate the effect of surface roughness on gas carburizing performance, (ii) develop a functional correlation between the surface roughness characteristics and the mass transfer coefficient, and (iii) model the observed correlation to predict carbon concentration profile and case depth variations.

Beyond the general knowledge of the surface roughness effects on momentum transfer, there has been little work done to correlate the mass transfer phenomena across a gas-solid interface. Several authors [6-8] have studied the effect of surface roughness on the mass transfer rate between solid and flowing liquid using an electrochemical method. It was found that rougher surfaces enhanced the rates of mass transfer in the case of natural and forced convection. The proposed mechanism was that surface roughness affected the transition from laminar to turbulent flow, and caused greater rates of mass transfer than in smoother parts. To the authors' best knowledge no similar work has been reported to relate the effect of surface roughness to carbon transfer across the gas-steel interface. This may be due to inherent limitations of contact profilometry and insufficient scale resolution, or limitations of conventional roughness analysis that previous researchers have used exclusively.

Carbon Transfer Mechanisms During Carburizing

The mass transfer mechanism during gas carburizing is a complex phenomenon which involves carbon transport from the atmosphere to the steel surface, surface chemical reactions, and diffusion of the absorbed carbon atoms down their concentration gradient. The endothermic atmosphere primarily consists of CO, H_2, and N_2 with smaller amounts of CO_2, H_2O, and CH_4. Among the several possible chemical reactions, carburizing most rapidly proceeds by CO molecules decomposition on the steel surface [9]:

$$2CO \rightarrow C_{\gamma-Fe} + CO_2, \quad (1)$$

$$CO + H_2 \leftrightarrow C_{\gamma-Fe} + H_2O. \quad (2)$$

The absorbed carbon atoms further diffuse down their chemical potential gradient and establish carbon concentration profile. The enriching hydrocarbon gas regenerates *CO* and H_2 by reducing CO_2 and H_2O and directing reactions (3) and (4) to the right:

$$CH_4 + CO_2 \leftrightarrow 2CO + 2H_2, \quad (3)$$

$$CH_4 + H_2O \leftrightarrow CO + 3H_2. \quad (4)$$

Figure 1 shows the schematic of the interface between gas atmosphere and steel during carburizing. Hypothetically, the rate of carbon transfer is influenced by the conditions of the steel surface: surface roughness increases the total area of the gas-solid interface, and therefore increases density of the sites for the dissociation of *CO* molecules. It is also hypothesized that cleanliness on the part's surface could have a similar effect to the surface roughness and may control the number of effective sites to catalyze the chemical reaction. Therefore, this paper presents an analysis of the combined effect of surface cleanliness and roughness on the kinetics of mass transfer during carburizing. The observed correlation will be used to mathematically model the evolution of the carbon concentration profile and to explain the case depth variations.

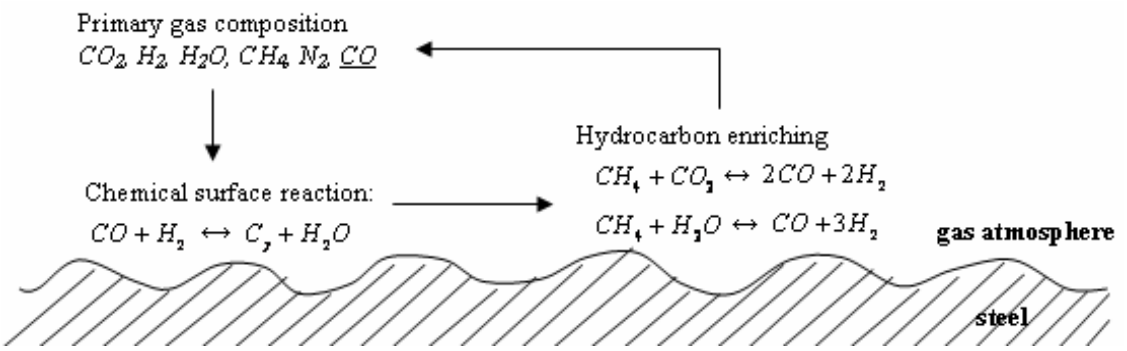

Figure 1. Schematic of the carbon transfer mechanism in gas carburizing.

Experimental Procedure

Material and Experimental Procedures

The steel used for this study was AISI 8620 with the chemical composition presented in Table 1. The cylindrical steel bars were supplied in hot rolled condition. Microstructural analysis revealed a mixture of ferrite and pearlite distributed uniformly in the transverse direction and

having a banded structure in the direction parallel to rolling. The steel bars were normalized at 900 ºC for 4 hours, which reduced the grain size from 6.5 to 8. The microstructure of the normalized steel is presented in Figure 2. The bars were machined into disks 3.125 cm in diameter and 1 cm in thickness and surface finished with a variety of operations as described below. The final parts were carburized at 925 ºC for 3 hours in endothermic atmosphere with natural gas enriching at Bodycote (Worcester, Massachusetts). Atmosphere carbon potential was controlled at 0.95 wt.% C using an oxygen probe. The parts were quenched in oil and tempered at 177 ºC for 2 hours.

Table 1. AISI 8620 steel chemical composition (wt.%).

C	Mn	P	S	Si	Ni	Cr	Mo
0.21	0.83	0.008	0.031	0.25	0.65	0.57	0.16

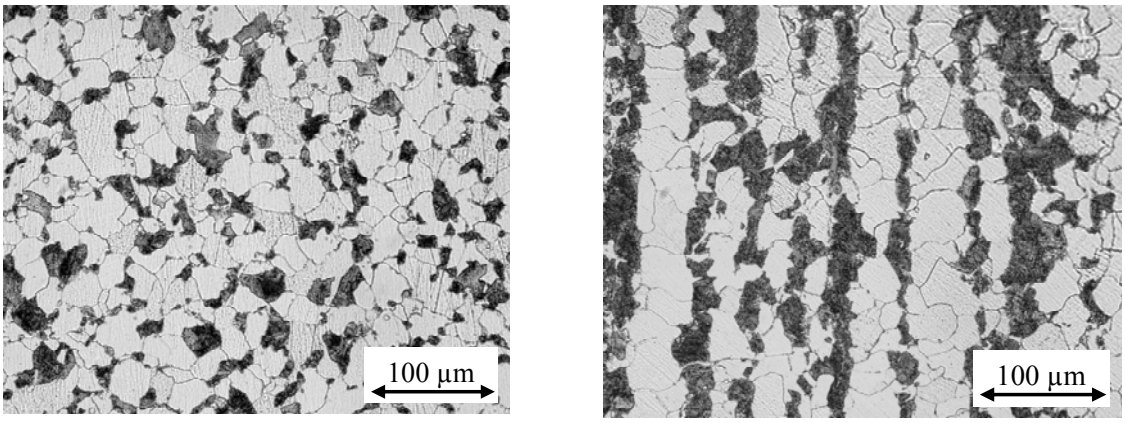

a) b)

Figure 2. Microstructure of AISI 8620 steel samples after normalizing, 2% nital etch.
a) transverse direction, b) longitudinal direction.

A full factorial experimental design included two factors: surface finish (roughness) and surface wash (intended to simulate a wide variety of surface cleanliness) on the parts prior to carburizing. The parts were finished by one of the five operations summarized in Table 2.

Table 2. Surface finishing operations.

Sandblasting	Particle size diameter - 0.09 cm , pressure 0.78 MPa, angle 90°
Wire brush - 1	2000 rpm, 25.4 cm/min feed rate
Wire brush - 2	3000 rpm, 5.08 cm/min feed rate
SiC: 120 grit	120 grit, average particle size - 116 µm
SiC: 800 grit	180 grit, average particle size - 12.2 µm

The finishing operations were selected such that they present a wide range of surface roughness from a near-mirror finish to a heavily-textured, markedly-rough surface. Prior to carburizing, the parts were washed in one of three solutions: 1) machine cutting liquid (ph = 8.9) to simulate as-machined condition, 2) alkaline solution (ph = 9.5) and 3) organic solution (ph = 10.3). An immersion system with good circulation assisted the cleaning through mechanical agitation: the cleaner activated the surface and promoted saponification and encapsulation of the soils, while agitation facilitated physical relocation of the surface contaminants.

Experimental Methods

The surface roughness was measured using a scanning laser microscope with Keyence LT 8010 confocal laser sensor. Five measurements per each surface were collected over a 0.4 x 0.4 mm^2 area with a 2 μm sampling interval. To capture maximum number of surface features, the following 3D roughness parameters were calculated:

$$Sa = \frac{1}{MN}\sum_{i}^{M}\sum_{j}^{N}|z|\left(x_i, y_j\right), \tag{5}$$

$$Sq = \sqrt{\frac{1}{MN}\sum_{i}^{M}\sum_{j}^{N}z^2\left(x_i, y_j\right)}, \tag{6}$$

and

$$St = |Sp| + |Sv|, \tag{7}$$

where *Sa* is the average roughness, *Sq* is the root-mean-square roughness, *St* is the peak-to-valley roughness, *Sp* is the maximum peak height, and *Sv* is the maximum valley depth.

In addition to the conventional roughness parameters, the surfaces were also characterized using area-scale fractal analysis [10-14]. The analysis is based on the following principle: triangular tiles of different size were virtually fitted to the surface to approximate the surface area. The scale of observation was defined as the area of individual tile, and the surface area was calculated as the total area of the fitted tiles using various scales. The relative surface area at every scale was obtained by dividing the measured surface area by the nominal area and plotted against the scale of observation in logarithmic coordinates. Since the surface area decreases with increasing scale, above some sufficiently large scale the relative area would equal one, and therefore would appear to be smooth. The scale at which this transition occurs is defined as the smooth-rough crossover (SRC) [11]. It has been shown that the fractal analysis is particularly

useful for providing an insight to characterizing various engineering surfaces and observing the surface related phenomena on the microscopic scale [13, 14]. Application of this technique would also allow characterization of the interaction between surface area and the dissociating *CO* molecules on the microscopic scale.

The carburizing performance was evaluated in terms of weight gain, microhardness and carbon concentration profiles. Laboratory scales sensitive to 10 μg were used for weight gain measurements. Microhardness transverse was measured with a Knoop indenter on an automated LECO Microhardness tester using a 500 g load and 20x objective lenses. Carbon concentration profiles were obtained by spectral analysis on LECO-OES with +/- 0.01 measurement error. A layer of the material of known depth was sequentially removed from the surface and analyzed for the chemical composition. This procedure repeated until a zero-gradient was reached, which was indicated by the bulk carbon concentration.

Results and Analysis

Surface Area Characterization

Figure 3 shows 3D topographic maps and SEM micrographs of the surfaces ranked from the smoothest (800 grit) to the roughest (sandblasted). All abrasive operations caused surface directionality and revealed systematic grooves across the surface. 800 grit ground samples appeared as near-mirror finish and were assumed to be isotropic. While 3D surface maps show surface area height distribution, SEM micrographs indicate the severity of the material deformation during the finishing operation: 800 grit < 120 grit < wire brush-2 < wire brush-1 < sand blasting.

Since carburizing proceeds by *CO* molecules decomposition, it is important to characterize the surface roughness at a scale comparable to the size of the dissociating *CO* molecule. At this scale, the relative area would be indicative of the intensity of their interaction. The size of *CO* molecule, estimated from *CO* bond length and radii of the composing atoms, depends on its orientation and may range from 1.58 nm to 2.8 nm. Therefore, it was proposed that the finer the scale used to characterize the surface roughness, the more representative it would be for the carburizing process and the better it would be to correlate the surface area with the mass transfer coefficient.

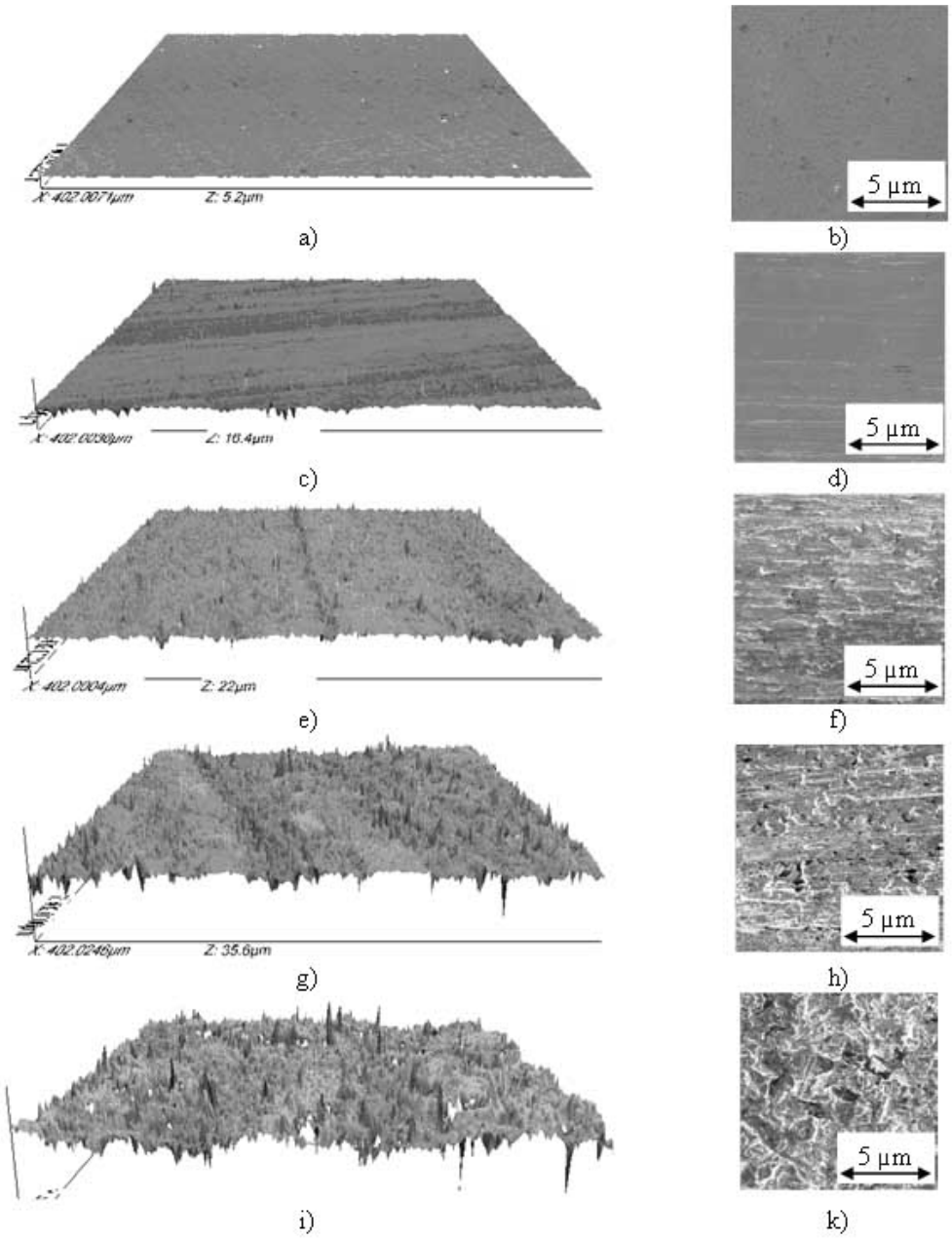

Figure 3. Qualitative representation of the surface finishes. 3D maps constructed from scanning laser microscope measurements and SEM micrographs of surfaces: a-b) 800 grit, c-d) 120 grit, e-f) wire brush-2, g-h) wire brush-1, and i-k) sandblasted samples.

The relative surface areas of the samples, calculated as the total surface area divided by the nominal area, are given in Figure 4. Statistical significance was evaluated in SAS using F-test with a 0.05 level of significance. The results indicated that the sandblasted surfaces were distinguishable at any scale below $2 \cdot 10^3$ μm^2; while the other four surface finishes were differentiable at scales below 200 μm^2. At sufficiently fine scales the relative surface area of the

sandblasted samples appeared to be nearly twice as large as the surface areas of the rest of the samples. This observation correlates to the severity of the material removal and the degree of plastic deformation induced during surface finishing.

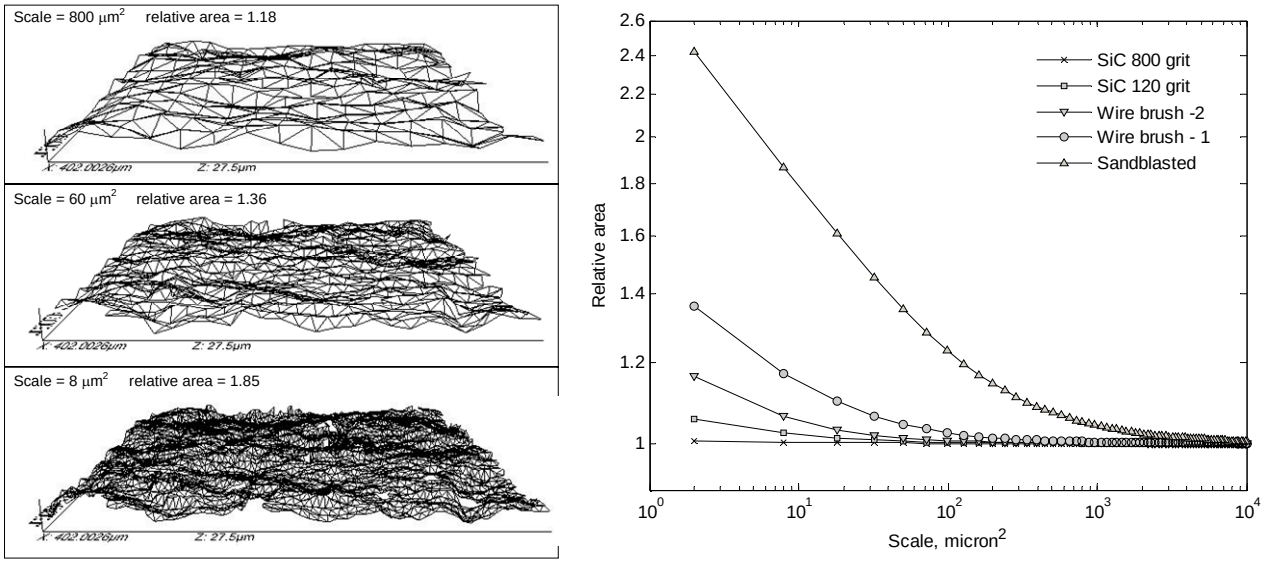

a) b)

Figure 4. Area-scale fractal analysis: a) surface area measurement using the patchwork method, b) mean relative areas of the surface finishes over a range of scales.

The conventional 3D roughness parameters on the parts' surfaces prior to carburizing are given in Table 3. Similar to the observed relative surface areas, the conventional parameters show a wide range of the surface roughness: 800 grit ground samples exhibited the finest surface finish while sandblasted samples were the roughest.

Table 3. Conventional roughness parameters of the parts prior to carburizing.

Surface finish	*Sa*, μm	*Sq*, μm	*St*, μm
Sandblasting	7.83+/-1.14	16.07+/-2.7	121.83+/-20.15
Wire brush - 1	1.46+/-0.12	1.94+/-0.21	33.56+/-3.53
Wire brush - 2	0.82+/-0.07	1.14+/-0.12	21.98+/-3.06
SiC: 120 grit	0.41+/-0.08	0.57+/-0.11	13.55+/-2.73
SiC: 800 grit	0.15+/-0.03	0.23+/-0.05	11.82+/-3.56

Weight Gain and Surface Carbon Concentration

The weight gain and the surface carbon concentration on the parts after carburizing are summarized in Table 4. Statistical analysis indicated that these data were primarily determined by the surface roughness and no particular trend in carbon absorption was observed due to the surface cleaning solutions. The rougher samples attained higher surface carbon concentration and revealed greater weight gain. Since the measured surface area of the sandblasted samples was larger than those of the other samples, it provided a greater number of sites available for *CO* molecules decomposition. This, in turn, increased the density of adsorbed carbon atoms and enhanced carbon diffusion flux from the steel surface to the bulk of the material.

Table 4. Weight gain [mg] and surface carbon content [wt.%] (in brackets) after carburizing.

Surface wash	Surface finish				
	Sandblasting	Wire brush - 1	Wire brush - 2	SiC: 120 grit	SiC: 800 grit
as-machined (cutting liquid, ph = 8.9)	72.28+/-0.81 (0.874+/-0.007)	68.85+/-0.35 (0.845+/-0.01)	68.10+/-0.51 (0.827+/-0.003)	67.85+/-1.66 (0.832+/-0.005)	68.34+/-1.07 (0.825+/-0.013)
alkaline wash (ph = 9.5)	72.35+/-0.28 (0.876+/-0.014)	68.78+/-0.37 (0.832+/-0.006)	68.26+/-0.47 (0.798+/-0.011)	67.27+/-0.89 (0.829+/-0.008)	67.43+/-0.30 (0.811+/-0.01)
organic wash (ph = 10.3)	72.48+/-0.28 (0.873+/-0.01)	69.10+/-0.22 (0.828+/-0.008)	68.26+/-0.57 (0.825+/-0.008)	68.42+/-1.45 (0.822+/-0.009)	67.60+/-1.18 (0.798+/-0.008)

No significant differences in the near surface microstructure were seen by optical or scanning electron microscopy. The grain size and the extent of intergranular oxidation were similar.

Total Carbon Flux and Mass Transfer Coefficient

Since no sooting was observed on the parts after carburizing, it was assumed that the carbon fluxes in the atmosphere and within the steel were balanced. Therefore, the total carbon flux into the workpiece can be calculated from the continuity equation of mass accumulation:

$$J_C = \frac{\partial}{\partial t}\left(\frac{\Delta M}{A}\right), \tag{8}$$

where J_C is the total carbon flux, $\Delta M/A$ is the weight gain per unit surface area, and t is the carburizing time. Given that carbon flux in the atmosphere is directly proportional to the

difference between carbon concentrations in the furnace (C_P) and at the steel surface (C_S), the mass transfer coefficient was calculated as follows [15]:

$$\beta = \frac{\frac{\partial}{\partial t}\int_{x_\infty}^{x_0} C(x,t)\,dx}{\left(C_P - C_S\right)} = \frac{\left(\Delta M / A\right)}{t\left(C_P - C_S\right)}. \qquad (9)$$

Figure 5 presents the total carbon flux and the mass transfer coefficient as a function of the peak-to-valley roughness and relative surface area. The calculated β ranges from $1.1 \cdot 10^{-5}$ to $2.5 \cdot 10^{-5}$ cm/s depending on the initial surface roughness. These values are slightly lower than those reported by Newmann and Wyss [5] and may have resulted from deviations in the gas atmosphere composition and possibly different method of carburizing atmosphere preparation [3]. On the other hand, β calculated in this work are in good agreement with the results of other researchers [1,3,4] and correlate well with the mass transfer coefficient models for the given carburizing temperature and carbon potential in the furnace [2].

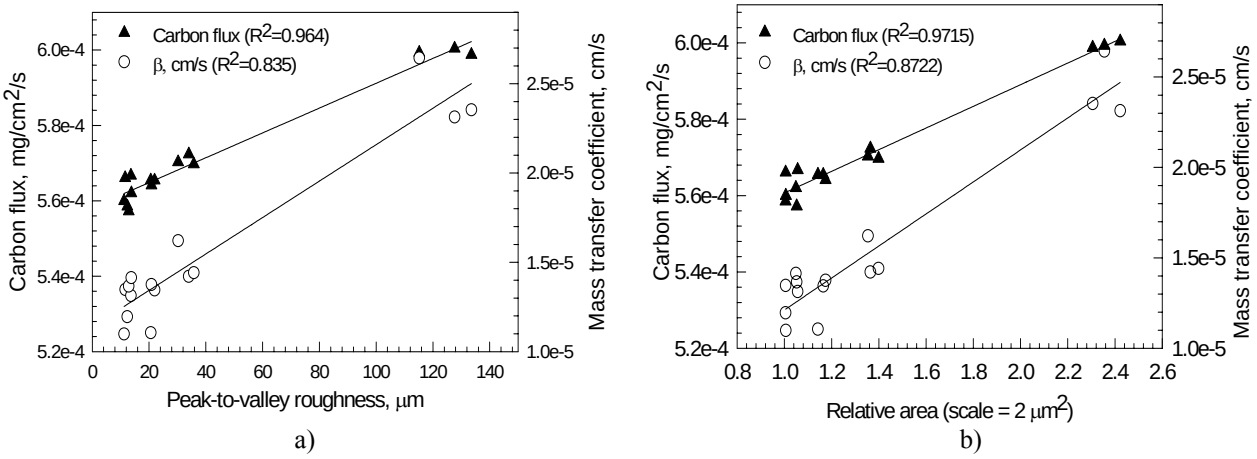

Figure 5. Total carbon flux and the mass transfer coefficient as a function of a) relative area at 2 μm^2 scale, and b) initial peak-to-valley surface roughness.

As hypothesized, both the carbon flux and the mass transfer coefficient increased with increasing surface roughness on the parts prior to carburizing. The R^2 values of the observed correlations indicate that the mass transfer characteristics are strongly dependent on the surface area available for the carburizing reaction. The relative surface area consistently provided higher coefficients of correlation for both – the measured characteristics (weight gain and surface

carbon concentration) and the calculated kinetic parameters. Therefore, it appears that the area-scale fractal analysis provides more adequate characterization of the surface roughness for this application and yields clear and direct physical interpretation for its influence on the carburizing performance.

To explain the observed phenomena, one should regard the steel surface as the interfacial area between the gas and solid phases where the carburizing reactions occur. Given the same process parameters, the samples with larger interfacial area (rougher surfaces) provide a greater number of sites available for the carburizing reaction. As a result, more carbon atoms are adsorbed at the steel surface, which establishes a steeper concentration gradient between the surface and the bulk of the workpiece. Such concentration gradients increase carbon flux within the steel and result in greater overall carbon uptake by the workpiece as observed in Table 5.

It is commonly accepted that the rate of carburization is determined by the combined control of surface reaction and carbon diffusion. In the initial time of carburizing surface reaction limits the process, therefore the weight gain at this stage is primarily determined by the surface area of the part, i.e. the number of sites available for the attachment of *CO* molecules and their decomposition. As such, even though in-situ monitoring of the instantaneous carbon flux in industrial carburizing is practically impossible, one may argue that the rougher surfaces enhance the instantaneous carbon flux through the gas-steel interface. From the kinetics standpoint, the greater rates of mass transfer establish steeper carbon gradient within the steel at near surfaces layers. According to Fick's laws of diffusion, the steeper concentration gradient further enhances carbon flux down the concentration gradient and will result in deeper case and more-carbon reach carburized layer

Modeling Carbon Concentration Profile

As a part of the project for the carburizing process control and optimization, it is equally important not only to identify the potential routes for the process improvement, but also to be able to control the optimized process performance. One of such control criteria is the effective case depth of the carburized layer. While the case depth during gas carburizing may be influenced by the various process parameters (temperature, carbon potential, gas carburizing atmosphere) and the steel alloy composition, it is the focus of this work to understand and model surface roughness effect on the carbon concentration profile and the corresponding case depth variability.

In a previous publication by the authors [16], a carburization model was developed to predict the carbon concentration profile and the corresponding case depth. This model is based on the finite difference approximation of the parabolic PDE governing carbon diffusion in steel and a set of boundary conditions, which account for the mass transfer in the atmosphere and the kinetics of the interfacial reactions. Figure 6-a compares the experimental and predicted carbon concentration profiles on the carburized parts with various initial surface roughness. While the prediction of carbon concentration profile is quite accurate, there is a large data variation, which arises from the fact that none of the existing mass transfer coefficient models accounts for the effect of the initial surface roughness. Furthermore, the experimentally determined relationship between the mass transfer coefficient and the surface roughness (Figure 5) was input as the boundary condition in the model and was plotted against the experimental carbon concentration profiles, as shown in Figure 6-b.

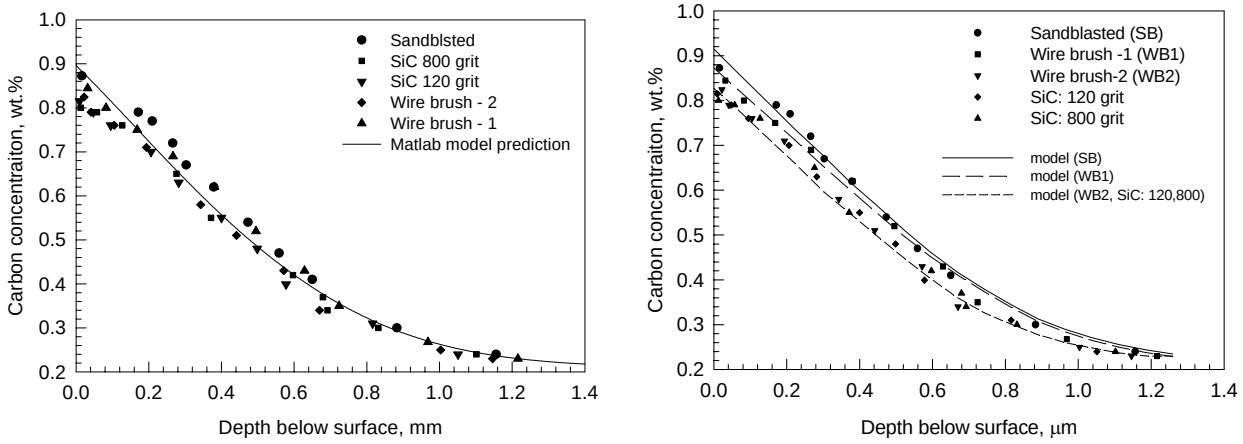

Figure 6. Carbon concentration profiles in the parts after carburizing: a) modeled with β from the referenced literature; b) modeled with $\beta = \beta$ (surface area) from Figure 5.

The carburization model with $\beta = \beta$ (surface area) shows very good agreement with the experimental data and adequately validates the model prediction. At near-surface layers the samples finished by sandblasting and wire brush-1 operation attained 0.05-0.1 wt.% more carbon than the parts with smoother surfaces. This difference remained significant until the depth of 0.4 wt.% C – corresponding to the effective case depth. Given that the parts were carburized in the same load, and therefore were subjected to identical carburizing conditions, the difference in

part-to-part surface roughness is the only the source of variation in the carbon concentration profiles and the effective case depth.

From the continuity equation of the mass accumulation and flux balance boundary condition, the weight gain represents the integrated area under the concentration profile. Therefore, the samples with rougher surfaces revealed larger carbon uptake and thus were characterized by the greater weight gain. Beyond the observation of higher carbon concentration in the parts with greater surface area, Figure 6 and Table 3 also suggest the presence of a threshold roughness value (Sq < 1.2 μm and St < 22 μm), below which the overall carbon uptake during carburizing becomes independent of the initial surface roughness. This observation agrees well with the observed weight gain and relative surface area, which were statistically insignificant for samples with wire brush-2, 120 grit and 800 grit surface finishes.

The total and effective case depths, summarized in Table 5, were obtained from the microhardness transverse (Rc 50) and the carbon concentration profiles (0.4 wt.%), respectively.

Table 5. Effective case depth based on carbon profiling and microhardness measurements.

Surface finish	Effective case depth to Rc 50	Effective case depth to 0.4 wt.% C	Total case depth (gradient method)
Sandblasting	0.86 mm	0.68 mm	0.93 mm
Wire brush - 1	0.84 mm	0.68 mm	0.89 mm
Wire brush - 2	0.83 mm	0.60 mm	0.81 mm
SiC: 120 grit	0.83 mm	0.60 mm	0.81 mm
SiC: 800 grit	0.83 mm	0.60 mm	0.81 mm

Although the observed case depths variation might not be considered critical, the data clearly suggest that carburizing parts in the same workload, and therefore, the same carburizing conditions will be affected by the final stage of the part's surface preparation. The total variation in the effective case depth up to +/- 0.04 mm and total case depth up to +/- 0.06 mm should be expected if the initial surface roughness varies from 0.23 to 18 μm (Sq) and 10 to 140 μm (St). This finding implies that the case depth variation is inevitable if an individual part consists of several segments with various surface finish requirements. If, however, the roughness on various segments of the part is kept below 1.2 μm (Sq) and 22 μm (St), these variations can be reduced or eliminated.

Conclusions

This paper presents the results and analysis of an experimental investigation of the effect of surface roughness and cleanliness on the mass transfer during gas carburizing and the corresponding case depth variation. Surface roughness was evaluated on the microscopic scale using area-scale fractal analysis. Based on the observed phenomena, the following conclusions have been made:

1. The rate of carburizing depends to a great extent on the surface roughness of the parts prior to carburizing. The calculated mass transfer parameters were directly proportional to the surface area available for carburizing, and showed good agreement with the data obtained by other researchers.

2. Carbon uptake by the steel surface increased with the increasing surface roughness, while smoother samples with surface roughness below 1.2 μm (Sq) and 22 μm (St) revealed no significant effect on the carbon concentration profile.

3. The previously developed carburization model and the observed correlation between surface area and the mass transfer coefficient were used to model the effect of surface roughness on the carbon concentration profile and the case depth variations.

4. Overall, the experimental data can further be used to determine an optimal initial surface roughness to maximize carbon uptake and minimize case depth variation, especially important for tolerance control and design considerations.

Acknowledgements

The support of the Center for Heat Treating Excellence (CHTE) at Worcester Polytechnic Institute (WPI) and the member companies is gratefully acknowledged. The authors would like to thank the Surface Metrology Lab at WPI, Surfract and TrueGage for their essential technical assistance in texture measurements and analysis. Special thank you goes to Bodycote, Caterpillar, DaimlerChrysler, Harley-Davidson, Houghton International for their support through facilities and work materials.

References

1. P. Stolar, and B. Prenosil "Kinetics of Transfer of Carbon from Carburizing and Carbonitriding Atmospheres," *Metallic Materials,* 22 (5) (1984), 348-353.

2. P. Si, Y. Zhang, S. Qin. And Y. Kong "Carbon Transfer Characteristics and Its Application on Gas Carburizing," *Heat Treatment of Metals*, 6 (1992), 51-55.

3. V.A., Munts, and A.P. Baskakov, "Mass Exchange in Carburization and Decarburization of Steel,"*Metal Science and Heat Treatment (English translation of Metallovedenie i Termicheskaya Obrabotka),* 25(1-2) (1983), 98-102.

4. M.F. Yan, Z. Liu, and G. Zu, "Study on Absorption and Transport of Carbon in Steel during Gas Carburizing with Rare-Earth Addition," *Materials Chemistry and Physics*, 70 (2) (2001), 242-244.

5. F. Neumann, and U. Wyss, "The Carburizing Effect of Gas Mixtures of the H_2-CH_4-H_2O-CO_2-CO System," *Harterei-Technische Mitteilungen*, 25 (4) (1970), 253-266.

6. G.H. Sedahmed and L.W. Shemilt, "Forced Convection Mass Transfer at Rough Surfaces in Annuli, *Letters in Heat and Mass Transfer*, 3 (5) (1976) 499-511.

7. M.G. Fouad, G.H. Sedahmed, H.A. El-Abd, "The Combined Effect of Gas Evolution and Surface Roughness on the Rate of Mass Transfer," *Electrochimics Acta*, 18 (1973), 279-281.

8. M.G. Fouad, and A. Zatout, "Mass-Transfer Rates at Rough Surfaces," *Electrochimica Acta*, 14 (9) (1969), 909-919.

9. R. Collin, S. Gunnarson, and D. Thulin, "Mathematical Model for Predicting Carbon Concentration Profiles of Gas-Carburized Steel," *Journal of the Iron and Steel Institute (London)*, 210 (1972), 785-789.

10. ASME B46 2002 National Standard B46.1, *Surface Texture, Surface Roughness, Waviness and Lay*, (New York, NY: American Society of Mechanical Engineers, 2002).

11. C.A. Brown, P.D. Charles, W.A. Johnsen, S. Chester, "Fractal Analysis of Topographic Data by the Patchwork Method," *Wear*, 161 (1-2) (1993), 61-67.

12. C.A. Brown, W. A. Johnsen, and R.M. Butland, "Scale-Sensitive Fractal Analysis of Turned Surfaces," *CIRP Annals - Manufacturing Technology*, 45 (1) (1996), 515-518.

13. Brown, C. A. and G. Savary, "Describing Ground Surface Texture Using Contact Profilometry and Fractal Analysis," *Wear*, 141 (2) (1991), 211-226.

14. A.J. Terry, and C. A. Brown, "Comparison of Topographic Characterization Parameters in Grinding," *CIRP Annals - Manufacturing Technology*, 46 (1) (1997), 497-500.

15. O. Karabelchtchikova and R.D. Sisson, Jr., “Carbon Diffusion in Steels – a Numerical Analysis based on Direct Integration of the Flux,” *Journal of Phase Equilibria and Diffusion*, 27 (6) (2006), 598-604.

16. O. Karabelchtchikova, Md. Maniruzzaman, and R.D. Sisson, Jr. “Carburization Process Modeling and Sensitivity Analysis using Numerical Simulation.” *Proc. MS&T 2006 Conference*, September 25-28 (2006) Cincinnati, OH, 375-386.

PAPER # 5: CARBON DIFFUSION IN STEEL – A NUMERICAL ANALYSIS BASED ON DIRECT FLUX INTEGRATION

(published in *Journal of Phase Equilibria and Diffusion,* 26 (6), 598-604)

Abstract

In the early 1970s Professor Dayananda developed a technique for the direct integration of fluxes from the concentration profiles in vapor-solid diffusion couples to determine diffusion coefficients and atomic mobilities. As part of a project to control and optimize the industrial carburization process in mild and low-alloyed steels, a modified integration analysis was applied to determine the mass transfer coefficient in the gas boundary layer and carbon diffusivity in austenite. Because carbon flux and surface carbon content vary with time during single-stage carburizing even with a fixed carbon potential in the atmosphere, a mass balance at the gas-solid interface must serve as boundary condition. This paper discusses the numerical modeling of the carburizing and focuses on calculating the mass transfer and carbon diffusivity parameters using the simulated concentration profiles. This approach validates the proposed method by comparing the calculated parameters with those used in simulation. The proposed method shows good predictability. The results were compared with previous determinations and predictions reported in the literature.

Introduction

Carburization is one of the oldest heat treatments used for surface hardening. Nonetheless, it experiences certain challenges associated with the process performance and reliability. As part of the process control and optimization study of industrial gas carburizing, this paper discusses modeling of the process and focuses on developing a method for calculating the coefficient of mass transfer at the gas boundary layer and the diffusion coefficient in steel during the process.

Carbon diffusivity is a main controlling parameter in the carburization heat treatment of steel, yet its value is difficult to measure. Often the coefficient of carbon diffusion is determined using solid-solid diffusion couple [1-3]. Application of such models to carburizing invariantly introduces a certain level of approximation and uncertainty due to a rough, though convenient,

assumption of constant surface concentration at the interface with time. More accurate modeling of the gas carburizing process must account for mass transfer from the carburizing gas atmosphere to the steel surface, surface reaction and further carbon diffusion into the steel. Mass transfer in the gas atmosphere is the rate limiting factor at the initial stages of carburizing [4,5] and carbon diffusion controls the process at longer times [6,7]; more often, however, carburizing is considered to be mixed controlled [8-11]. If these coefficients could be calculated from the carbon concentration profile as a function of various process parameters it would enable modeling and process control. This information could also be used for further process optimization.

The objective of this work is to develop a method for calculating the surface mass transfer and diffusion coefficients from carbon concentration profiles. The approach is based on numerical modeling of the carburizing process. Carbon diffusivity and the mass transfer coefficient from the literature are used to simulate carbon concentration profiles; and their comparison with the calculated coefficients from these concentration profiles is then used for validation of the method. Once tested, this technique will further be applied to the experimental data, where the coefficients are to be determined for a range of steels of various composition and various process parameters.

Available Methods for Measuring Carbon Diffusivity

Carbon diffusivity in austenite was first measured by Smith [12] using steady state method. The experimental setup included a steel tube which was carburized on the inside by natural gas decomposition and decarburized on the outside by wet hydrogen. The flux of carbon atoms was measured under steady state conditions by determining the number of carbon atoms per second carried by the wet hydrogen. Measuring the flux and carbon concentration profile, the coefficients of carbon diffusivities for a range of carbon concentration were determined.

Measurements of carbon diffusivity using diffusion-annealed couple were studied by various researchers [1-3,13,14]. In their analysis the coefficients of carbon diffusion were calculated from the concentration profiles using Boltzmann-Matano method [15]. The driving force for diffusion is the concentration gradient between the components of the diffusion couples and/or the differences in carbon activities due to the effect of alloying. While this approach to determining the coefficient of carbon diffusion in steel yields good approximation of the

diffusivity coefficient, it assumes time invariant carbon content at the interface of the two solids. When applied to carburizing this assumption implies that there is no resistance barrier to carbon transfer in the atmosphere and that diffusion in the steel is rate limiting. As a result, often we are not able to explain the effect of variations in furnace parameters, such as temperature, atmosphere characteristics and/or materials related parameters.

Dayananda developed a method of direct flux integration [16], which allowed calculation of the intrinsic diffusivities in solid-solid and solid-vapor diffusion couples. Assuming negligible interactions between fluxes at the lattice fixed frame of reference, the intrinsic flux of species within the solid is defined as

$$J = -C \cdot M \cdot \frac{\partial \mu}{\partial x} \cdot \frac{1}{N_{Av}}, \tag{1}$$

where C and M are carbon concentration and atomic mobility of the component, $\partial\mu/\partial x$ is the gradient in chemical potential and N_{Av} is Avogadro number. While the above equation is valid for all sections of the diffusion couple, the limitation to its usefulness, as pointed by Dayananda [16], is that the instantaneous intrinsic flux cannot be measured directly. To compensate for this limitation, the continuity equation was used which allowed the estimation of the cumulative intrinsic flux of atoms diffusing past the marker plane with time by integrating the corresponding area under the concentration profile:

$$\int_{x_0}^{x_\infty} C(x,t)\,dx = \frac{1}{N_{Av}} \int_0^t -C \cdot M \cdot \frac{\partial \mu}{\partial x}\,dt, \tag{2}$$

where x_0 is the initial location of the interface between the two components of the diffusion couple, x_∞ is the depth beyond which no concentration gradient exists, and t is the diffusion time. Based on the assumption of constant surface concentration, application of the Boltzmann parameter and Fick's law of diffusion yielded

$$D = C \cdot M \cdot \frac{\partial \mu}{\partial C} \cdot \frac{1}{N_{Av}}. \tag{3}$$

Dayananda's method of direct flux integration is extensively used in analysis of solid-solid and vapor-solid diffusion couples [17-21]. Considering carburizing process as diffusion in a vapor-solid diffusion couple, the goal of this paper is to develop a modified method for direct flux integration which would account for the surface boundary condition. As such, with slight modifications, the proposed method would allow one to calculate not only concentration dependent carbon diffusivity but the mass transfer coefficient as well.

Kinetics of Carbon Transfer in Carburizing

The process of gas carburizing of steel can be viewed as diffusion in a vapor-solid diffusion couple. Carbon transfer from the atmosphere to the solid is determined by the rate limiting process, which kinetically becomes the controlling stage of carburizing. The maximum carburizing rate is obtained when the carbon transfer from the atmosphere is equal or greater than the carbon diffusion rate in the solid state. Such diffusion controlled process has no deficiency of carbon supplied to the interface for its further transport into the solid. In this case the assumption of constant surface carbon content can be justified. In practice, however, the carbon transfer from the atmosphere to the solid boundary is often reported to be the rate limiting factor [4,5] especially at the start of the carburizing process. After this initial stage, the process becomes mixed controlled [8-11] and should be modeled correspondingly.

Gas carburizing is modeled using parabolic PDE for carbon diffusion in steel and a set of boundary conditions accounting for the mass transfer coefficient:

$$\frac{\partial C}{\partial t} = \frac{\partial}{\partial x}\left(D\frac{\partial C}{\partial x} \right) + u \cdot \frac{D}{r + ux} \cdot \frac{\partial C}{\partial x}, \tag{4}$$

where $u = -1$ for convex surface, $u = 0$ for plane surface and $u = 1$ for concave surface, D is the coefficient of carbon diffusion in steel, x is the distance from the surface, r is the radius in case of convex or concave surfaces.

The boundary condition is specified by assuming a mass balance at the steel surface:

$$\beta\left(C_P - C_S \right) = -D\frac{\partial C}{\partial x}, \tag{5}$$

where $\partial C/\partial x$ is carbon concentration gradient at the surface and β is the mass transfer coefficient (cm/s), which accounts for all the phenomena at the phase boundary between gas atmosphere and steel [4]. Therefore, the two primary parameters governing carburizing are the mass transfer coefficient (β) and carbon diffusivity (D) in austenite.

Numerical Approach to the Parameters Calculation

Carbon Profiles Simulation

Since the analytical solution to carbon diffusion in steel (Equation 4) with the flux balance boundary conditions (Equation 5) is not available for concentration dependent diffusivity, the method proposed in this paper is based on a numerical analysis. A computer program was written in the MATLAB, which transformed the governing PDE with its corresponding boundary conditions into a set of finite difference equations. Initially carbon concentration profiles were generated with the mass transfer coefficient (β) and carbon diffusivity (D) from the literature. Then these concentration profiles were analyzed to determine the β and D coefficients. As such, this approach served two purposes: 1) preliminary computer experiments tested the technique's capability using numerically simulated data, and 2) calculated values of the parameters were validated by comparing them against the parameters used for the concentration profiles generation.

Dusinberre numerical method [23] was employed in the study as it enables one to relate boundary conditions to the rate of carbon transfer at the gas boundary layer and across the steel surface. Concentration profiles were computed using an iterative method for generating the case into a solid of semi-infinite geometry initially at uniform concentration. The method is second order accurate and provides a stable convergent solution. Assuming a simple plane geometry and one-dimensional diffusion, the following expression transforms continuum Equation 4 to the finite difference expression

$$C_i^{t+\Delta t} = \frac{\Delta t}{(\Delta x)^2}\left[D_i^t \left(C_{i-1}^t - 2C_i^t \left(\frac{(\Delta x)^2}{D_i^t \Delta t} - 2 \right) + C_{i+1}^t \right) + \frac{\left(D_{i+1}^t - D_{i-1}^t\right)\left(C_{i+1}^t - C_{i-1}^t\right)}{4} \right]. \quad (6)$$

To account for the mass transfer at the surface, carbon concentration at the boundary nodes was calculated as

$$C_{surf}^{t+1} = \frac{1}{N_1} \cdot \left[2N_2 \cdot C_P + \left[N_1 - \left(2N_2 + 2 \right) \right] C_{surf}^{t} + 2C_{x_1}^{t} \right], \tag{7}$$

where

$$N_1 = \frac{D \cdot \Delta t}{\left(\Delta x \right)^2} \quad \text{and} \quad N_2 = \frac{\beta}{D} \cdot \Delta x \,. \tag{8}$$

The two stability criteria were assured to be fulfilled simultaneously: $N_1 > 2$, and $N_1 > 2N_2 + 2$, where N_2 is the equivalent Biot number, which relates the mass transfer resistance within the steel and at the steel surface. The maximum stable time increment from the previously determined grid space interval, D and β values was calculated as

$$\Delta t < \frac{\left(\Delta x \right)^2}{2\beta \cdot \Delta x + 2D}. \tag{9}$$

The input diffusivity values for carbon profiles simulation were calculated from the equations for carbon diffusion in austenite reported in the literature [10-12,24-33]. These equations were subdivided in two categories: the equations that depend on temperature only and those that consider carbon content in the steel as well. To account for variation of diffusivity with concentration, the values were re-calculated for instantaneous carbon concentration level along every space and time increment. Each of the two sets of the diffusivity equations was used to calculate the mean values which served as input for carbon diffusivity in the MATLAB code execution.

It was assumed that no volume change takes place in the crystal lattice of austenite during carburizing, which is a valid assumption for interstitial diffusion processes [29]. The results of the numerically simulated carbon profiles are given in Figure 1, and the adequacy of the prediction was tested by comparing the simulation results with the available analytical solution for the flux balance boundary condition and constant carbon diffusivity [34].

$$\frac{C\left(x,t\right) - C_0}{C_P - C_0} = erfc\left(\frac{x}{2\sqrt{Dt}} \right) - \exp\left(\frac{\beta x + \beta^2 t}{D} \right) \cdot erfc\left(\frac{x + 2\beta t}{2\sqrt{Dt}} \right). \tag{10}$$

Given the sufficiently small spatial increment used for the calculation, the numerical solution for any time greater than 0.25 hour accurately reproduced the analytical solution in Equation 10. This comparison validated the accuracy of the numerical calculation and gave confidence to further use the code for modeling carburizing using concentration dependent diffusivities.

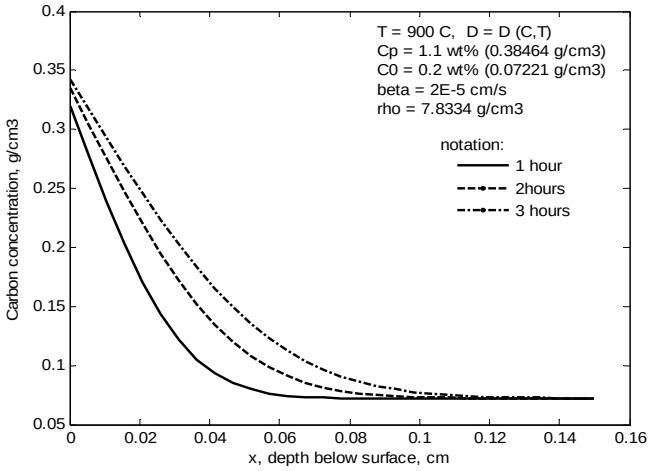

Figure 1. Numerically calculated carbon concentration profiles after 2 hours of carburizing at T = 900 °C and Cp = 1.1 wt.%.

Calculation of the Mass Transfer Coefficient

From the flux balance condition at the steel interface and continuity equation of the mass accumulation within the solid, the rate at which the total mass of the solid changes per unit cross section area is

$$\int_{x_\infty}^{x_0} C(x,t)\,dx = \int_{t_0}^{t_f} J dt = \frac{\Delta m}{A}, \tag{11}$$

where m is the mass and A is the surface area of the workpiece.

The total quantity of the species diffusing through the surface is found by integrating the concentration profile over the depth of the carburized layer. Further differentiation of the total weight gain by the steel over the carburizing time yields the following expression for the total flux of carbon atoms through the vapor/solid interface:

$$J^t = \frac{\partial(\Delta m/A)}{\partial t} = \beta\left(C_P - C_S^t\right). \tag{12}$$

Assuming time dependent nature of the process, the mass transfer coefficient can be found as

$$\beta^t = \frac{\frac{\partial}{\partial t}\int_{x_\infty}^{x_0} C(x,t)\,dx}{\left(C_P - C_S^t\right)} = \frac{\left(\Delta m / A\right)\Big|_{t_0 \to t}}{t\left(C_P - C_S^t\right)}. \qquad (13)$$

If weight gain is expressed in [g/cm^2], time in [s], and carbon concentration in [g/cm^3], calculated by this method mass transfer coefficient will have units of [cm/s].

An example of such calculation of the mass transfer coefficient is shown in Figure 2. As follows from Equation 16 the data needed for the calculation includes: 1) total weight gain obtained by integrating total flux over carburizing time, and 2) time evolution of the surface carbon concentration. The input value for β of $2\cdot10^{-5}$ cm/s was used for the concentration profiles generation, while the calculated value of $2.046\cdot10^{-5}$ cm/s was obtained by application of the described above method. The predictability was found to be dependent on selection of the spatial grid size parameter. The predicted values corresponding to the initial time of carburizing were affected by the numerical error arising from the finite difference approximation; therefore, such initial transient part should not be used.

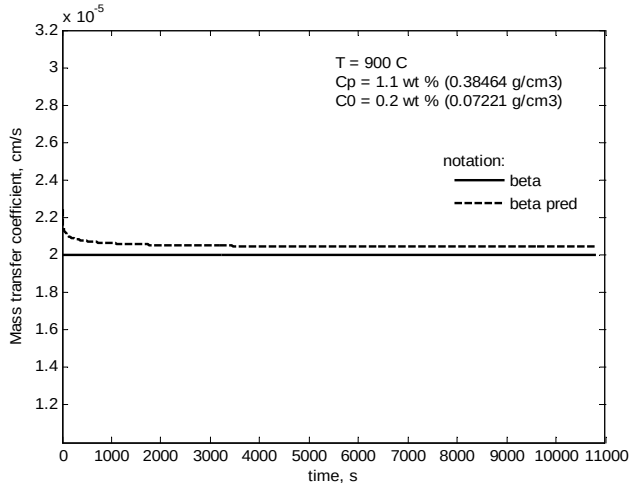

Figure 2.Comparison of the calculated values of the mass transfer coefficient with the one used in carbon concentration profile simulation.

According to Rimmer and co-authors [35] the mass transfer coefficient in "technical" carburizing atmospheres, consisting of endogas and natural gas enrichment, may range from $1.3\cdot10^{-5}$ to $2.7\cdot10^{-5}$ cm/s. The result of β calculation for a range of input parameters is shown in

Figure 3. The observed R^2 of the parameters correlation suggests that the accuracy of the calculation is independent of the parameters magnitude and gives a relative error of only 2.56% as seen from the slope of the fitted relationship.

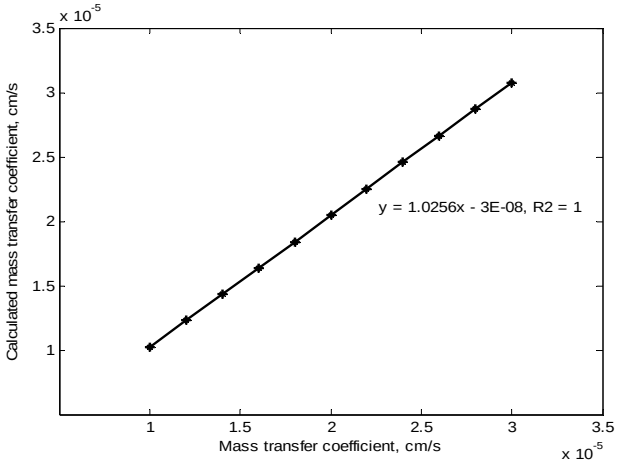

Figure 3. Correlation of the mass transfer coefficient used in simulation and the corresponding calculated values for a range of input parameters

Calculation of the Coefficient of Carbon Diffusion

As in β calculation, the weight gain of the diffusing species in steel during carburizing was found by integrating the concentration profile over distance at which the gradient exists

$$\frac{d}{dt}\int_{x_\infty}^{x_0} C(x,t)\,dx - J(x_0) = 0. \tag{14}$$

Assuming an isotropic media, the flux of the diffusing substances through a unit area is proportional to the concentration gradient measured normal to the section:

$$J(x_0) = -D(x_0)\cdot\frac{dC}{dx}(x_0,t). \tag{15}$$

By equating the above two equations, the following expression for the diffusion coefficient from the concentration profiles can be derived

$$D(x_0) = -\left(\frac{dC(x_0,t)}{dx}\right)^{-1}\cdot\frac{d}{dt}\int_{C_0}^{C} x\,dC \quad . \tag{16}$$

Based on the proposed method, carbon diffusivity calculation requires at least two different concentration profiles for time differentiation of the corresponding weight gain. The diffusivity calculation involves the product of the two components: negative inverse of the slope at any position of the concentration profile and differentiated with respect to time integrated area under the corresponding section of the profile. The results of the diffusivity coefficient calculation as opposed to the actual diffusivity values used for the profiles generation are shown in Figure 4.

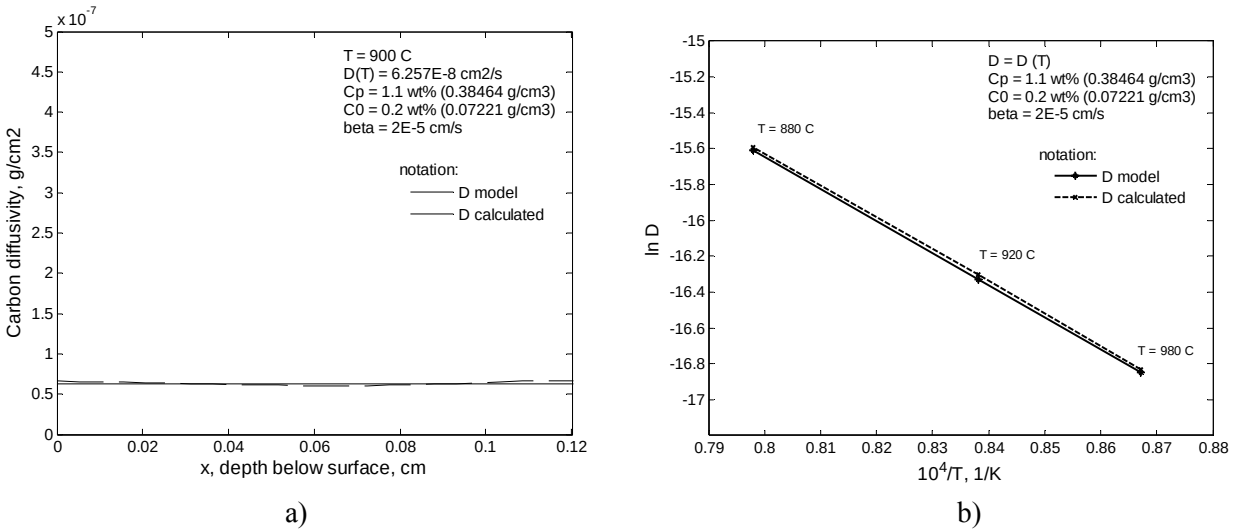

a) b)

Figure 4. Comparison of the predicted values of carbon diffusion coefficient D=D(T) with the modeled values, used in the concentration profile simulation: a) as a function of distance, b) Arrhenius type plot.

As in the case of calculating the mass transfer coefficient, the predicted values of carbon diffusivities have some error due to the numerical approximation. This error is observed at depths where carbon gradient asymptotically approaches zero. The corresponding rate of the weight gain change (term 2 in Equation 16) becomes negligible, and its further multiplication by the inverse of the slope causes erroneous result. As such, it follows that this method can successfully be applied to the range of concentration profile with concentration gradient greater than zero.

While prediction of the diffusivities independent of carbon concentration is very accurate (Figure 4), the technique applied to determining concentration dependent coefficients of diffusion have some prediction error at the near-surface layer (Figure 5). This difference between the input diffusivity and the calculated values arises from the estimation of the finite

difference at the surface and consecutive recalculation of the carbon diffusion coefficient corresponding to the instantaneous carbon content at every depth of the profile.

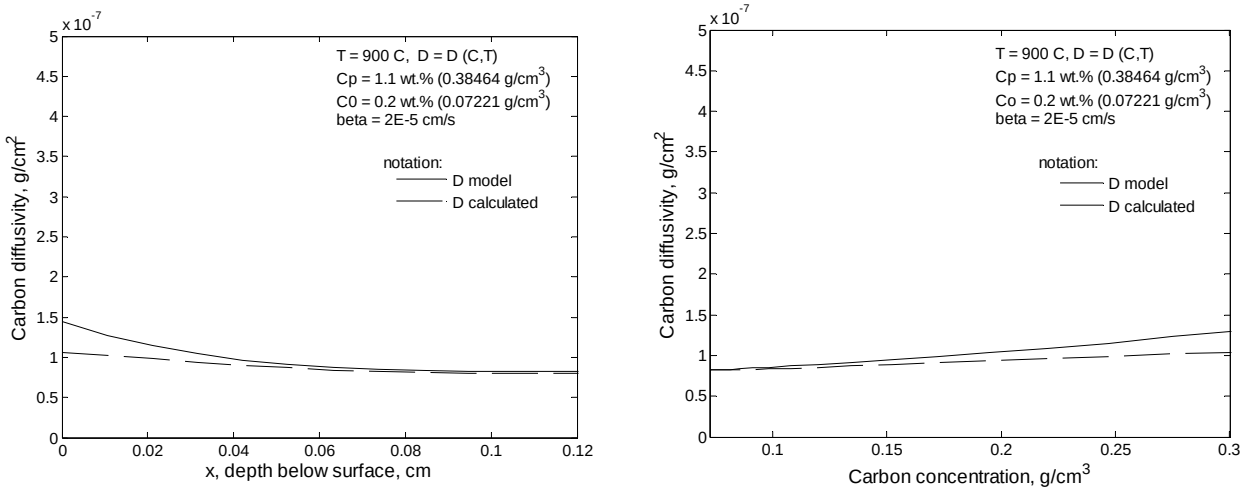

Figure 5. Comparison of the predicted values of carbon diffusion coefficient D=D(C,T) with the modeled values, used in carbon concentration profile simulation: a) as a function of depth, b) as a function of carbon content.

Conclusions

In this paper the carburizing process was modeled using a finite difference method. The model prediction was validated by comparing the generated concentration profiles with the analytical solution for constant diffusivity. The ongoing work uses these numerical simulations as a new method to calculate the mass transfer and concentration dependent carbon diffusivity in austenite from the carbon concentration profile. The adequacy of the method was validated by comparing the calculated coefficients against the models used in the profiles generation.

The proposed method revealed good predictability and can be applied to determine the mass transfer coefficient in any vapor-solid diffusion system and any size of the steel part with no restriction on Biot number. Successful application of the method requires available data on surface carbon concentration evolution with time and carbon concentration profile. To the authors' best knowledge, no time dependent mass transfer models were available in the published literature; therefore, at this moment it was not possible to test the prediction power to the variable mass transfer coefficient. Although it is clear that the proposed method may also be used for time dependent parameter calculation.

Similar to the mass transfer coefficient, the calculation of carbon diffusivity from the concentration profiles was capable of predicting the values which agreed quite well with the input diffusivity models. The calculated values were slightly larger than the input values due to finite difference approximation.

Overall, since the proposed method for the mass transfer parameters calculation involves measurement of slopes and areas under the concentration profiles, it is possible that such calculation using experimental data will have some level of uncertainty associated with it. Nonetheless, successful implementation of this technique gives a method for further analyses and will be validated using the experimental data. As such, the calculated mass transfer and carbon diffusivity values can then be related to the process parameters and materials characteristics and may further be used for the carburizing process control and optimization.

Acknowledgements

The support of the Center for Heat Treating Excellence (CHTE) at Worcester Polytechnic Institute and the member companies is gratefully acknowledged. The authors also would like to thank Prof. Sullivan, Dr. Md. Maniruzzaman, and Dr. V. Tenishev for their assistance and valuable discussions.

List of References

1. C. Wells and R.F. Mehl, Rate of Diffusion of Carbon in Austenite in Plain Carbon , in Nickel and in Manganese Steels, American Institute Mining Metallurgical Engineers, Technical Publication, 1940, 1180.
2. K.E. Blazek and P.R. Cost, Carbon Diffusivity in Iron-Chromium Alloys, *Transactions of the Japanese Institute of Metals,* 1976, **17**(10), p 630-636
3. W. Batz, and R.F. Mehl, Diffusion Coefficient of Carbon in Austenite, *Transactions of AIME*, 1950, **188**, p 553-560
4. P. Stolar and B. Prenosil, Kinetics of Transfer of Carbon from Carburising and Carbonitriding Atmospheres, ***Metallic Materials*** (English translation of Kovove Materialy), 1984, **22**(5), p 348-353
5. B.A. Moiseev, Y.M. Brunzel', and L.A. Shvartsman, Kinetics of Carburizing in an Endothermal Atmosphere, *Metal Science and Heat Treatment* (English translation of Metallovedenie i Termicheskaya Obrabotka Metallov), 1979, **21**(5-6), p 437-442

6. H.W. Walton, Mathematical Modeling of the Carburising Process for Microprocessor Control, *Heat Treatment of Metals,* 1983, **10**(1), p 23-26

7. E.L. Gyulikhandanov and A.D. Khaidorov, Carburizing Low-Carbon Heat-Resistant Steels Containing Molybdenum and Titanium, *Metal Science and Heat Treatment* (English Translation of Metallovedenie i Termicheskaya Obrabotka Metallov), 1991, **33**(5-6), p 344-348

8. M. Yan, Z. Liu, and G.Zu. , The Mathematical Model of Surface Carbon Concentration Growth during Gas Carburization, *Materials Science Progress*, 1992, **6**(3), p 223-225, in Chinese

9. T. Turpin, J. Dulcy, and M. Gantois, Carbon Diffusion and Phase Transformations during Gas Carburizing of High-Alloyed Stainless Steels: Experimental Study and Theoretical Modeling, *Metallurgical Transactions A*, 2005, **36**(10), p 2751-2760

10. A. Ruck, D. Monceau, and H.J.Grabke, Effects of Tramp Elements Cu, P, Pb, Sb and Sn on the Kinetics of Carburization of Case Hardening Steels, *Steel Research,* 1996, **67**(6), p 240-246

11. R. Collin, S. Gunnarson, and D. Thulin, Mathematical Model for Predicting Carbon Concentration Profiles of Gas-Carburized Steel, *Journal of the Iron and Steel Institute*, 1972, **210**, p 785-789

12. R.P. Smith, The Diffusivity of Carbon in Iron by Steady-State Method, *Acta Metalurgica*, 1953, **1**, p 578-587

13. S.K. Bose and H.J. Grabke, Diffusion Coefficient of Carbon in Fe-Ni Austenite in the Temperature Range 950-1100 Degree C, *Zeitschrift fuer Metallkunde*, 1978, **69**(1), p 8-15

14. S.K. Roy, H.J. Grabke, and W. Wepner, Diffusivity of Carbon in Austenitic Fe-Si-C Alloys, *Archiv fuer das Eisenhuettenwesen,* 1980, **51**(3), p 91-96

15. C. Matano, On the Relation between the Diffusion-Coefficients and Concentrations of Solid Metals, *Japanese Journal of Physics*, 1933, **8**(3), p 109-113

16. M.A. Dayananda, Atomic Mobilities in Multicomponent Diffusion and Their Determination, *Transactions of AIME*, 1968, **242**, p 1369-1372

17. M.A. Dayananda and C.W. Kim, Zero-Flux Planes and Flux Reversals in Cu-Ni-Zn Diffusion Couples, *Metallurgical Transactions A*, 1979, **10**(9), p 1333-1339

18. P.T. Carlson, M.A. Dayananda, and R.E. Grace, Diffusion in Ternary Ag- Zn- Cd Solid Solutions, *Metallurgical Transactions A,* 1972, **3**(4):, p 819-26

19. A.L. Hurley and M.A. Dayananda, Multiphase Diffusion in Ag-Zn Alloys, *Metallurgical Transactions A*, 1970, **1**(1), p 139-43

20. N.R. Iorio, M. A. Dayananda, and R.E. Grace, Intrinsic Diffusion and Vacancy Wind Effects in Ag-Cd Alloys, *Metallurgical Transactions A*, 1973, **4**(5), p 1339-1346

21. G.H. Cheng, M.A. Dayananda, and R.E. Grace, Diffusion Studies in Ag-Zn Alloys, *Metallurgical Transactions A*, 1975, **6**(1), p 21-27

22. J. Dulcy, P. Bilger, D. Zimmermann, and M. Gantois, Characterization and optimization of a carburizing treatment in gas phase: Definition of a new process, *Metallurgia Italiana*, 1999, **91**(4), p 39-44

23. W.H. McAdams, Heat Transmission, New York, McGraw-Hill, 1954, p 43-50

24. B. Million, K. Bacilek, J.Kucera, P. Michalicka, and A. Rek, Carbon Diffusion and Thermodynamic Characteristics in Chromium Steels**,** *Zeitschrift fuer Metallkunde* (Materials Research and Advanced Techniques), 1995, **86**(10), p 706-712

25. J. Kucera, and K. Stransky, The Dependence of Carbon Diffusion Coefficients in Austenitic Ternary Alloys on Concentration of Additive Elements, *Acta Technica CSAV* (Ceskoslovensk Akademie Ved), 2003, **48**(4), p 353-364

26. R.P. Smith, The Diffusivity of Carbon in γ-Fe-Co Alloys, *Transactions of AIME*, 1964, **230**, p 476-480

27. M.M. Thete, Simulation of Gas Carburising: Development of Computer Program with Systematic Analyses of Process Variables Involved, *Surface Engineering*, 2003, **19**(3), p 217-228

28. G.G. Tibbetts, Diffusivity of Carbon in Iron and Steels at High Temperatures, *Journal of Applied Physics*, 1980, **51**(9), p 4813-4816

29. J.I. Goldstein and A.E. Moren, Diffusion Modeling of the Carburization Process, *Metallurgical Transactions A*, 1978, **9**(11), p 1515-1525

30. G.E. Totten and M.A.H. Howes, Steel Heat Treatment Handbook, Marcel Dekker, Inc., NY, 1997

31. L. Sproge and J.Agren, Experimental and Theoretical Studies of Gas Consumption in the Gas Carburizing Process, *Journal of Heat Treating*, 1988, **6**, p 9-19

32. J. Agren, Revised Expression for the Diffusivity of Carbon in Binary Fe-C Austenite, *Scripta Metallurgica*, 1986, **20**(11), p 1507-1510

33. R.M. Asimow, Analysis of the Variation of the Diffusion Constant of Carbon in Austenite with Concentration, *Transactions of AIME,* 1964, **230**(3), p 611-613

34. J. Crank, *The Mathematics of Diffusion*, 1st ed., Oxford, UK, Clarendon Press, 1956, p 42-62

35. K.E. Rimmer, E. Schwarz-Bergkampf, and J. Wunning, Surface Reaction Rate in Gas Carburizing, *Haerterei-Technische Mitteilungen*, 1975, **30**(3), p 152-160

PAPER # 6: CALCULATION OF GAS CARBURIZING KINETIC PARAMETERS FROM CARBON CONCENTRATION PROFILES BASED ON DIRECT FLUX INTEGRATION

(published in *Defect and Diffusion Forum,* vol. 266: 171-180)

Abstract

Initiated by the need of industry for gas carburizing process control and optimization, this paper focuses on understanding the effect of the time, temperature and carbon potential on the mass transfer coefficient and carbon diffusivity in austenite. A method for direct flux integration has previously been proposed to calculate these kinetic parameters from the experimental carbon concentration profiles. AISI 8620 steel discs were gas carburized at different levels of atmosphere carburizing potential for selected austenizing temperatures. Analyses of the carburized parts included experimental measurement of weight gain, surface carbon concentration and carbon concentration profiles. The time-dependent weight gain and surface carbon content measurements allowed calculation of the time average mass transfer coefficient, while carbon concentration profiles were used to calculate the concentration dependent carbon diffusivity for selected process parameters. Excellent agreement was found between the calculated mass transfer coefficient and carbon diffusivity values and those reported in the literature. The calculated values served as input in the previously developed carburizing model validating the predicted results by comparison with the experimental concentration profiles.

Introduction

Gas carburizing is one of the oldest heat treatment processes used for surface hardening. During the process, low carbon steel is exposed to a high carbon potential atmosphere, which causes carbon atoms to diffuse down the chemical potential gradient and establishes carbon gradient at near-surface layer. Mechanical properties of the carburized layer depend on the number of interrelated factors and include the effect of process parameters, base material and surface characteristics. Although the mechanism of carburizing is well understood, there are certain challenges in the process performance and reliability. As part of the process control and optimization study of industrial gas carburizing, this paper focuses on the development and

experimental validation of the method for calculating the mass transfer coefficient in the atmosphere and carbon diffusivity in austenite.

Carbon diffusivity is a main controlling parameter in the carburization heat treatment of steel, yet its value is difficult to measure. The carbon diffusion coefficients have been determined using solid-solid diffusion couple [1-3]. Application of such models to carburizing introduces a certain level of approximation and uncertainty due to a rough, though convenient, assumption of constant surface concentration at the interface with time. More accurate modeling of the gas carburizing process must account for the mass transfer from the carburizing gas atmosphere to the steel surface, surface chemical reactions and further carbon diffusion into the steel. Mass transfer in the gas atmosphere is the rate limiting factor at the initial stages of carburizing [4,5] and carbon diffusion controls the process at longer times [6,7]; more often, however, carburizing is considered to be mixed controlled [8-11]. If these coefficients could be calculated from the carbon concentration profile as a function of various process parameters it would enable modeling and process control.

The objective of this work is to experimentally validate the previously developed method of direct flux integration [12] to calculate the mass transfer coefficient in the carburizing atmosphere and carbon diffusivity in austenite from the experimental carbon concentration profiles. Calculations performed for a range of carburizing process conditions will enhance understanding of the effect of the process parameters on the kinetics mass transfer during gas carburizing. This knowledge can further be applied to optimize and control the carburizing process.

Kinetics of Carbon Transfer in Carburizing

The process of steel gas carburizing can be viewed as diffusion in a vapor-solid diffusion couple. The mass transfer coefficient (β) defines the flux of carbon atoms from the atmosphere to the steel surface and the coefficient of carbon diffusion in austenite (D) determines the rate of mass transfer within the steel. Carbon transfer from the atmosphere to the steel is determined by the rate limiting process, which kinetically becomes the controlling stage of carburizing. The maximum carburizing rate is obtained when the carbon transfer from the atmosphere is equal or greater than the carbon diffusion rate in the steel. Such a diffusion-controlled process has no deficiency of carbon supplied to the interface for its further transport into the solid. In practice, however, the process is mixed controlled, where both the mass transfer in the atmosphere and

carbon diffusivity contribute [8-11]. Assuming that no sooting occurs during the process, the mass balance at the gas-steel interface can be expressed as follows:

$$\beta\left(C_P - C_S\right) = -D\frac{\partial C}{\partial x},$$

where C_P is the carburizing potential in the atmosphere, C_S is the surface carbon concentration and $\partial C/\partial x$ is the carbon concentration gradient at the gas-steel interface. From Equation 1 it is clear that the two control parameters governing the rate of carburizing and determining the final carbon profile are the mass transfer coefficient (β) and carbon diffusivity (D) in austenite.

Considering the carburizing process as the diffusion in vapor-solid diffusion couple, the goal of this paper is to experimentally validate the previously developed method of direct flux integration to calculate β and D [12]. Historically, the coefficient of mass transfer in the atmosphere was calculated from the lumped analysis using wire or foil [4,13-16]. An additional experimental setup would be required to calculate the carbon diffusivities in austenite. On the contrary, the modified method of direct flux integration offers an advantage of calculating both of these kinetic parameters from a simple experimental setup. Once proved to be accurate and effective, the methods can serve as a tool for understanding the effect of process parameters on the kinetics of the mass transfer during gas carburizing, and can successfully be used for the process control and optimization.

Experimental Procedure

Material used for this study was AISI 8620 steel. The chemical composition is given in Table 1. The cylindrical steel bars were supplied in hot rolled condition. Microstructural analysis revealed a mixture of ferrite and pearlite distributed uniformly in the transverse direction and having a banded structure in the longitudinal direction parallel to the direction of rolling. The steel bars were normalized at 900 ºC for 4 hours, which reduced the grain size from 6.5 to 8 (ASTM E112) and reduced the banded anisotropy as seen in Figure 1.

Table 1. AISI 8620 steel chemical composition [wt.%]

C	Mn	P	S	Si	Ni	Cr	Mo
0.21	0.83	0.008	0.031	0.25	0.65	0.57	0.16

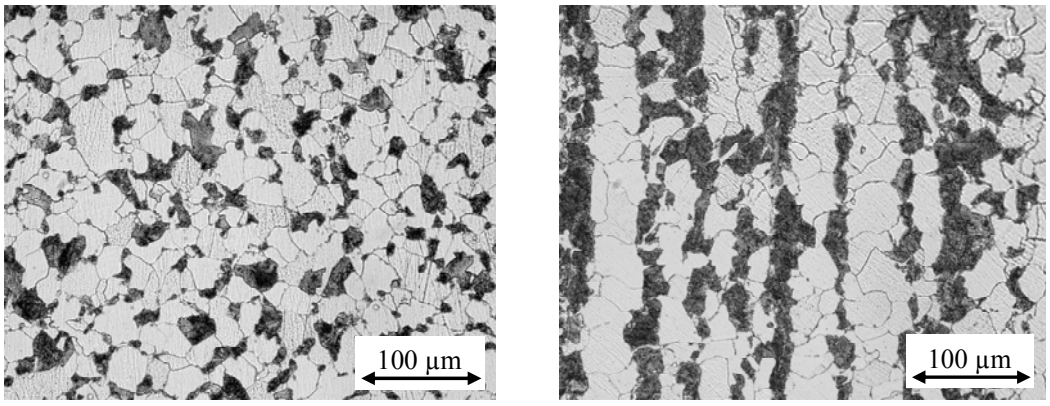

a) b)

Figure 1. Microstructure of AISI 8620 steel samples after normalizing, 2% nital etch: a) transverse direction, b) longitudinal direction.

The bars were machined into disks 3.125 cm in diameter and 1 cm in thickness and were carburized in an Integral Quench furnace with an endothermic carburizing atmosphere produced by blending the carrier endogas with natural gas enriching. A total of six combinations of the carburizing process parameters were explored: temperature (900, 925, and 950 ºC) and the atmosphere carbon potential (0.9 and 1.1 wt.% C). For every combination of the experimental factors, the parts were carburized for 15, 30, 60, and 120 min, which allowed recording time-dependent weight gain, surface carbon concentration evolution and the carbon concentration profiles. The weight gain measurements were collected on laboratory scales sensitive to 0.1 mg. Surface carbon concentration and carbon concentration profiles were measured by spectral analysis using LECO-OES with +/- 0.01 wt.% C measurement error. A layer of the material of exact known depth was sequentially removed from the surface and analyzed for its chemical composition. This procedure repeated until a zero-gradient was reached, which indicated the bulk carbon content.

Results and Analysis

Weight Gain and Surface Carbon Evolution

Figure 2 shows the experimental measurements of weight gain and surface carbon evolution during carburizing. According to the flux balance boundary condition at the gas-steel interface, the instantaneous surface carbon concentration is determined by the balance between the carbon flux in the atmosphere and the rate of carbon diffusion in steel. Correspondingly, the observed surface carbon concentration was explained primarily by the effect of carbon potential in the atmosphere, and to a much smaller degree, by the effect of carburizing temperature.

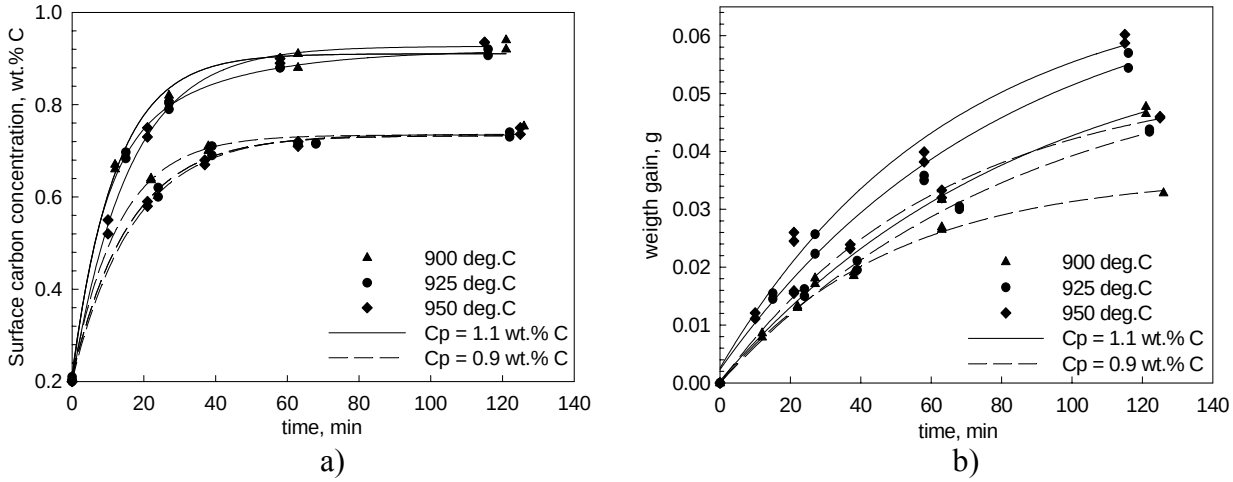

Figure 2. Surface carbon concentration (a) and weight gain (b) evolution during carburizing.

Since the experimental weight gain is the measure of total carbon flux into the steel, it accounts both for the rate of carbon transfer in the atmosphere and the rate of carbon diffusion in the steel. Therefore, the data reveal a clear increasing trend in weight gain with an increasing driving force for carburizing ($C_P - C_S$) and the carburizing temperature.

Calculation of the Mass Transfer Coefficient

Figure 3 shows the mass transfer coefficients calculated from the experimental weight gain and surface carbon concentration using the previously developed method of direct flux integration [12]. The calculated β range from $1.2 \cdot 10^{-5}$ to $2 \cdot 10^{-5}$ cm/s depending on the carburizing conditions and agree well with the results of other researchers [4,15-17]. It was observed that the

mass transfer coefficient decreases with carburizing time and can be explained by the following considerations. In the initial time of carburizing the process is controlled by the rate of mass transfer from the atmosphere to the steel surface. As time proceeds, carburizing becomes diffusion controlled and limits the amount of carbon flux entering the surface. The corresponding increase in the surface carbon concentration increases carbon activity at the steel surface [13], and therefore decreases the overall driving force for carburizing (a_c^{gas} - a_c^{surf}).

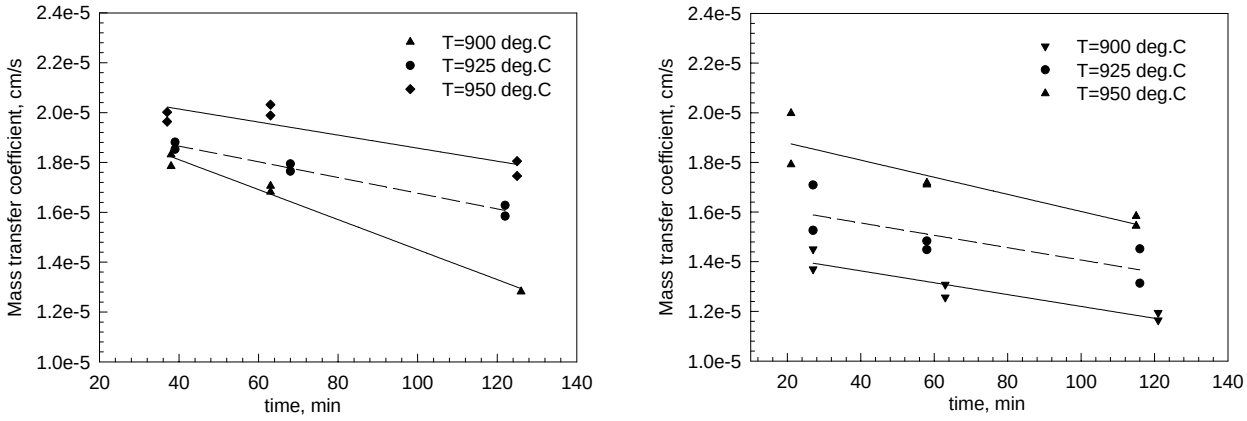

Figure 3. Calculated mass transfer coefficient in the atmosphere with: a) Cp=0.9 wt.%, and b) Cp=1.1. wt.% C

The mass transfer coefficient is often expressed as the ratio between the rate coefficient for the chemical reactions at the steel surface and the carbon activity at the steel surface ($\beta = k/a_c^{surf}$) [4,13,18]. Grabke [19] also reported the carburizing reaction rate to be a function of the surface carbon concentration ($\beta = k/C_S$). Since carbon activity is directly proportional to the degree of carbon saturation at the steel surface [13], the overall mass transfer coefficient should also decrease with surface carbon evolution, i.e. with increasing carburizing time. Despite all these arguments, it has been a common practice to assume constant with time β for modeling and controlling the carburizing process.

As follows from Figure 3, the mass transfer coefficient increases with a decreasing carburizing potential in the atmosphere. This observation agrees well with the measurements of other researchers using carburized wire and foils [4,14-16]. While the effect of carbon potential on the mass transfer coefficient is well established, there is a discrepancy in the reported effect of temperature on the mass transfer coefficient. Wunning [20] and Rimmer et.al [21] studied

carburizing of foils in an endothermic atmospheres and reported β to be independent of the carburizing temperature. Opposed to these results, a number of studies [14,22,23] observed significant change in β due to the effect of temperature. As the rate of carbon diffusion increases with increasing temperature, a greater carbon demand is established, allowing for more carbon to enter the surface and diffuse down the concentration gradient. Therefore, the mass transfer coefficients calculated in this work were observed to be thermally activated and increase with increasing carburizing temperature.

Calculation of the Carbon Diffusion Coefficient

Figure 4 shows the carbon diffusivities calculated from the experimental carbon concentration profiles at 925 °C, while Figure 5 shows the diffusivities for various carburizing temperatures and carbon concentration. The coefficients of carbon diffusion calculated in this work agree well with other carbon diffusivity models [10,24-27]. The calculated activation energy for carbon diffusion in austenite decreased with increasing carbon concentration and agrees well with the referenced diffusion data [28]. Overall, this validates the method of direct flux integration for calculating the mass transfer coefficient in the atmosphere and carbon diffusivity in austenite from a simple experimental setup.

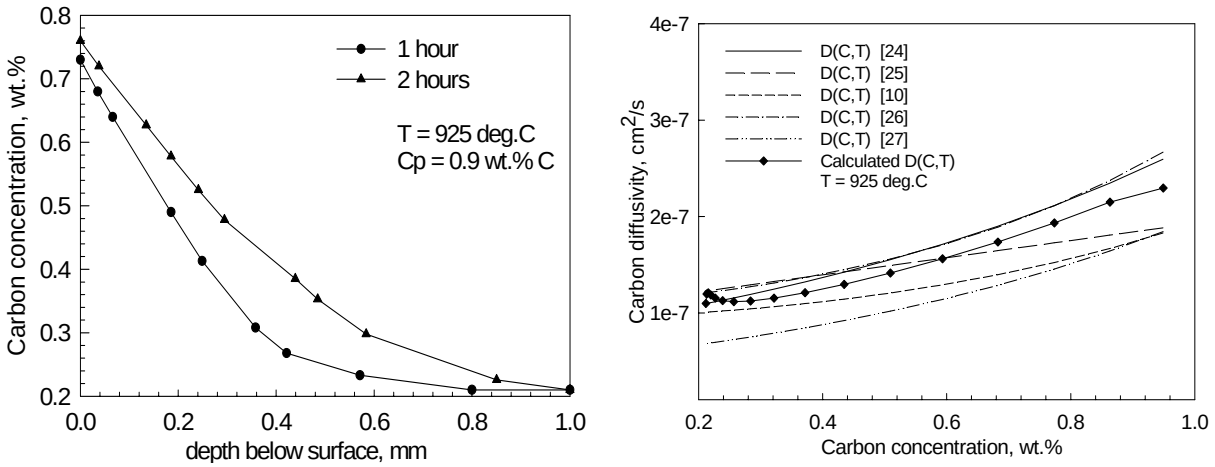

a) b)

Figure 4. Calculation of the coefficient of carbon diffusion: a) experimental carbon concentration profiles, b) the calculated carbon diffusivity.

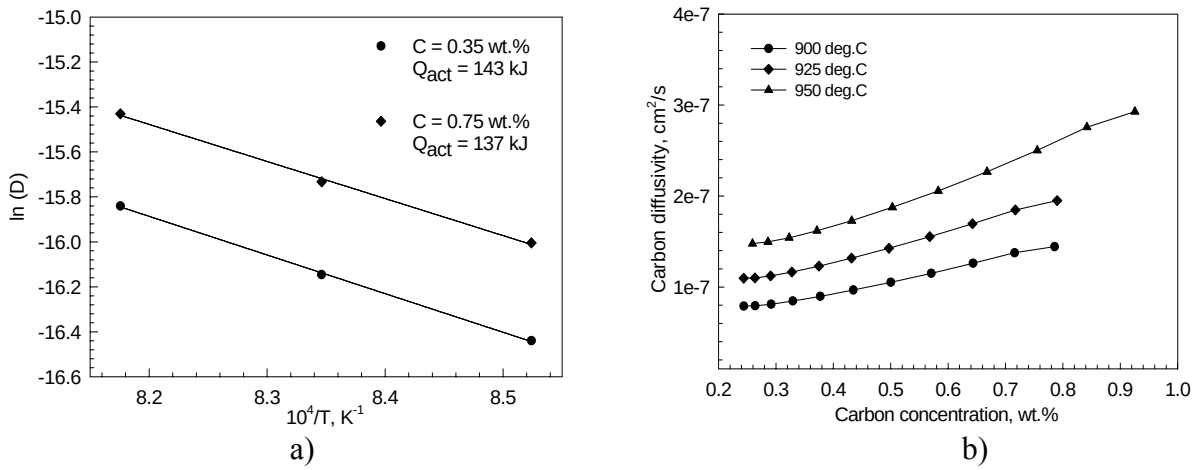

Figure 5. Calculated coefficient of carbon diffusion in austenite: a) Arrhenius type plot, b) as a function of carbon content.

Model Validation

In a previous publication by the authors [29], a carburization model was developed to predict the carbon concentration profile. This model is based on the finite difference approximation of the parabolic partial differential equation governing carbon diffusion in steel and a set of boundary conditions, which account for the mass transfer in the atmosphere and across the gas-steel interface assuming flux balance at the steel surface. The calculated time-dependent mass transfer coefficient and concentration dependent carbon diffusivity were input as the boundary condition in the model. The predicted carbon concentration profiles were plotted against the experimental data as shown in Figure 6.

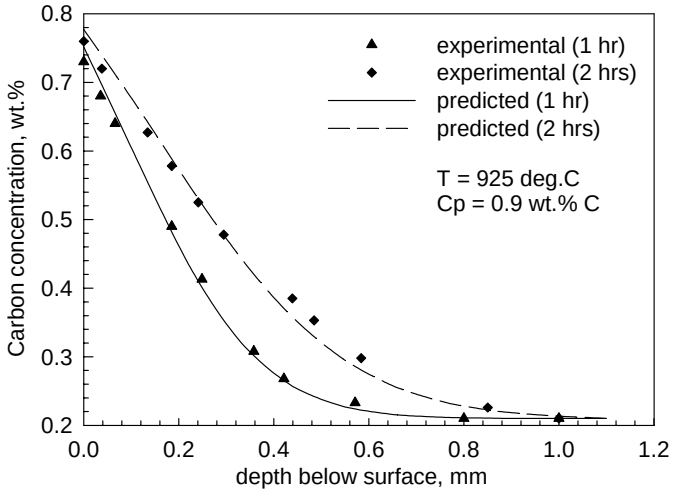

Figure 6. Carbon concentration profiles in the parts after carburizing.

Comparison of the experimental data and the predicted profiles using the calculated β and D further validates the developed method of direct flux integration. With only a simple experimental setup it allows calculation of both the mass transfer coefficient and concentration dependent carbon diffusivity in austenite, and can be successfully used as a tool for the carburizing process control and further optimization.

Conclusions

This paper focused on development and experimental validation of the developed method for calculating the mass transfer coefficient in the atmosphere and carbon diffusivity in austenite during gas carburizing. The proposed method revealed good predictability and can be applied to determine the kinetics control parameters in any vapor-solid diffusion system and is independent of the steel part size.

The mass transfer coefficient was calculated from the experimental weight gain and surface carbon evolution. The calculations were performed for a range of carburizing conditions and facilitate understanding the effect of process parameters on the kinetics of mass transfer during carburizing. Concentration dependent carbon diffusivities were calculated from the experimental profiles and reveal good agreement with other diffusivity models. The calculated kinetic parameters served as input in the previously developed carburizing model. The method was validated by comparing the predicted carbon concentration profiles with the experimental data.

Since the proposed method for the mass transfer parameters calculation involves measurement of slopes and areas under the concentration profiles, it is possible that such calculation using experimental data will have some level of uncertainty associated with it. Nonetheless, implementation of this technique and successful experimental validation provides an effective method for calculation of the main control parameters from a simple experimental setup. Overall, analysis of the calculated mass transfer and carbon diffusivity help facilitate understanding the effect of the process parameters on the mass transfer coefficient and carbon diffusivity in austenite and can further be used for the carburizing process control and optimization.

Acknowledgements

The support of the Center for Heat Treating Excellence (CHTE) at Worcester Polytechnic Institute and the member companies is gratefully acknowledged. Special thank you goes to Caterpillar for their support through facilities and experimental work.

References

1. C. Wells and R.F. Mehl: American Institute Mining Metallurgical Engineers, Technical Publication, (1940), p. 1180
2. K.E. Blazek and P.R. Cost: Transactions of the Japanese Institute of Metals, Vol. 17, n. 10 (1976), p. 630
3. W. Batz, and R.F. Mehl: Transactions of AIME, Vol.188 (1950), p. 553
4. P. Stolar and B. Prenosil: Metallic Materials (Kovove Materialy), Vol. 22, n. 5 (1984), p. 348.
5. B.A. Moiseev, Y.M. Brunzel' and L.A. Shvartsman: Metal Science and Heat Treatment (Metallovedenie i Termicheskaya Obrabotka Metallov), Vol. 21, n. 5-6 (1979), p. 437
6. H.W. Walton: Heat Treatment of Metals, Vol 10, n. 1 (1983), p. 23
7. E.L. Gyulikhandanov and A.D. Khaidorov: Metal Science and Heat Treatment (Metallovedenie i Termicheskaya Obrabotka Metallov), Vol. 33, n. 5-6 (1991), p. 344
8. M. Yan, Z. Liu, and G.Zu: Materials Science Progress, Vol. 6, n. 3 (1992), p. 223
9. T. Turpin, J. Dulcy, and M. Gantois: Metallurgical Transactions A, Vol. 36, n.10 (2005), p. 2751
10. A. Ruck, D. Monceau, and H.J.Grabke: Steel Research, Vol. 67, n. 6 (1996), p. 240
11. R. Collin, S. Gunnarson, and D. Thulin: Journal of the Iron and Steel Institute, Vol. 210 (1972), p. 785
12. O. Karabelchtchikova and R.D. Sisson, Jr.: Journal of Phase Equilibria and Diffusion, Vol. 27, n. 6 (2006), p. 598
13. R. Collin, S. Gunnarson and D. Thulin: Journal of the Iron and Steel Institute, Vol. 210, n. 10 (1972), p. 777

14. V.A. Munts and A.P. Baskakov: Metal Science and Heat Treatment (Metallovedenie i Termicheskaya Obrabotka Metallov), Vol. 22, n. 5-6 (1980), p. 358

15. V.A. Munts and A.P. Baskakov: Metal Science and Heat Treatment (Metallovedenie i Termicheskaya Obrabotka), Vol. 25, n. 1-2 (1983), p. 98

16. P. Si, Y. Zhang, S. Qin and Y. Kong: Heat Treatment of Metals, Vol. 6 (1992), p. 51

17. F. Neumann and U. Wyss: Harterei-Technische Mitteilungen, Vol. 25, n. 4 (1970), p. 253

18. R. Collin: Canadian Mining Journal, (1975), p. 121

19. H.J. Grabke: Proceedings of the 3rd International Congress, Amsterdam, Holland, p. 928 (1964)

20. J. Wunning: Haerterei-Technische Mitteilungen, Vol. 23, n. 3 (1968), p. 101

21. K. Rimmer, E. Schwarz-Bergkampf and J. Wunning: Haerterei-Technische Mitteilungen, Vol. 30, n. 3 (1975), p. 152

22. B.A. Moiseev, Y.M. Brunzel', and L.A. Shvartsman: Metal Science and Heat Treatment (Metallovedenie i Termicheskaya Obrabotka Metallov), Vol. 21, n. 5-6 (1979), p. 437

23. T. Sobusiak: Proceedings of the 3rd International Congress on Heat Treatment of Materials, Shanghai, China: Metals Society (Book 310), London, England (1984)

24. G.G. Tibbetts: Journal of Applied Physics, Vol. 51, n. 9 (1980), p. 4813

25. J.I. Goldstein and A.E. Moren: Metallurgical Transactions A, Vol. 9, n. 11 (1978), p. 1515

26. G.E. Totten and M.A.H. Howes, in: *Steel Heat Treatment Handbook*, Marcel Dekker, Inc., NY, 1997

27. A. Muroga, I. Niimi, Y. Tsunekawa and M. Okumiya: Nippon Kinzoku Gakkaishi (Journal of the Japan Institute of Metals), Vol. 52, n. 5 (1988), p. 495

28. L.H. Van Vlack, in: *Elements of Materials Science and Engineering*, 4th ed., Addison-Wesley Publishing Co., Inc., Reading, MA (1980)

29. O. Karabelchtchikova, Md. Maniruzzaman and R.D. Sisson, Jr.: Proceedings of the 2006 MS&T, Cincinnati, OH, p. 375 (2006)

PAPER # 7: EFFECT OF ALLOY COMPOSITION ON CARBURIZING PERFORMANCE OF STEEL

(submitted to *Metallurgical Transactions*)

Abstract

This paper investigates the effect of alloy composition on the gas carburizing performance of AISI 1018, 4820, 5120 and 8620 steels. The mass transfer coefficients and carbon diffusivities were calculated from the experimental measurements using the method of direct flux integration. Although steels with high concentration of austenite-stabilizing elements (Si, Ni) increased carbon diffusivity in austenite, they significantly reduced the kinetics of carbon transfer from the atmosphere to the steel surface and resulted in lower weight gain. Despite lowering the carbon diffusivities, steels alloyed with carbide-forming elements (Cr, Mo) significantly increased the mass transfer coefficient in the atmosphere and enhanced the rate of carbon profile evolution. The experimentally determined carbon diffusivities were in good agreement with the carbon diffusivities obtained from the thermodynamic and kinetic databases in DICTRA. Overall, using the concentration dependent mass transfer coefficient and carbon diffusivity in various alloy steels helped explain the experimentally observed variations in the carbon concentration profiles and the effective case depths. Recommendations are made to help achieve better case depth uniformity within a carburizing workload.

Introduction

Gas carburizing is an important heat treatment process used for surface hardening of automotive and aerospace steel components. Despite its worldwide application, the process faces certain challenges in the process control and case depth variability. Carburizing performance of steel is influenced by the furnace design, the process parameters (i.e. gas atmosphere composition, carburizing temperature and time), and by the steel composition. Considerable research has been done to investigate the effect of these process parameters on the carburizing performance. In practice, however, even with a well-controlled process, some variation in the effective case depth and surface carbon concentration are observed, which remain unresolved.

Therefore, the goal of this work is to develop a better understanding of the effect of steel composition on the kinetics of carbon transfer during the process and on the overall carburizing performance of steel. Specifically, the objective is to qualitatively and quantitatively investigate the contribution of the major alloying elements on the mass transfer coefficient in the gas atmosphere and on the carbon diffusivity in austenite.

The effect of alloy composition on the rate of gas carburizing has been investigated by many researchers [1-11]. Wada et.al. [1-3] studied the effect of alloy composition on carbon activity in austenite and developed thermodynamic models for several ternary Fe-C-X systems. Others researchers [4-8] studied the effect of alloy composition on carbon mobility and carbon diffusivity in austenite. Most of these investigations were based on the analysis of diffusion couples. Application of such models to gas carburizing, introduces a certain level of uncertainty due to the assumption of a constant surface concentration. Therefore, the most common approach to account for the effect of steel composition involves adjusting the effective carbon potential in the gas atmosphere by an 'alloying factor' [9-11]. While this empirically developed correction factor yields acceptable results, it does not provide a clear relationship between the alloy composition and the coefficients of mass transfer from the atmosphere to the steel surface or the carbon diffusivity in austenite. Therefore, to explore the nature of their relationship, the calculations and data analysis in this work are based on the modified method of direct flux integration [12]. This method enables calculation of the mass transfer coefficient and the carbon diffusivity in austenite from a simple experimental setup and has previously been validated [12].

Thermodynamics of Mass Transfer During Gas Carburizing

The process of gas carburizing can be viewed as diffusion in a vapor-solid diffusion couple. Carbon transport during the process is governed by the gradient in chemical potential and is determined by the rate limiting process, which kinetically becomes the controlling stage of carburizing. The maximum carburizing rate is obtained when carbon transfer from the gas atmosphere is equal to or greater than the carbon diffusion rate in the steel. In practice, however, the process is mixed controlled [10,13] and is governed both by the mass transfer coefficient and by the carbon diffusivity in steel. According to the thermodynamics of irreversible processes [14], the driving force for mass transfer during carburizing is the gradient in carbon chemical

potential. The chemical potential is determined by the carburizing temperature and the thermodynamic carbon activity:

$$\mu_C = \mu_C^0 + RT \ln a_C, \tag{1}$$

where μ_C is the chemical potential of carbon, R is the universal gas constant, T is the process temperature in Kelvin and a_C is the carbon activity in austenite.

Most of the available models for carbon activity have been developed for ternary Fe-C-X systems [1-3]. Such models are based on the characteristic distribution of carbon atoms in the matrix of alloyed austenite and the localized forces of their interactions. The presence of Si and Ni in steel increases the carbon activity and the coefficient of carbon diffusion in austenite [9,14,15]. Nevertheless, the presence of these elements in steel impedes the carburizing process. In comparison, Cr and Mn decrease the carbon diffusivity in austenite, though these elements accelerate the overall carburizing performance of steel [9,14,15]. These phenomena become more convoluted as the composition of alloy steels grows increasingly complex. Since carburizing of alloy steels helps attain necessary steel hardenability, it is critically important to understand the effect of alloying elements on the carburizing response of medium- and high-alloy steels to help ensure repeatable and well-controlled results.

Gas carburizing is modeled using the 2nd order PDE with a flux balance boundary condition at the gas-steel interface [10]:

$$\sum_i^n \frac{k_i}{a^{surf_i}} \left(a_c^{gas} - a_c^{surf} \right) = -D \frac{da_c^{surf}}{dx}, \tag{2}$$

where k_i is the rate coefficient of the atmosphere chemical reactions, a^{surf} and $a_C{}^{gas}$ are the carbon activity at the steel surface and gas atmosphere, respectively, D is the carbon diffusivity in austenite and x is the depth below the steel surface. The summation sign ($\sum$) indicates that several chemical carburizing reactions can take place simultaneously. For carbon concentration profiles with less than 1 wt.% C, the mass transfer coefficient is often expressed as the ratio between the rate coefficient for the chemical reactions and the carbon activity at the steel surface ($\beta = \sum_i^n k_i / a^{surf_i}$) [16,17]. The mass transfer coefficient (β) has been reported to be a complex

function of the atmosphere gas composition, carburizing potential and temperature [17-20]. To the authors' best knowledge, there has been little work published to quantitatively relate the effect of alloy composition to the rate of carbon transfer in the gas atmosphere and across the gas-steel interface. Using a concentration dependent β would allow modeling the carbon concentration profiles to help explain the observed variations in the effective case depth and the carbon concentration evolution in various alloy steels.

The carbon diffusivity in austenite (D) is another critical parameter, which is influenced by the carburizing temperature and steel composition [21]. For low-alloy steels, this influence may be negligible, while for medium- and high-alloy steels the effect of alloying elements may be significant and should be taken into consideration. Understanding the effect of alloying on the carburizing performance requires knowledge of thermodynamic data including the activity coefficient and carbon mobility in the FCC lattice of alloyed austenite. Such experimental data are scarce and are not always readily available in the published literature. Therefore, the mass transfer coefficient and carbon diffusivity calculations in this work were performed using the method of direct flux integration, which allow calculation of both kinetic parameters from a simple experiment.

Experimental Procedure

Four steel grades with the same bulk carbon concentration were selected for this work. These included plain carbon steel (AISI 1018), and three medium-alloyed steels (AISI 4820, 5120, 8620), with the chemical composition given in Table 1. The steel grades were selected such that they provide various combinations of (low-high) concentration of the major alloying elements (Ni, Mo, Cr and Si). Carburizing AISI 1018 was intended to serve as the baseline for evaluating the effect of steel composition on carburizing performance.

The AISI 5120 and AISI 8620 steel bars were received in the hot rolled condition, while AISI 4820 and AISI 1018 were supplied in the annealed and cold finished condition. Microstructural analysis revealed a mixture of ferrite and pearlite uniformly distributed in the transverse direction and having a banded structure in the longitudinal direction, parallel to the direction of rolling. All steel bars were normalized for 4 hours at 900 ºC, which minimized the differences in prior rolling conditions and reduced the grain size from 6.5 to 8 (ASTM E 112).

Table 1. Chemical composition of steels (wt.%).

AISI steel designation	C	Mn	P	S	Si	Ni	Cr	Mo
1018	0.2	0.8	0.01	0.029	0.26	0.1	0.07	0.03
4820	0.2	0.6	0.007	0.02	0.28	3.28	0.12	0.26
5120	0.2	0.79	0.007	0.01	0.23	0.05	0.77	0.02
8620	0.19	0.87	0.013	0.031	0.19	0.42	0.57	0.21

The normalized bars were machined into disks 3.1 cm in diameter and 1 cm in thickness. The samples were carburized at 925 ºC for 1 and 2 hrs in an Integral Quench furnace at an industrial research facility. The endothermic atmosphere was produced by blending the endothermic carrier gas with natural gas enrichment and the carbon potential in the furnace was controlled at 1.1 wt.% C using an oxygen probe and IR analyzers. The weight gain measurements upon carburizing were collected on laboratory scale sensitive to 0.1 mg. Surface carbon concentration and carbon concentration profiles were measured by spectral analysis using LECO-OES with an accuracy of $\pm$ 0.01 wt.% C. A layer of the material of exact known depth was sequentially removed from the surface and analyzed for chemical composition. In order to measure the carbon concentration profiles, this procedure was repeated until a zero carbon gradient [for three consecutive measurements] was reached, which indicated the bulk carbon concentration.

Results and Discussion

Figure 1 shows the experimentally measured carbon concentration profiles in the carburized parts after 1 and 2 hrs. Although all parts were carburized in the same basket under the same carburizing conditions, the laboratory analysis revealed distinct differences among these steels in the carbon concentration profiles and the total weight gain (ΔM). It was observed that plain carbon steel exhibited the maximum carbon uptake. Depending on the level of alloying and on the nature of carbon and alloying elements atomic interactions, the carbon concentrations profiles in the alloy steels were lower than in the plain carbon steel.

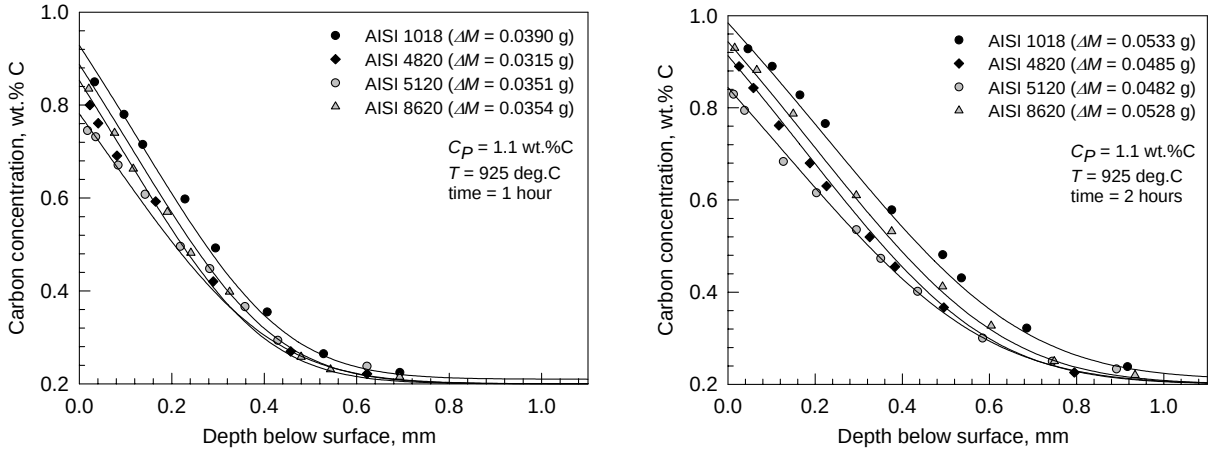

a) b)

Figure 1. Carbon concentration profiles after 1 and 2 hours carburizing.

If the effective case depth is defined as the depth to 0.4 wt.% C, the measured case depth variation was found to be ± 0.03 mm after 1 hr carburizing and ± 0.06 mm after 2 hr carburizing. From Figure 1-a, the primary differences in the carbon concentration profiles after 1 hr were observed at near surface layer up to a depth of 0.4 mm. This observation was attributed to the rate of carbon transfer from the atmosphere to the steel surface, which is kinetically the rate limiting process at the initial stage of carburizing [17]. As time proceeds, the process becomes mixed controlled [10,13], where both the mass transfer coefficient and the carbon diffusivity contribute to the carbon profile evolution (Figure 1-b). During this stage, the instantaneous carbon flux across the gas-steel interface is determined by the balance between the carbon flux from the gas atmosphere to the steel surface and the rate of carbon diffusion in steel. Therefore, the overall observed differences in the carburizing performance of various alloy steels are due to the effect of alloying elements on the carbon activity at the steel surface (affecting the rate of carbon transfer across the gas-steel interface) and the carbon diffusivity in austenite.

By definition, carbon potential (C_P) in the atmosphere is defined as the amount of carbon that is in equilibrium with the surface carbon concentration in unalloyed austenite. For the given carburizing temperature and C_P of 1.1 wt.%, the thermodynamic carbon activity in austenite and the corresponding activity coefficients for various alloy steels were calculated using Thermo-Calc [22] and are given in Table 2. Of the three alloy steels, AISI 5120 steel (with high-Cr and zero-Ni concentrations) provides the highest equilibrium carbon concentration and, therefore, it exhibit the strongest tendency to reduce the carbon activity from its unalloyed counterpart,

i.e. AISI 1018. AISI 8620 steel with a more balanced combination of the austenite-stabilizing and carbide-forming elements also increases the equilibrium carbon concentration from that of the plain carbons steel but to a smaller degree. The opposite effect is observed in case of AISI 4820 steel, which chemical composition significantly reduces the equilibrium concentration of carbon in austenite and increases the thermodynamic carbon activity in steel. These data will further be used throughout the paper to help explain the effect of steel composition on the kinetic carburizing parameters.

Table 2. Thermodynamic characteristics of various steels calculated at 925 °C and C_P =1 wt.%.

Parameters	AISI 1018	AISI 4820	AISI 5120	AISI 8620
a_C	0.803	0.803	0.803	0.803
Equilibrium *C* concentration, wt.%	1.029	0.964	1.043	1.039
γ, activity coefficient	15.85	16.94	15.63	15.67

Mass Transfer Coefficient

From the flux balance condition at the steel interface and the continuity equation of mass accumulation within steel, the total amount of diffused carbon atoms per unit area can be estimated from the area under the carbon concentration profile and the integrated carbon flux:

$$\int_0^{x_\infty} C(x,t)\,dx = \int_{t_0}^{t_f} J_C\,dt = \frac{\Delta M}{A}, \tag{3}$$

where x_∞ is the depth beyond which no concentration gradient exists, J_C is the carbon flux, t is the diffusion time, $\Delta M/A$ is the weight gain per unit area of the carburized part. Further differentiation of the weight gain over carburizing time yields the following expression for the total carbon flux through the gas-steel interface:

$$J_C{}^t = \frac{\partial}{\partial t}\left(\frac{\Delta M}{A}\right) = \beta\left(C_P - C_S^t\right) \tag{4}$$

Assuming a time-dependent nature of the process, the rate of carbon transfer at the gas steel interface can be characterized by the instantaneous mass transfer coefficient:

$$\beta^t = \frac{1}{\left(C_P - C_S^t\right)} \cdot \frac{\partial}{\partial t} \int_{x_\infty}^{x_0} C(x,t)\,dx \tag{5}$$

or by the average mass transfer coefficient:

$$\beta^{avg} = \frac{1}{t\left(C_P - C_S^t\right)} \cdot \left(\frac{\Delta m}{A}\right)\Bigg|_{t_0 \to t}. \tag{6}$$

Table 3 presents the measured weight gain and the surface carbon concentration in the parts after 1 and 2 hr carburizing. The carbon flux and the average mass transfer coefficient were calculated from the experimental data according to Equations (4) and (6).

Table 3. Calculation of the mass transfer coefficient.

Steel	Carburizing time	Experimental data			Calculated data	
		weight gain, g	C_S, wt.%	C_S, g/cm^3	J_C, g/cm^{2}s	β^{avg}, cm/s
AISI 1018	1 hr	0.0390	0.88	0.30974	1.92×10^{-5}	1.818E-05
	2 hrs	0.0533	0.95	0.33438	1.72×10^{-5}	
AISI 4820	1 hr	0.0315	0.75	0.26492	9.59×10^{-6}	8.91E-06
	2 hrs	0.0485	0.82	0.28964	8.23×10^{-6}	
AISI 5120	1 hr	0.0351	0.83	0.29173	1.40×10^{-5}	1.341E-05
	2 hrs	0.0482	0.92	0.32336	1.28×10^{-5}	
AISI 8620	1 hr	0.0354	0.85	0.29992	1.58×10^{-5}	1.519E-05
	2 hrs	0.0528	0.92	0.32382	1.46×10^{-5}	

While the parts were subjected to the same carburizing conditions, the calculated mass transfer coefficients ranged from 8.91×10^{-6} to 1.82×10^{-5} cm/s depending on the steel composition. AISI 4820 steel exhibited the slowest kinetics of the mass transfer from the gas atmosphere to the steel surface and revealed the least weight gain after carburizing. As follows from Table 2, austenite-stabilizing elements (Ni and Si) reduce the equilibrium carbon concentration and increase the carbon activity (a_C^{surf}) at the steel surface. This decreases the mass transfer coefficient and the corresponding carbon flux [$J_C \propto (a_C^{gas} - a_C^{surf})$] entering the steel surface. In comparison, carbide-stabilizing alloying elements (Cr, Mo) decrease the carbon activity and

correspondingly increase the total carbon flux across the gas-steel interface. As a result, the calculated mass transfer coefficients for AISI 5120 and AISI 8620 were greater than that of AISI 4820 and revealed larger weight gain and higher surface carbon concentration upon carburizing.

Carbon Diffusivity in Austenite

As with the mass transfer calculation, the weight gain of carbon atoms diffusing into the steel across any arbitrary plane parallel to the gas-steel interface can be found by integrating the concentration profile over the distance at which the gradient exists:

$$\frac{d}{dt}\int_{C'}^{C_0} x dC - J_C\left(x_0\right) = 0 \ , \tag{7}$$

where C' is the carbon concentration at the given depth (x_0) and C_0 is the bulk carbon concentration. Assuming an isotropic media, the flux of the diffusing substances through a unit area is proportional to the concentration gradient measured normal to the section:

$$J_C\left(x_0\right) = -D\left(x_0\right)\cdot\frac{dC}{dx}\left(x_0, t\right). \tag{8}$$

By equating the above two equations, the following expression for calculating carbon diffusivity from the concentration profiles can be derived [12]:

$$D\left(x_0\right) = -\left(\frac{dC\left(x_0, t\right)}{dx}\right)^{-1}\cdot\frac{d}{dt}\int_{C'}^{C_0} x dC \ . \tag{9}$$

Overall, calculation of the carbon diffusivity involves the product of two components: i) negative inverse of the slope at any position x_0 on the carbon concentration profile and ii) integrated area under the concentration profile differentiated with respect to carburizing time. Figure 2 presents the carbon diffusivities calculated from the experimental carbon concentration profiles [shown in Figure 1]. The calculated data were compared with the carbon diffusivities to those calculated from the thermodynamic and kinetic databases in DICTRA [22]. A good agreement was observed between the sets of data.

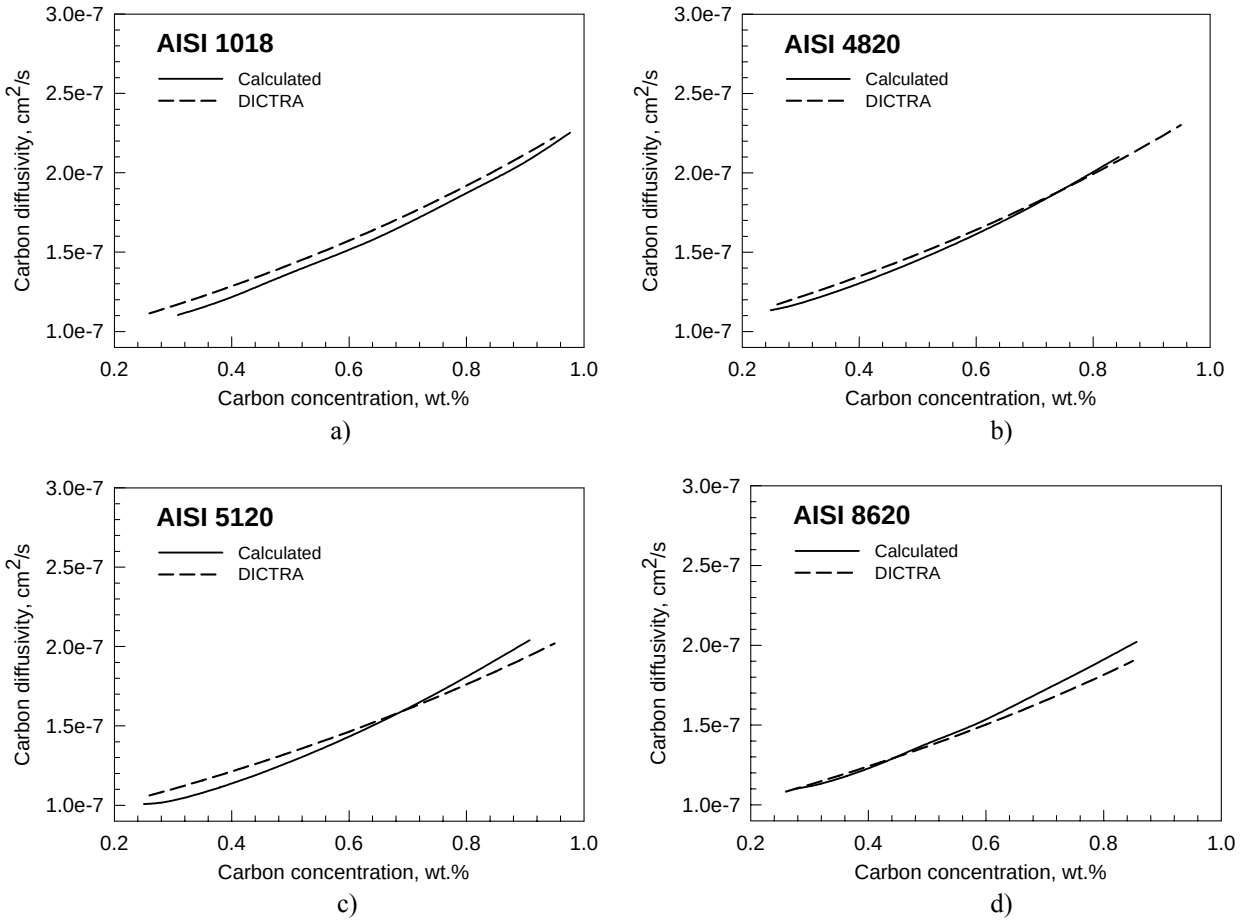

Figure 2. Comparison of the calculated carbon diffusivities with those from DICTRA: a) AISI 1018, b) AISI 4820, c) AISI 5120, d) AISI 8620.

Figure 3 compares the carbon diffusivity in austenite for various alloy steels. It was observed that despite the lowest mass transfer coefficient associated with AISI 4820, the presence of strong austenite-stabilizers (Ni, Si) increases the carbon diffusivity in austenite. This observation was attributed to weaker bonding energy and negative atomic interactions between the austenite-stabilizing elements and carbon atoms. Carbide-forming elements (Mo, Cr) induce positive atomic interactions and tend to attract interstitially diffusing carbon atoms. Such deviations from randomness impede the long-range diffusion of carbon atoms in the austenite matrix, and therefore decrease the effective carbon diffusivity. Since the effect of carbide-forming elements is offset by the addition of austenite-stabilizing elements, the calculated carbon diffusivities in AISI 8620 and 1020 steels were found to be between those of AISI 4820 and 5120.

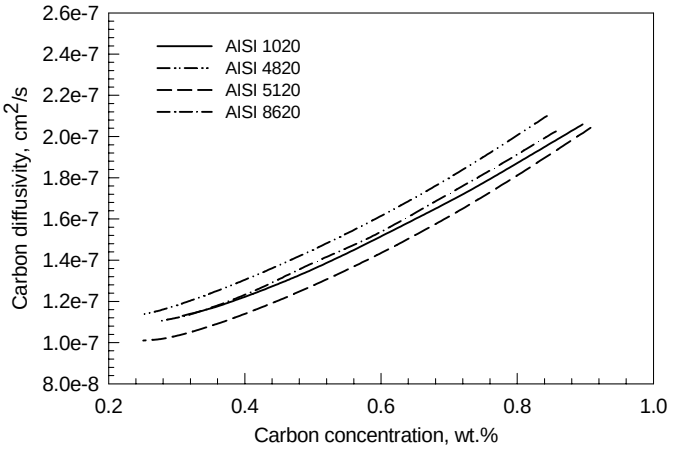

Figure 3. Comparison of the coefficients of carbon diffusion for various alloyed steels.

Overall, the implication of this work is that medium- and high-alloy steels with high-Cr and low-Ni concentrations significantly reduce the carbon diffusivity in steel and, therefore, require longer carburizing time to achieve the desired case depth. Carburizing such steel parts together with high-Ni steel components will inevitably lead to case depth variations within the same workload. Therefore, it is recommended that such steel components be carburized in a separate load and the carburizing time should be adjusted accordingly to achieve the desired case depth.

The importance of understanding and quantifying the effect of chemical composition of alloy steel on their carburizing performance should not be underestimated. For a given carburizing temperature and gas carburizing atmosphere, the mass transfer coefficient and the carbon diffusivity in austenite vary with the steel composition. This implies that various steels may require different carburizing times to achieve a desired case depth. Using the concentration dependent β and D in the available carburizing models can help achieve better case depth uniformity.

Conclusions

This paper investigated the effect of alloy composition on the kinetics of mass transfer during gas carburizing and on the overall carburizing performance of various alloy steels. The principal conclusions of this work are:

1. Gas carburizing performance of various alloy steel is strongly affected by the alloy composition and should be taken into account when carburizing medium- and high-alloy steels to ensure repeatable and well-controlled results.

2. AISI 4820 steel with high concentration of austenite-stabilizing elements (Ni, Si) exhibited the slowest kinetics of the mass transfer from the gas atmosphere to the steel surface. Although, the austenite-stabilizing elements increased the carbon diffusivity in austenite, the rate of carburizing was limited by the flux entering the steel surface, which significantly lowered the final carbon concentration profile compared to that of plain carbon steel with the same bulk carbon concentration.

3. While carbide-forming elements (Cr, Mo) in AISI 5120 and 8620 lowered the carbon diffusivity in austenite, they increased the rate of carbon transfer from the atmosphere to the steel surface and accelerated the rate of carburizing.

4. Carbon diffusivities calculated from the experimental data using the method of direct flux integration were compared to the carbon diffusivities obtained from the thermodynamic and kinetic databases in DICTRA and showed good agreement.

5. Understanding and quantifying the contribution of alloy composition on the mass transfer coefficient and carbon diffusivity in austenite helps explain the observed variations in the carbon concentration profiles of various alloy steels. Most importantly, it is recommended that the carburizing process time is adjusted by the steel composition to achieve the desired carburizing results with better case depth uniformity.

Acknowledgements

The support of the Center for Heat Treating Excellence (CHTE) at Worcester Polytechnic Institute and the member companies is gratefully acknowledged. The experimental work was performed at Caterpillar Inc. and its support through facilities and experimental work is greatly appreciated.

References

1. T. Wada, H. Wada, J.F. Elliott and J. Chipman: *Metall. Trans.*, 1971, vol. 2, n. 8, pp. 2199-08.

2. T. Wada, H. Wada, J.F. Elliott and J. Chipman: *Metall. Trans.*, 1972, vol. 3, n. 6, pp. 1657-67.

3. T. Wada, H. Wada, J.F. Elliott and J. Chipman: *Metall. Trans.*, 1972, vol. 3, n. 11, pp. 2865-72.

4. B. Jonsson: *Z. MetaIlkd.*, 1994, vol. 85, n. 7, pp. 502-9.

5. S.S. Babu and H.K.D.H. Bhadeshia: *J. Mater. Sci. Lett.*, 1995, vol. 14, n. 5, pp. 314-16.

6. S.K. Bose and H.J. Grabke: *Z. MetaIlkd.*, 1978, vol. 69, n. 1, pp. 8-15.

7. S.K. Roy, H.J. Grabke and W. Wepner: *Arch. Eisenhuettenwes.*, 1980, vol. 51, n. 3, pp. 91-96.

8. M.A. Krishtal: *Diffusion Process in Fe Alloys*, Israel program for scientific translations, Jerusalem, 1970, (1963), pp. 90-133.

9. C. Dawes and D.F. Tranter: *Heat Treat. Met.*, 2004, vol. 31, n. 4, pp. 99-108.

10. R. Collin, S. Gunnarson and D. Thulin: *J. Iron Steel Inst.*, 1972, vol. 210, n. 10, pp. 785-89.

11. R. Collin: *Can. Min. J.*, 1975, pp. 121-24.

12. O. Karabelchtchikova and R.D. Sisson, Jr.: *J. Phase Equilib. Diff.*, 2006, vol. 27, n. 6, pp. 598-04.

13. T. Turpin, J. Dulcy, and M. Gantois: *Metall. Trans. A*, 2005, vol. 36A, n.10, pp. 2751-60.

14. A.A. Zhukov and M.A. Krishtal: *Met. Sci. Heat Treat.*, 1975, vol. 17, n. 7-8, pp. 626-33.

15. M.A. Krishtal and A.I. Volkov: *Met. Sci. Heat Treat.*, 1979, vol. 21, n. 7-8, pp. 617-22.

16. M.A. Krishtal., A. P. Mokrov and P.N. Zakharov: *Met. Sci. Heat Treat.*, 1973, vol. 15, n. 11-12, pp. 1043-46.

17. P. Stolar and B. Prenosil: *Metall. Mat.*, 1984, vol. 22, n. 5, pp. 348-53.

18. V.A. Munts, and A.P. Baskakov: *Met. Sci. Heat Treat.*, 1983, vol. 25, n. 1-2, pp. 98-2.

19. J. Wunning: *Haerterei Tech. Mitt.*, 1968, vol. 23, n. 3, pp. 101-9.

20. K. Rimmer, E. Schwarz-Bergkampf and J. Wunning: *Haerterei Tech. Mitt.*, 1975, vol. 30, n. 3, pp. 152-60.

21. J. Agren: *Scripta Metall.*, 1986, vol. 20, n. 11, pp. 1507-510.

22. Thermo-Calc Software Inc., Stokholm, Sweden, 2006.

PAPER # 8: MULTI-OBJECTIVE OPTIMIZATION OF GAS CARBURIZING PROCESS IN BATCH FURNACES WITH ENDOTHERMIC CARBURIZING ATMOSPHERE

(submitted to *Metallurgical Transactions*)

Abstract

A methodology for optimization of the gas carburizing heat treatment in terms of cost, cycle time and quality of the carburized parts has been developed. The optimization strategy is based on 1) modeling the effect of process parameters (carbon potential, temperature and time) on the mass transfer coefficient and carbon diffusivity in austenite; 2) correlating the observed variations in the process parameters on the kinetics of carburizing; and 3) developing a robust multi-objective optimization technique to achieve the desired case depth with minimum cost and minimum case depth variation. The index of performance for the process optimization involves both the surface carbon concentration and the case depth. While the first parameter depends on accurate control of the atmosphere and the carbon potential in the furnace, the case depth is primarily influenced by the furnace temperature and the duration of the carburizing process. The application of this optimization technique provides a tradeoff between minimizing the case depth variation and total cycle cost and results in significant energy reduction by shortening cycle time and thereby enhancing furnace capacity.

Introduction

Gas carburizing is an important heat treatment used for surface hardening of steel components for automotive and aerospace industries. Although the process has been successfully used in industry for over 50 years, the carburizing cycles are generally designed through plant trials and empirical methods, and therefore, they are rarely optimized [1].

From a customer's perspective, the quality requirements for the carburized parts include achieving desired surface hardness and case depth with limited case depth variation. Meeting these quality requirements helps ensure adequate performance of the carburized parts and helps avoid premature failure in service. Carburized parts with insufficient case depths are subject to

rejections [2] or additional rework [1], which significantly increase the total processing cost. From a manufacturer's perspective, the carburizing heat treatment cycles should be time- and cost-efficient. Anticipated shortages in natural gas supply and energy resources demand industry to search for optimized process conditions and efficient energy utilization [3]. In the competitive market this would require finding global optimal solutions to meet the specified quality requirements while shortening cycle time and reducing energy consumption.

Optimization of the industrial carburizing parameters is typically pursued by trial and error. In addition to being time consuming and expensive, this approach yields suboptimal results at the best [1]. Palaniradja et.al. [2] reported their optimization work based on Taguchi experimental approach, where the authors considered three levels of the carburizing temperature, carbon potential and time and evaluated their effect on the surface hardness and case depth. While statistical analysis determined 'the best' combination within the selected process parameters, such approach indicates only the direction to optimal conditions rather than the global optimum itself. Another common optimization approach is to approximate the experimental data with a second-order response surface model [4]. Application of such regressive models may yield an adequate solution, although these models ignore the functional relationship between the process variables and the carburizing performance measurements and, therefore, cannot be used unless extensive experimental data are available. Sahay and Mitra [1] built an optimization model using numerical and analytical approach, where the carburizing process parameters were correlated to the plant performance metric and to the overall cycle cost. Using an extensive search method, the authors optimized the boost stage temperature and time based on the minimum carburizing cycle cost as the optimization criterion.

Optimization of the gas carburizing process parameters in this paper is the conclusive chapter in a series of experimental and theoretical investigations on gas carburizing process control and optimization [5-7]. The previously presented carburizing model [5] was extensively used in this work to simulate the carbon concentration profiles and the corresponding case depth. A method of direct flux integration was developed which allowed calculation of the mass transfer coefficient and carbon diffusivity from the experimental data [6,7]. These kinetic parameters were used to model the relationship between the controllable input parameters (carbon potential, temperature and time) and the carburizing performance (surface carbon concentration and case depth). The optimization strategy is based on 1) modeling the effect of the process parameters on the mass

transfer coefficient and carbon diffusivity in austenite; 2) correlating the observed variations in the process parameters on the kinetics of carburizing; and 3) developing a robust multi-objective optimization technique to achieve the desired case depth with minimum cost and minimum case depth variation.

Model Formulation and Optimization Framework

The mass transfer mechanism during gas carburizing consists of three stages: 1) carbon transport from the atmosphere to the steel surface through a boundary layer, 2) chemical reaction at the steel surface, and 3) carbon diffusion in steel. The two control parameters determining the final carbon concentration profile are: the mass transfer coefficient (β) defining the flux of carbon atoms from the atmosphere to the steel surface and the coefficient of carbon diffusion in steel (D) at the austenizing temperature. The mass transfer coefficient is a complex function of the atmosphere gas composition, carburizing potential and temperature [7,8], while carbon diffusivity depends on the carburizing temperature, carbon concentration and steel alloy composition [7,9].

Carbon concentration profiles and the effective case depth were modeled numerically using a carbon potential- and temperature-dependent mass transfer coefficient and the concentration-dependent carbon diffusivity in austenite [5,7]. The model is based on the finite difference approximation of the parabolic equation governing carbon diffusion in steel and a flux balance boundary condition accounting for the mass transfer coefficient in the atmosphere and the kinetics of the interfacial carburizing reactions:

$$\frac{\partial C}{\partial t} = \frac{\partial}{\partial x}\left(D\frac{\partial C}{\partial x} \right), \tag{1}$$

$$\beta\left(C_P - C_S \right) = -D\frac{\partial C}{\partial x}, \tag{2}$$

where C is the carbon concentration in steel at any location x below the surface, D is the carbon diffusivity in austenite, β is the mass transfer coefficient, C_P is the carburizing potential in the atmosphere, C_S is the carbon concentration at the steel surface.

Figure 1 shows a framework developed for the carburizing process optimization. The index of performance for optimization was to find a combination of process parameters that would allow

achieving the target case depth of 0.6 mm with minimum cycle cost and minimum case depth variation. The effective case depth was defined as the depth to 0.4 wt.% C. This criteria corresponds to Rc 50 or greater and is generally accepted for carburizing process evaluation in industrial settings.

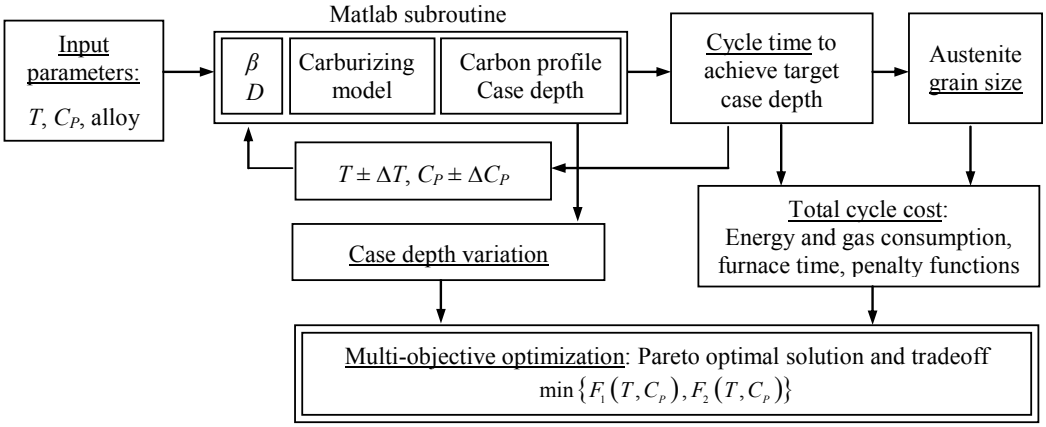

Figure 1. Framework for the carburizing process optimization.

The primary controllable process parameters include the carburizing temperature (T), carbon potential in the gas atmosphere (C_P) and the process time. Increasing carburizing temperature enhances the mass transfer coefficient in the atmosphere (β) and carbon diffusivity in austenite (D), and thus shortens the time necessary to achieve the desired case depth [7]. Such a solution, however, may decrease furnace life and promote excessive austenite grain growth. While increasing C_P enables a greater rate of carbon transfer from the atmosphere to the steel surface, it also increases the tendency of such carburizing atmospheres to soot when C_P approaches the carbon saturation limit in austenite. When soot occurs the carburized parts' quality degrades due to non-uniform case depth, and the overall process cost increases by the furnace downtime during the burn-out cycle. Both of these constraints on high levels of T and C_P were imposed on the overall cycle cost by means of penalty functions discussed further in this work.

While the effect of steel composition influences the carbon saturation limit in austenite, the mass transfer coefficient in the atmosphere and the carbon diffusivity in austenite [7], this factor might have a significant contribution to the results of the process optimization in case of medium- and high- alloyed steels. Such calculations need to be specific for particular steel, where the carbon saturation limit in austenite, β and D should be adjusted for a particular steel composition. In this work, all calculations were performed for optimizing the carburizing performance of AISI 1020 plan carbon steel.

Multi-objective Pareto optimization

Multi-objective optimization of the gas carburizing process is based on determining a set of carburizing process parameters to produce the desired case depth while meeting cost and quality requirements. If the quality objective function, i.e., case depth variation is defined as F_1 and the cost objective function is defined as F_2, the generic problem formulation can be expressed as follows:

$$\min\left\{F_1\left(T,C_P\right),\ F_2\left(T,C_P\right)\right\}, \tag{3}$$

subject to the following constraints:

$$880\ ^{\circ}\mathrm{C} \le T \le 1000\ ^{\circ}\mathrm{C},$$
$$0.9\ \text{wt.\%C} \le C_P \le 0.9\ \text{wt.\%C}.$$

Depending on the nature of the process there might be several potential solutions to multi-objective optimization problems, and a particular set of optimal solutions is referred to as Pareto frontier [10,11]. Often, the objective functions exhibit a conflicting nature: as one objective improves, another one deteriorates. Therefore finding the Pareto frontier in the space of conflicting multi-objective functions determines a set of solutions that are non-dominated to each other but are superior to the rest of solutions [12].

The Pareto frontier uses both effectiveness and efficiency of optimization and can be successfully used to characterize the tradeoff properties within the multi-objective carburizing process performance. Specifically, the Pareto optimal solution along the Pareto frontier with the best tradeoff between the minimum case depth variation and the minimum total cycle cost can be obtained by calculating a tradeoff- Υ parameter [10]:

$$\Upsilon = \frac{dF_2\left(T,C_P\right)}{dF_1\left(T,C_P\right)}. \tag{4}$$

The regions with two extreme conditions $\Upsilon \to 0$ or $\Upsilon \to \infty$ along the Pareto frontier imply that there is a little tradeoff between the objectives F_1 and F_2, while the region with $\Upsilon \to -1$ yields nearly an exact tradeoff between the two objectives. This region is defined as the Pareto optimal solution and corresponds to the optimal combination of T and C_P with the best tradeoff in $\min\left\{F_1\left(T,C_P\right),F_2\left(T,C_P\right)\right\}$

Results and Analysis

Time to Achieve Target Case Depth

Figure 2 shows evolution of the case depth (at 0.6 mm below steel surface) at various carburizing temperatures. The elevated temperatures increase both the rate of carbon transfer from the atmosphere to the steel surface and the rate of carbon diffusion in austenite. Therefore, at the first approximation – ignoring the cost penalties for excessive austenite grain growth and furnace deterioration, increasing the carburizing temperature from 875 °C to 975 °C would shorten the cycle time by a factor of 2.

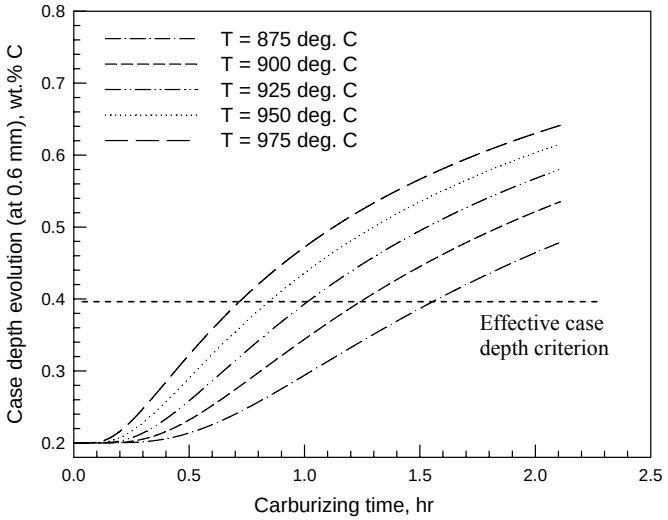

Figure 2. Case depth evolution at various carburizing temperatures and Cp of 1.1 wt.% C.

Figure 3 presents the results of the carburizing model simulation and shows the cycle time necessary to achieve the target case depth under various combinations of the carburizing temperature (T) and the atmosphere carbon potential (C_P). Since elevated C_P and T increase the driving force for carbon transfer from the atmosphere to the steel surface and enhance the rate of carbon diffusion in steel, respectively, high level combinations of these two factors require ~ 1.5 hrs to achieve the target case depth. Low level combinations of T and C_P significantly reduce the kinetics of carburizing and require up to ~ 5 hrs to achieve the same target case depth.

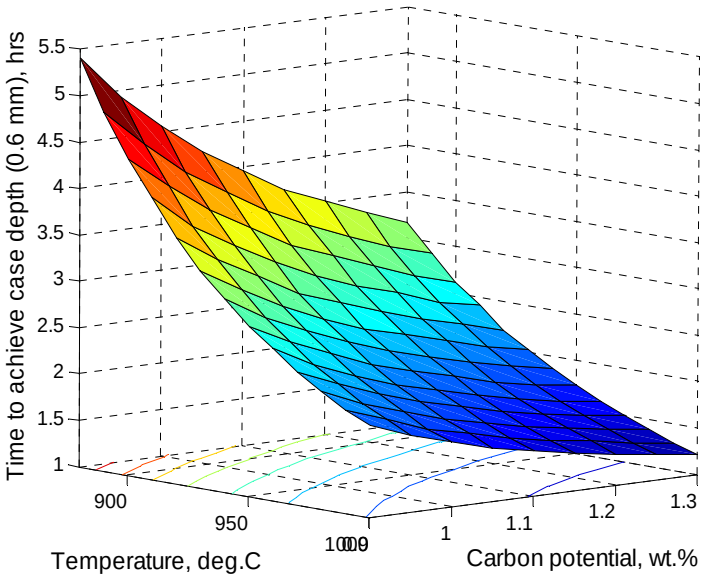

Figure 3. Carburizing time required to achieve the target case depth of 0.6 mm for the cycles with various combinations of carburizing temperature and carbon potential.

Case Depth Variation

There are multiple factors contributing to case depth variations in the carburized parts. These may include non-uniform temperature distribution in the carburizing chamber and variation in carbon potential in the gas atmosphere. Even in a well-controlled furnace, a temperature gradient may persist in the carburizing chamber throughout the carburizing cycle due to non-uniform heating and due to the specifics of the parts racking and workload characteristics. Dawes and Tranter [13] reported that an average temperature variation of 10 °C from the temperature set point may cause a 0.05 wt.% C variation in the atmosphere carbon potential.

The effect of the process parameters on the variations in the effective case depth was simulated using the carburizing model [5], where the temperature (T) and the atmosphere carbon potential (C_P) were allowed to vary by $\Delta T = \pm$ 10 °C and $\Delta C_P = \pm$ 0.05 wt.% C from the set points, respectively. In order to eliminate bias, it was assumed that ΔT and ΔC_P variations are constant and do not change with the magnitude of the carburizing T and C_P. For every combination of T and C_P the simulations were performed for 2 worst case scenarios: 1) $T + \Delta T$, $C_P + \Delta C_P$ and 2) $T - \Delta T$, $C_P - \Delta C_P$. The variations in the target case depth are shown in Figure 4 and were calculated as (±) half the difference in the corresponding case depths for the two worst case scenario of ΔT and ΔC_P variation.

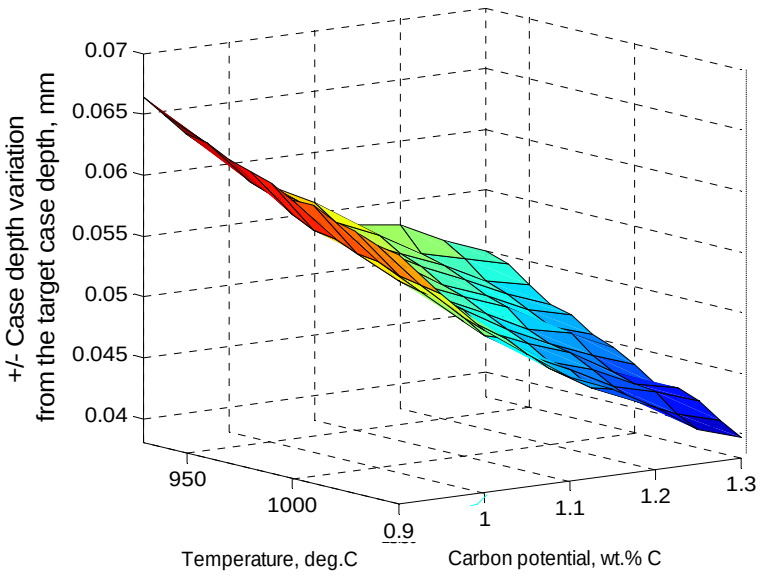

Figure 4. Case depth variations [mm] from the target case depth of 0.6 mm.

Since the carbon diffusivity increases exponentially with increasing process temperature [9], a variation of ± 10 °C from the temperature set point will cause more pronounced variations in the carbon diffusivity for the cycles with high level combinations of T and C_P. Consequently, larger variations in case depth should be expected. However, as seen from Figure 2, such cycles, with high level combinations of T and C_P, require significantly shorter time to achieve the desired case depth. Therefore, the overall case depth variations were notably smaller in the carburizing cycles with high level combinations of T and C_P as opposed to the cycles with low level combinations of these factors.

Total Carburizing Cycle Cost

Although Figure 2 suggests that shortening the processing time can be achieved by carburizing parts at higher T and C_P, finding an optimal combination of these process parameters can only be feasible if the corresponding cost factors are accounted for in the model. The overall cycle cost was calculated from several cost constituents, which included labors and furnace operating cost, gas and energy consumption, and cost penalty associated with additional rework in case of excessive austenite grain growth:

$$\mathrm{Cost}_{\mathrm{total}} = \mathrm{Cost}_{\substack{\mathrm{furnace}\\ \mathrm{operating}}} + \mathrm{Cost}_{\substack{\mathrm{gas}\\ \mathrm{consumption}}} + \mathrm{Cost}_{\substack{\mathrm{energy}\\ \mathrm{consumption}}} + \mathrm{Cost}_{\substack{\mathrm{penalty}\\ \mathrm{high\ T,\ Cp}}}, \qquad (5)$$

with

$$\text{Cost}_{\substack{\text{furnace}\\\text{operating}}} = \left(\frac{\$\, furnace}{hr} + \frac{\$\, operator}{hr} \right) \cdot t_{Carb}, \tag{6}$$

$$\text{Cost}_{\substack{\text{gas}\\\text{consumption}}} = \frac{ft^3}{hr} \cdot \frac{\$}{ft^3} \cdot t_{Carb}, \tag{7}$$

$$\text{Cost}_{\substack{\text{energy}\\\text{consumption}}} = \left(Energy_{\substack{heatup\\to\ T}} + Energy_{\substack{hold\\at\ T}} \cdot t_{Carb} \right) \cdot \frac{\$}{\text{KWt}}, \tag{8}$$

where t_{Carb} is the carburizing cycle time at constant carbon potential and temperature.

Since excessive austenite grain growth at the elevated temperatures has a negative effect on the quality of the carburized parts, this factor should be accounted for as a cost penalty in the overall cost model. The grain growth kinetics for a particular combination of the carburizing process parameters was simulated using a Beck type model [14] assuming an initial austenite grain diameter of 40 μm:

$$d^n - d_0^n = k_0 \cdot \exp\left(-\frac{Q}{RT} \right) \cdot t\,, \tag{8}$$

where d is the mean grain diameter at the end of isothermal hold at temperature T, d_0 is the initial grain diameter, k_0 is the pre-exponential rate constant, R is the gas constant, Q is the overall activation energy for grain growth, t is the holding time and n is the grain growth exponent. The coefficients k_0, Q and n were obtained by fitting the model to the experimental data according to the work of Sahay et.al. [1]. The final austenite grain size diameter was calculated for every combination of the carburizing temperature and time. No additional rework charges were applied unless the austenite grain size exceeded 55 μm. These charges involved the cost of furnace operating time and energy consumption during the rehardening operation, which included heating to 850 °C and holding the parts at constant temperature for 1 hr.

The estimated prices for energy, natural gas, furnace operating time and annual maintenance cost were obtained from the public resources of the Department of Energy [15] and from the CHTE industrial heat treating partners. Although the actual cost numbers are furnace-specific and may differ from one manufacturer to another, the cost-model approach provides a framework for optimizing the carburizing process parameters based on the gradient descent of the cost function rather than the actual cost numbers. The overall cost model accounts for the major

contributing cost factors and it can easily be adjusted to a particular manufacturer if the data are available.

Gas consumption for an electrically fired batch furnace with a rich endothermic atmosphere and a carburizing chamber of 3 m^3 was calculated from Equation (7) based on the previous experimental data [16]. Energy consumption was simulated using CHT-bf software [17] for the same batch furnace during heating and isothermal holding at various carburizing temperatures. Instantaneous energy consumption during heating the furnace to the carburizing temperature and energy utilized for maintaining the furnace at the constant temperature were used to calculate the average hourly energy consumption as shown in Figure 5.

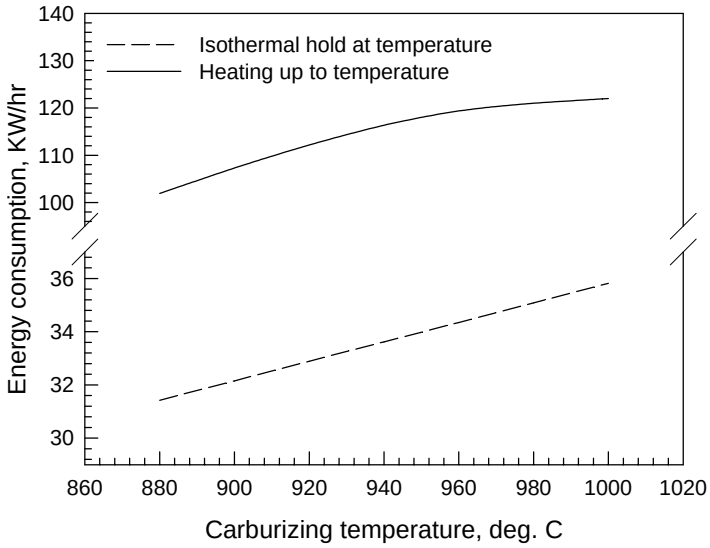

Figure 5. Energy consumption to heat up and maintain furnace at the carburizing temperature.

The overall cost for the carburizing cycles, with various combinations of the process temperature, the atmosphere carbon potential, and the time to achieve the target case depth (see Figure 2), were calculated from Equation (5) and are shown in Figure 6. The values of the total cycle cost were normalized with respect to the maximum cost value. Further, these data were used to search for the optimal solutions based on the gradient of the total cycle cost rather than the absolute values. This method helped finding a global minimum in the cost function for all corresponding combinations of T and C_P with a fast algorithm convergence rate.

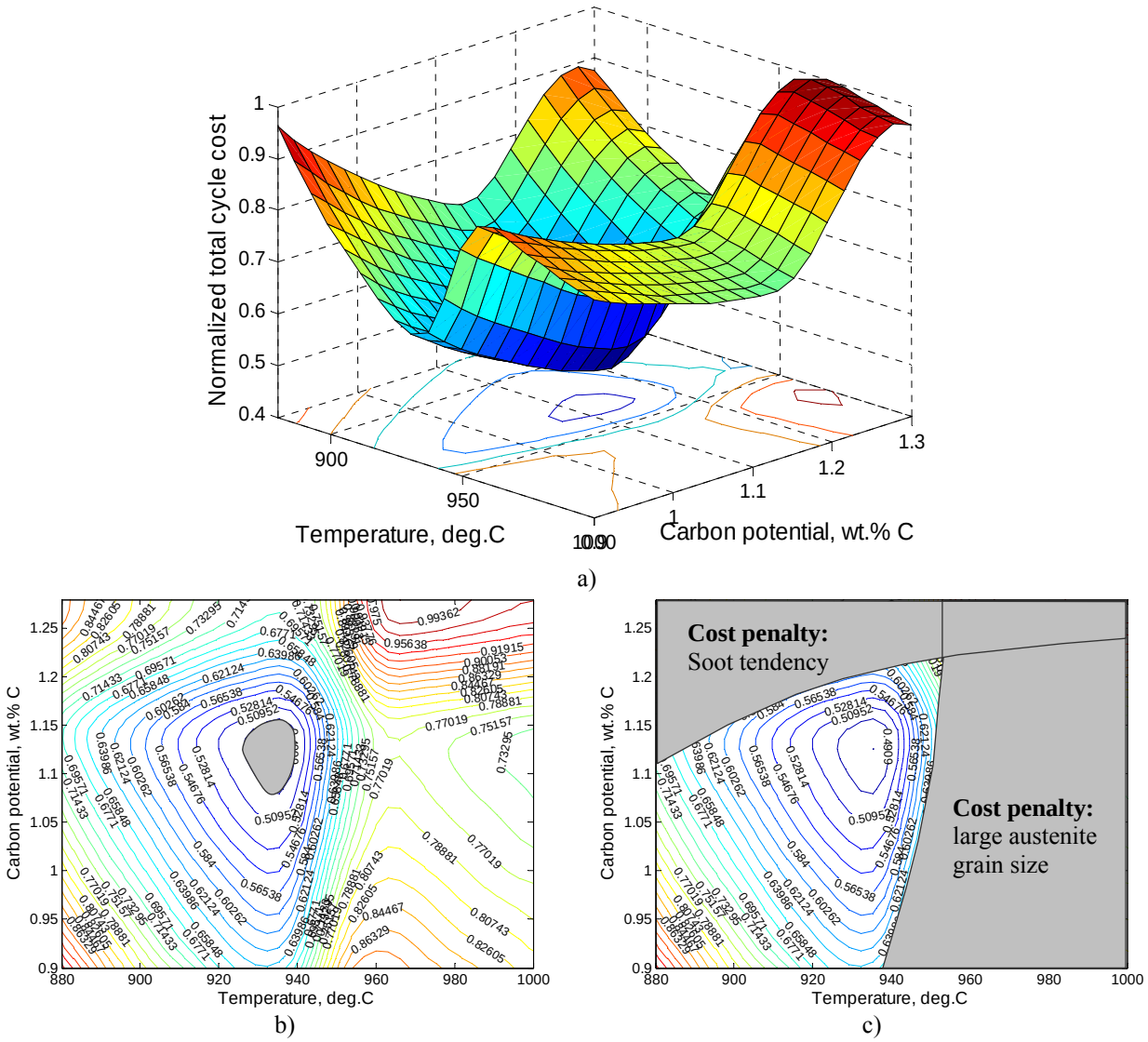

Figure 6. Normalized total cost for various carburizing cycles producing the target case depth: a) 3D surface representation, b) contour representation of the optimal conditions, c) contour representation for regions where cost penalty functions were applied.

Many heuristics can be proposed by evaluating the contour of Figure 6-b. There is a succinct range of controllable process parameters (T and C_P), where the target case depth can be achieved with minimum cycle time and minimum overall cost. The optimal range of T and C_P centers around 926-940 °C and 1.08-1.15 wt.% C, respectively, within which the target case depth is achieved in 2.4 hrs with cost < 50% of all explored combinations. Depending on the acceptable cost range, the optimal combinations of T and C_P can be controlled with tighter tolerances.

Increasing the carburizing temperature beyond ~ 940 °C from the optimal T and C_P combination sharply increases the total process cost due to rework required for large austenite grain size (refer to Figure 6-c). Exceeding carbon potential of ~ 1.15 wt.% C also increases the total cycle cost as it increases the atmosphere tendency to form soot and will require more frequent burnout cycles. While a combination of high T and C_P significantly shortens the cycle time required to achieve the desired case depth (refer to Figure 2), such process settings should be avoided due to high operating cost and the corresponding issues with the austenite grain size rework and furnace maintenance. In contrast, the carburizing cycles with low level combinations of T and C_P [below 920 °C and 1.05 wt.% C, respectively] require lower hourly gas- and energy-consumption, the kinetics of carburizing is so low that it requires significantly longer carburizing time to achieve the desired case depth. As a result, cost of the furnace operating time is much higher than the hourly savings in the gas and energy resources and results in higher overall cycle cost.

Multi-Objective Cost and Quality Optimization

Due to the inherent complexity presented in Figure 6, optimization of the carburizing process in the previous sections was based only on a single criterion: achieving the target case depth with minimum total cycle cost. Such approach helped determine several possible combinations of the carburizing process parameters (T and C_P) that would allow achieving the target case depth with minimum cost, process time, and the most optimal use of the energy resources. However, this methodology is based on sequential considerations of the variables and is most likely to be suboptimal since it addresses only the manufacturing requirements and does not carry any information on the quality of the carburizing performance, and particularly, case depth variation. For any given furnace, the variation in the case depth depends on the duration of the carburizing cycle and increases with increasing temperature and carbon potential in the atmosphere. Therefore, successful gas carburizing requires the resolution of both quality (austenite grain size and case depth variation) and cost (furnace time, gas and energy consumption) objectives. To identify the global optimal solution for meeting customers' and manufacturers' requirements, these objective functions should be considered simultaneously.

Defining the quality objective function, i.e., case depth variation as F_1 and the cost objective function as F_2, the multi-objective optimization problem focuses on finding a set of T and C_P

minimizing both objective functions simultaneously: $\min\{F_1(T,C_P),\ F_2(T,C_P)\}$. Analytically, one can evaluate two objectives either based on the trade-off of dF_1/dF_2 or dF_2/dF_1 represented in Figure 7-b and reach the same conclusion. Defining *min* F_1 (cost) as the primary objective, the goal is to search for Pareto optimal solution with the best tradeoff between the optimization functions. Such a combination of T and C_P would minimize F_1 (cycle cost) as much as possible without sacrificing much of F_2 (case depth variation).

From a practical standpoint, the range of acceptable cycle cost was set within the lower 10% cost range of all explored combinations, i.e. 0.48-0.58 on the normalized cost scale. Figure 7-a shows the range and the distribution of T and C_P, which produce the desired case depth within the range of [cost] interest. The Pareto space was obtained by rearranging and ranking these data in terms of the objective functions F_1 and F_2, as shown in Figure 7-b, where every data point represents a unique combination of T and C_P. The shaded area represents all possible solutions, while the heavy line indicates the Pareto optimal frontier for minimization of both objective functions – minimum total cycle cost and minimum case depth variation.

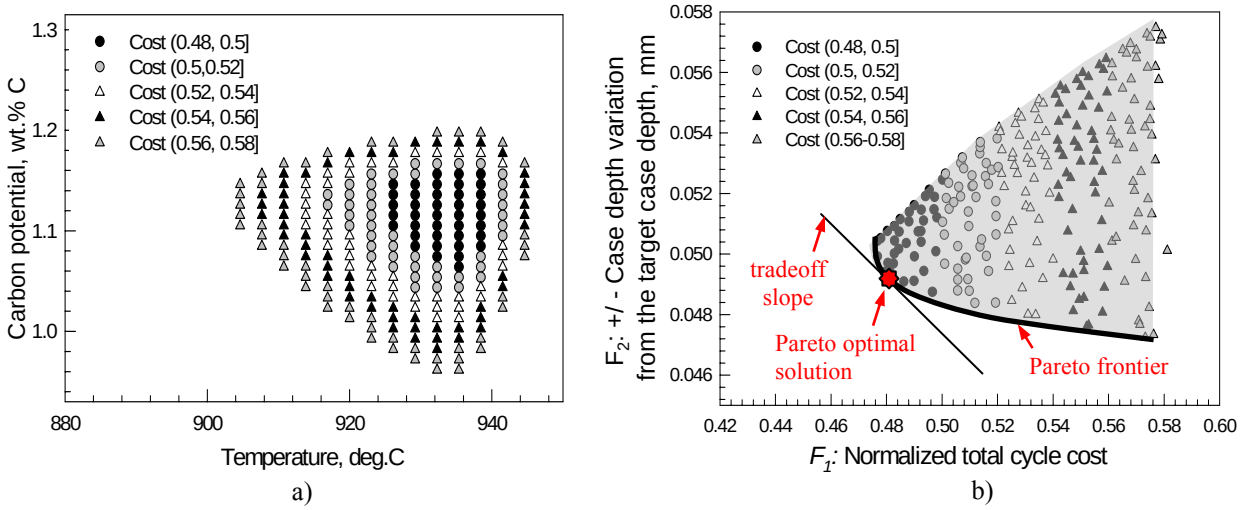

Figure 7. Pareto space: a) Carbon potential and temperature distribution within the range of interest (cost < 58 %); b) Pareto optimal frontier for bi-objective minimization problem.

The tradeoff between the minimum case depth variation and the minimum total cycle cost along the Pareto frontier were obtained by calculating the Υ parameter (Equation 4) for any two given sampling points of (T and C_P). Graphically, for regions with two extreme situations, $\Upsilon \to 0$ or $\Upsilon \to \infty$ along the Pareto frontier there is a little tradeoff between the objectives F_1 and

F_2. For region with $\Upsilon \to -1$ (Figure 7-b) there is nearly an exact tradeoff between the two objectives. This data point corresponds to the optimal combination of T and C_P with the best tradeoff in $\min\left\{F_1\left(T,C_P\right),F_2\left(T,C_P\right)\right\}$: carburizing temperature of 938.5 ºC and carbon potential of 1.14 wt.% C. Specifically, this combination of the carburizing parameters allows achieving the target effective case depth of 0.6 mm in 2.23 hrs with corresponding ± 0.05 mm case depth variation and minimum total cycle cost.

Conclusions

Optimization of gas carburizing process in this work was accomplished by simultaneously shortening the carburizing cycle time to achieve the desired case depth and minimizing the overall cycle cost. The cost function used for optimization included the cost of gas and energy resources, furnace operating time and cost penalties due to rework of parts with large austenite grain size and additional furnace maintenance due to operation at high temperature and/or high carbon potential. Multi-objective process optimization was performed using a Pareto frontier analysis, which helped determine the optimal set of parameters with the most optimal combination of carburizing temperature and atmosphere carbon potential and the best tradeoff between minimizing total cycle cost and minimizing case depth variation. Overall, application of this optimization technique will meet the carburizing quality requirements and achieve significant energy reduction, while shortening cycle time and thereby enhancing furnace capacity.

References

1. S.S. Sahay and K. Mitra "Cost Model Based Optimization of Carburizing Operation," *Surface Engineering*, 20 (5) (2004), 379-384.

2. K. Palaniradja, N. Alagumurthi and V. Soundararajan "Optimization of Process Variables in Gas Carburizing Process: A Taguchi Study with Experimental Investigation on SAE 8620 and AISI 3310 Steels," *Turkish Journal of Engineering and Environmental Sciences*, 29 (2005), 279-284.

3. F. Kuhn "Energy Situation in Europe and Conservation in Some Industrial Furnace Uses,"*Industrial Heating*, 50 (11) (1983), 25-30.

4. B.M. Khusid, E.M. Khusid and B.B Khina "Optimization of Properties of Carburized High-Chromium Steels," *Journal of Materials Science*, 30 (1995), 2989-2998.

5. O. Karabelchtchikova, M. Maniruzzaman, R.D. Sisson, Jr. "Carburization Process Modeling and Sensitivity Analysis using Numerical Simulation." *Proc. MS&T*, Cincinnati, OH, Sept. 25-28, (2006), 375-386.

6. O. Karabelchtchikova and R.D. Sisson, Jr., "Carbon Diffusion in Steels – a Numerical Analysis based on Direct Integration of the Flux", *Journal of Phase Equilibria and Diffusion*, 26 (6) (2006), 598-604.

7. O. Karabelchtchikova and R.D. Sisson, Jr., "Calculation of Gas Carburizing Kinetic Parameters from Carbon Concentration Profiles based on Direct Integration of the Flux", *Defect and Diffusion Forum*, 266 (2007), 171-180.

8. P. Stolar and B. Prenosil, "Kinetics of Transfer of Carbon from Carburizing and Carbonitriding Atmospheres," *Metallic Materials*, 22 (5) (1984), 348-353.

9. J. Agren, "Revised Expression for the Diffusivity of Carbon in Binary Fe-C Austenite," *Scripta Metallurgica*, 20 (11) (1986), 1507-1510.

10. C.A. Mattson and A. Messac "Pareto Frontier Based Concept Selection Under Uncertainty, with Visualization," Optimization and Engineering, Special Issue on Multidisciplinary Design Optimization (in press).

11. Alexander V. Lotov, Vladimir A. Bushenkov, Georgy K. Kamenev "Interactive Decision Maps: Approximation and Visualization of Pareto Frontier" (2004) Springer-Verlag New York, LLC.

12. N. Nariman-Zadeh, K. Atashkari, A. Pilechi, A. Jamali, and X. Yao, "Thermodynamic Pareto Optimization of Turbojet Engines Using Multi-Objective Genetic Algorithms," *International Journal of Thermal Sciences*, 44 (11) (2005), 1061-1071.

13. C. Dawes and D. F. Tranter, "Production Gas Carburizing Control," *Heat Treatment of Metals*, 31(4) (2004), 99-108.

14. F.J. Humphrey and M. Hatherly: "Recrystallization and Related Annealing Phenomenon" 281-285, 1996, Oxford, Elsevier Science.

15. Department of energy, Energy Information Administration: www.eia.doe.gov

16. O. Karabelchtchikova, S.A. Johnston and R.D. Sisson, Jr, "Gas Carburizing Atmosphere Development. Part I: Thermodynamics of Carburizing Endothermic Atmospheres with Various Enriching Hydrocarbon gases", submitted to *Metallurgical Transactions B*.

17. J. Kang, Y. Rong and W. Wang, "Numerical Simulation of Heat Transfer in Loaded Heat Treatment Furnaces," *Journal of Physics*, 4 (120) (2004), 545-553.

CHAPTER IV

RESEARCH CONCLUSIONS

This thesis presents a series of research papers that expand our fundamental understanding of the mass transfer during gas carburizing and provide a strategy for the carburizing process control and optimization. The research methodology was based on theoretical developments and experimental investigations and included modeling the thermodynamics of the gas carburizing endothermic atmosphere [Paper # 1], modeling the kinetics of mass transfer at the gas-steel interface [Paper # 4] and modeling the carbon diffusion in steel [Papers # 3 and 5]. The developed models accurately predict: 1) the atmosphere gas composition during the enriching stage of carburizing, 2) the kinetics of carbon transfer at the gas-steel interface, and 3) the carbon diffusivity in austenite for various process conditions and alloy composition. Experimental investigations focused on understanding the effects of the process parameters [Paper # 6], steel composition [Paper # 7] and the initial surface roughness [Paper # 4] on the kinetics of mass transfer during carburizing. The results of these investigations were combined with the models to determine the critical kinetic parameters for the boundary conditions and process modeling. This approach allowed the study of various stages of carbon transfer from the gas atmosphere to the steel surface individually, yet linked them together to allow the overall process modeling, control and optimization.

The 'boost' stage of gas carburizing was optimized by analyzing the thermodynamics and kinetics of carburizing reactions with enriching natural gas, propane, and a mixture of these two gases [Paper # 2]. The same atmosphere carbon potential was obtained by using 2.3 vol. % (total gas flow) of enriching C_3H_8 as opposed to 6.5 vol.% of natural gas, which lowered hourly enriching gas consumption by 65 %. Greater carbon availability of the C_3H_8 molecules and the thermodynamics of their step-reaction decomposition provided a faster rate of carbon potential evolution, which shortened the total carburizing cycle time while producing a similar microstructure, case depth and carbon gradient characteristics. Although enriching with a mixture of natural gas and C_3H_8 (1:1) enhanced the rate of carbon potential evolution, the effect was primarily dominated by C_3H_8. Simultaneous addition of natural gas and C_3H_8 lowered the activity of C_3H_8 and increased the amount of residual CH_4 remaining in the furnace. Therefore,

enrichment of the carburizing atmosphere with pure C_XH_Y is preferred to gas mixtures enrichment. Overall, gas carburizing with propane enrichment was found to provide a lower-cost alternative to endothermic carburizing atmospheres with more efficient energy utilization. Using such atmosphere also helps lower the environmental impact by reducing gas consumption and emission of the by-product gases without impairing the carburizing performance. Accelerating the rate of the carbon potential evolution would permit carburizing larger workloads with greater efficiency, reducing total cycle time required to achieve a desired case depth and increasing furnace capacity.

A method of direct flux integration was developed to calculate the mass transfer coefficient in the atmosphere and carbon diffusivity in austenite from the experimental carbon concentration profiles [Paper # 5]. The calculations were performed for a range of carburizing conditions and facilitate understanding the effect of process parameters on the kinetics of mass transfer during carburizing [Paper # 6]. The mass transfer coefficient in the atmosphere was found to increase with decreasing carbon potential in the furnace and increasing carburizing temperature. As the rate of carbon diffusion increases with increasing temperature, a greater carbon demand is established, allowing for more carbon to enter the steel surface and diffuse down the carbon concentration gradient. The calculated kinetic parameters served as input in the developed carburizing model [Paper # 3], and were successfully validated by comparing the predicted carbon concentration profiles with the experimental data.

The rate of carburizing and the kinetics of mass transfer at the gas-steel interface depend on the surface roughness of the parts prior to carburizing [Paper # 4]. Given the same process parameters, the parts with larger interfacial area (rougher surfaces) provide a greater number of sites for *CO* molecules decomposition, which increases the density of the absorbed carbon atoms and enhances the rate of carbon diffusion. Carbon uptake by the steel surface increased with the increasing surface roughness, while smoother samples with surface roughness below 1.2 μm (Sq) and 22 μm (St) revealed no significant effect on the carbon concentration profile. Therefore, if the initial surface roughness on the parts or on the various segments of the same part is controlled below 1.2 μm (Sq) and 22 μm (St), the observed case depth variations can be reduced or eliminated. Overall, the experimental data can further be used to determine an optimal initial surface roughness to maximize carbon uptake and minimize case depth variation, especially important for tolerance control and design considerations.

Gas carburizing performance of various alloy steels is strongly affected by the alloy composition [Paper # 7]. Therefore, alloy composition should be taken into account when carburizing medium- and high-alloy steels to ensure repeatable and well-controlled results. AISI 4820 steel with high concentration of austenite-stabilizing elements (Ni, Si) exhibited the slowest kinetics of the mass transfer from the gas atmosphere to the steel surface. Although, the austenite-stabilizing elements increased the carbon diffusivity in austenite, the rate of carburizing was limited by the flux entering the steel surface, which significantly lowered the final carbon concentration profile compared to that of plain carbon steel with the same bulk carbon concentration. While carbide-forming elements (Cr, Mo) in AISI 5120 and 8620 lowered the carbon diffusivity in austenite, they increased the rate of carbon transfer from the atmosphere to the steel surface and accelerated the rate of carburizing. Understanding and quantifying the contribution of alloy composition on the mass transfer coefficient and carbon diffusivity in austenite helped explain the observed variations in the carbon concentration profiles of various alloy steels. In addition, a recommendation was made to adjust the carburizing process time by the steel composition to achieve the desired carburizing results with better case depth uniformity.

Finally, the overall optimization of the atmosphere gas carburizing process was based on the multi-objective Pareto optimization [Paper # 8], which linked all the observed correlations between the controllable process parameters (carbon potential, temperature and time) and the kinetics of carbon transfer in the gas atmosphere, at the gas-steel interface and within the steel [Papers # 1-7]. Specifically, the multi-objective optimization was performed to determine a set of process parameter to achieve the target case depth with the best tradeoff combination between minimizing case depth variation and minimizing total cycle cost. The cost function used for optimization included the cost of gas and energy resources, furnace operating time and the corresponding cost penalties due to operation at high temperature and/or high carbon potential. Overall, application of this optimization technique will meet the carburizing quality requirements and achieve significant energy reduction, while shortening cycle time and thereby enhancing furnace capacity.